1-1-1981

Geological interpretations of a detailed bouguer gravity survey of the Chattolanee Dome, near Baltimore, Maryland.

David A. Chapin

GEOLOGICAL INTERPRETATIONS OF A DETAILED BOUGUER GRAVITY SURVEY OF THE CHATTOLANEE DOME, NEAR BALTIMORE, MARYLAND

by

David A. Chapin

A Thesis

Presented to the Graduate Committee

of Lehigh University

in Candidacy for the Degree of

Master of Science

in

Department of Geological Sciences

Lehigh University

1981

This thesis is accepted and approved in partial fulfillment of the requirements for the degree of Master of Science.

June 3, 1981

____

____
Professor in Charge

____
Chairman of Department

ACKNOWLEDGMENTS

I am deeply grateful to my advisor, Dr. Kenneth P. Kodama for his patient help and useful criticisms. I would also like to express my appreciation to the other members of my thesis committee, Dr. Charles B. Sclar and Dr. Emery T. Cleaves (from the Maryland Geological Survey), for their helpful guidance in pinning down my research objectives.

Special thanks are due to Dr. Peter D. Muller of the Maryland Geological Survey. Much of my geological understanding of Piedmont structure is due to him. He and Dr. Jonathan Edwards, Jr. (also from the Maryland Geological Survey) were especially helpful guiding me with my fieldwork. The Phoenix Dome traverse could not have been completed without their help.

Fellow graduate students, Stephen Perry and Susan Gawarecki deserve my special gratitude. Both provided me with useful hints and served as a sounding board for my ideas.

My appreciation is due to Claude Wessels of the Gravity and Astronomy Division of the National Geodetic Survey (National Ocean Survey). I was able to borrow a LaCoste and Romberg Gravity Meter through him and his office. All of my gravity reductions were calculated by his computer program. The accuracy of my survey was in a large part attributable to his invaluable aid.

The nature of my research involved innumerable people. Thanks are due to the following people: Bryan McCoy, plant geologist for the Arundel Corp. for permitting me to visit his quarries. The good people at the Balto. City Dept. of Public Works Field Section and the Balto. County Dept. of Public Works Survey Office for allowing me to use their elevation data.

Very special recognition is due to my beautiful wife, Rita, who was patient enough to put up with this nonsense. Without her constant encouragement, this study could not have been completed.

This study was supported by a Student Technical Assistantship from the Maryland Geological Survey for the summer of 1980, and by a University Fellowship from Lehigh University for 1980-81. This support is greatly appreciated.

Table of Contents

List of Figures

List of Tables

ABSTRACT

A gravity survey of the Chattolanee Gneiss Dome was conducted to allow the determination of detailed models of its subsurface structure. 425 gravity stations were occupied with a LaCoste and Romberg and/or a Worden gravity meter in a net pattern over a 160 square kilometer area. Readings were taken at 2nd order benchmarks and elevations were accurate to +/- 0.08 m.

A simple bouguer anomaly map (bouguer density = 2.67 g/cc) shows a 5 km. wide flat-bottomed gravity trough over the dome with the axis of the trough dipping eastward.

Trend surface analysis produced a second-order surface at a 94% correlation. The conclusions reached by this analysis were: 1) Local anomalies were superimposed on a large trough-shaped regional anomaly. Local anomalies were insignificant and unmappable. 2) The subsurface body that produced the regional signal was relatively simple in shape. 3) Residuals probably represent noise in the data rather than local events.

The densities of 167 rock samples from 10 different lithologies were measured. The Baltimore Gneiss (2.683 g/cc) is among the least dense of the Piedmont rocks.

Gravity modeling of the data was accomplished using a two-dimensional Talwani-type computer routine. Models

suggest: 1) To the south of the dome, the Baltimore Mafic Complex overthrusts the metasedimentary rocks of the dome along a 30 to 45 degree southward-dipping fault. Serpentine probably underlies the gabbroic rocks of the mafic complex. 2) To the east, the Ruxton Fault may be a high-angle normal fault which cuts across an older low-angle reverse fault. The reverse fault dips eastward. 3) The east side of the dome is truncated by an eastward-dipping normal fault. 4) The Slaughterhouse Gneiss is apparently a thin unit (<200 m.). 5) The valley between the Chattolanee and Towson Domes is floored by metasedimentary rocks (<700 m. thick) which form an overturned syncline that plunges to the south. 6) The Chattolanee Dome is underlain (at depths <2 kms.) by a wedge of higher density metasediments - presumably Wissahickon - which thicken westward. 7) The dome's root zone may be below its eastern end.

Modeling of a separate gravity traverse northward across the Phoenix Dome indicates that the western region of the dome is probably the bottom limb of a rootless nappe.

The geophysical data suggest two possible deformational schemes for the Baltimore Gneiss Dome terrain. One sequence of deformational events could be: 1) Extreme ductile deformation, forming nappes; 2)

Thrusting of the Baltimore Mafic Complex from the south; 3) Westward imbricate thrusting of the whole package; 4) Late-stage normal faulting. This scheme is one of increasingly shallower deformational styles.

The preferred scheme of deformational events is based on the assumption that the wedge of dense material under the Chattolanee Dome is the bottom limb of a nappe, making folding, rather than faulting the predominant deformational style. In this model thrusting of the Baltimore Mafic Complex from the south is penecontemporaneous with napping of the Chattolanee and Phoenix Domes. This is followed by late-stage normal faulting.

The data suggest two possible structural relationships between the Chattolanee and Phoenix Domes: 1) The Chattolanee Dome may be the root zone for the Phoenix Nappe. 2) The two domes represent two different layers of a stack of nappes.

This study proposes that the domes were emplaced by tectonic shortening rather than true diapiric doming. This may have been caused by a continental-continental collision in Taconic time.

1. INTRODUCTION

The Maryland Piedmont is one of the most intensely studied areas of the Piedmont Province. In order to better delineate the geology of this structurally complex region, a detailed gravity survey of the Chattolanee Dome was conducted. The Chattolanee Dome is one of seven gneiss bodies cropping out in the Maryland Piedmont (Fig. 1-1).[1] Parts of the Phoenix Dome and the Towson Dome were also studied, but in less detail. The study area involves the following U. S. Geological Survey 7 1/2 minute quadrangles:

- Cockeysville (all)
- Baltimore West (northern section)
- Reisterstown (all)
- Ellicott City (northeast corner)
- Hereford (central section)

The Chattolanee Dome is an elongate, oval-shaped gneiss body in map view (Fig. 1-1). Its long axis trends east - west and the dome is approximately 12.5 km. east -

---

[1] These gneiss bodies have been called domes. While this study demonstrated that at least three of the gneiss bodies may not be true structural domes, the term 'dome' will continue to be used throughout this report, unless otherwise stated.

west by 6 km. north - south.

1.1 Objectives

The main objective of this study was to determine the overall subsurface structure of the Chattolanee Dome and its structural relationship with adjoining domes.

Specific questions about the structure were:

1. Is the Chattolanee Dome allocthonous or autocthonous?

2. What is the relationship between the Slaughterhouse Gneiss and the Baltimore Gneiss?

3. A major fault (Ruxton Fault) truncates the western end of the Towson Dome. What is the attitude of this fault?

4. What is the nature of the Baltimore Mafic Complex - metasedimentary terrain contact on the southern edge of the Chattolanee Dome?

5. What is the subsurface structure of the Phoenix Dome?

1.2 General Geology and Previous Work

Many important concepts have been developed during the geological investigation of the Maryland Piedmont. Williams [1891] from Johns Hopkins University pioneered the first application of petrographic methods used to solve geologic problems in America. Williams used petrologic methods learned in Germany to interpret Piedmont geology.

Eskola [1949] visited the Baltimore area in 1946 and developed his now classic theory concerning the origin of mantled gneiss domes based upon the geology of this region.

Figure 1-1: Index Map of the Baltimore Gneiss Domes

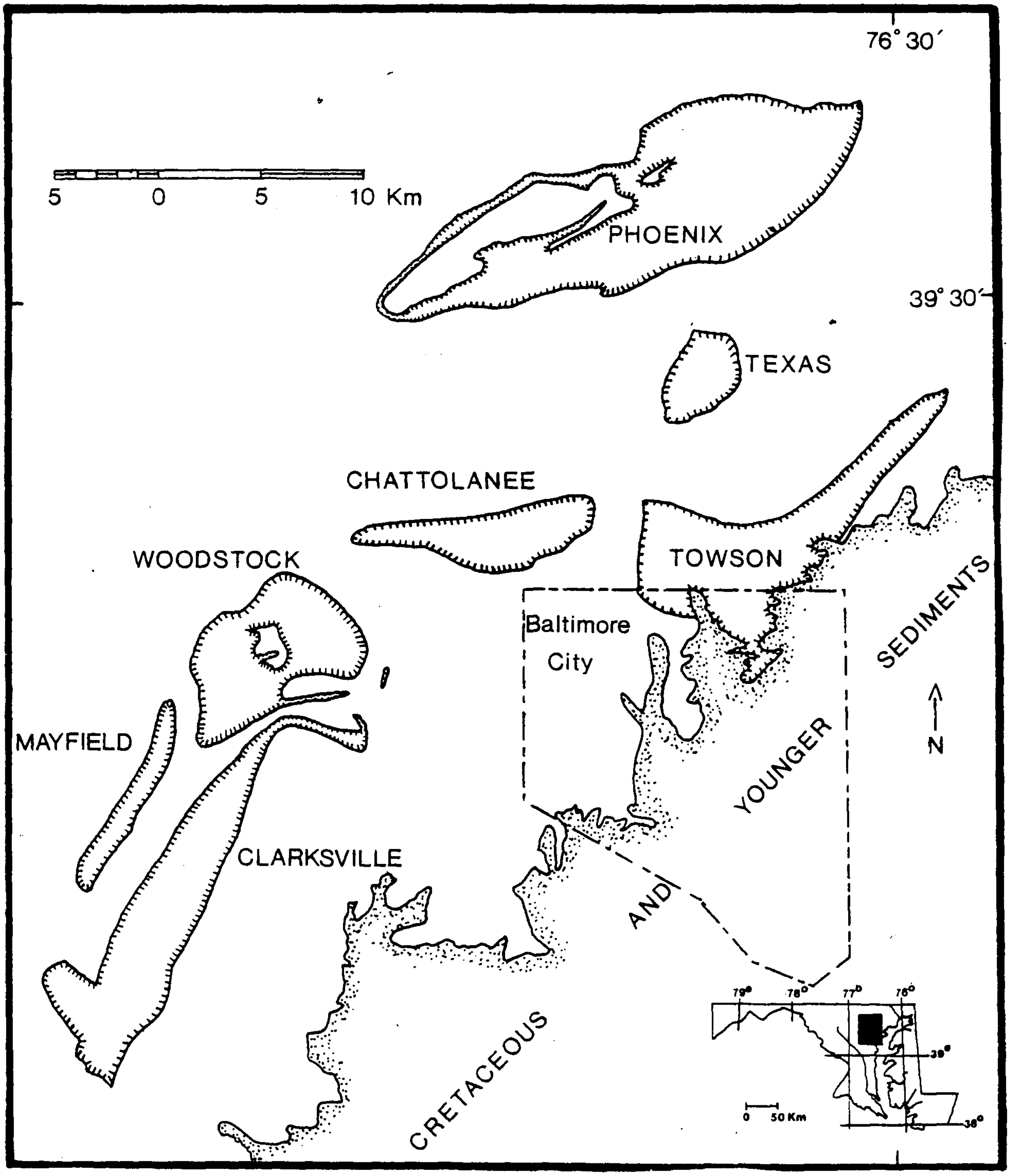
76° 30′
5 0 5 10 Km
PHOENIX
39° 30′
TEXAS
CHATTOLANEE
WOODSTOCK
TOWSON
Baltimore City
SEDIMENTS
MAYFIELD
YOUNGER
CLARKSVILLE
AND
CRETACEOUS
N
79° 78° 77° 76°
39°
38°
0 50 Km

The general structure of the Piedmont near Baltimore was first studied by Williams [1892]. The work of Williams, his students, and other workers is reviewed by Higgins [1972]. Table 1-1 lists the most important contributions.

The mantling of metasediments over gneiss into dome-like structures near Baltimore was first noted by Mathews [1904] and Mathews and Miller [1905]. Reconnaissance mapping of the area was completed by Mathews [1925] and by Knopf and Jonas [1925, 1929]. Broedel [1937] was the first to perform structural analysis on the gneiss domes.

These first generation workers determined:

1. The gneiss that cores each dome (Baltimore Gneiss) is the oldest rock in the stratigraphic sequence [Williams, 1892].

2. A quartzite (the Setters Formation) unconformably overlies the gneiss [Williams, 1892].

3. The general structure of the gneiss is anticlinal [Mathews, 1904; Broedel, 1937].

4. Marble (the Cockeysville Formation) conformably overlies the quartzite [Mathews and Miller, 1905].

5. Schists conformably overlie the marble [Mathews and Miller, 1905].

6. These schists may be the same schists (Wissahickon) that outcrop in the Philadelphia

GENERAL GEOLOGY	
Reconnaissance Mapping	Williams, 1892 Mathews, 1904 Mathews, 1933 Knopf and Jonas, 1925 Mathews, 1925 Knopf and Jonas, 1929 Broedel, 1937 Cleaves and others, 1968 Crowley, 1976a Crowley, 1976b
Detailed Mapping	Crowley and Cleaves, 1974 Crowley and others, 1975 Crowley and others, 1976 Crowley, 1977 Crowley and Reinhardt, 1979 Crowley and Reinhardt, 1980 Muller, in prep.
General Petrology	Williams, 1891 Hopson, 1964
Age Dating	Tilton and others, 1958 Tilton and others, 1959 Wetherill and others, 1966 Wetherill and others, 1968 Tilton and others, 1970 Higgins, 1972
Geophysics	Bromery, 1967a Bromery, 1967b Bromery, 1967c Bromery, 1968 Higgins and others, 1973 Higgins and others, 1974a Hansen, 1974 Higgins and others, 1974b Zietz and others, 1978 Edwards and Hansen, 1979 Fisher and others, 1979 Zietz and others, 1980 Daniels, in prep.

Table 1-1: Summary of Previous Work

Stratigraphic Nomenclature	Knopf and Jonas, 1923 Fisher, 1963 Southwick and Fisher, 1967 Crowley and others, 1971 Higgins and Fisher, 1971 Higgins, 1972 Crowley, 1976a Fisher and others, 1979
INDIVIDUAL ROCK UNITS	
Baltimore Gneiss	Olsen, 1972 Wagner and Crawford, 1975 Olsen, 1977
Setters Formation	Fisher, 1971
Cockeysville Formation	Mathews and Miller, 1905 Miller, 1905 Choquette, 1957 Choquette, 1960
Wissahickon Group	Knopf and Jonas, 1923 Cloos and Anderson, 1950 Reed and Jolly, 1963 Fisher, 1963 Southwick, 1969 Fisher, 1970 Fisher, 1971 Fisher, 1978
Baltimore Mafic Complex	Williams, 1886 Cohen, 1937 Herz, 1950 Herz, 1951

Table 1-1, continued

area [Knopf and Jonas, 1923, 1925, 1929].

7. A terrain of gabbroic rocks (the Baltimore Mafic Complex) exists southeast of the metasedimentary terrain.

8. The western side of the Towson Dome is truncated by the Ruxton Fault [Mathews and Miller, 1905; Broedel, 1937].

The petrology and structure of the Maryland Piedmont has been updated and synthesized by Hopson [1964]. Hopson agreed with all these major conclusions.

Recent work involves more detailed geologic mapping of the Maryland Piedmont. The Maryland Geological Survey has undertaken an extensive 7 1/2 minute geologic mapping program in the Baltimore area. This mapping project [Crowley 1977; Crowley and Cleaves, 1974; Crowley and Reinhardt, 1979, 1980; Crowley and others, 1975, 1976; Muller, in prep.] has provided new insights as to the geology of the Piedmont.

1.2.1 Previous Geophysical Work

Gravity and magnetic studies of this area was first undertaken by Bromery [1967a; 1967b; 1967c; 1968]. These studies involved areal mapping of gravity and magnetic anomalies. The gravity map had a station spacing of approximately 1 km. and was not dense enough to study local structures smaller than about 0.5 km.

Bromery's aeromagnetic maps were used by Fisher and others [1979] to study large scale Piedmont structures and, in particular, the Baltimore Gneiss Dome Terrain.

1.3 Stratigraphic Nomenclature and Rock Descriptions

Stratigraphic nomenclature has been subject to much debate, particularly concerning subdivision of the Glenarm Series. All workers agree that there are six major crystalline rock units in the study area. They are: 1) Baltimore Gneiss; 2) Setters Formation; 3) Cockeysville Formation; 4) Wissahickon Group; 5) Baltimore Mafic Complex; 6) Late-stage granitic intrusives (not examined in this study).

The stratigraphy for this study (Table 1-2) generally follows Fisher and others [1979] because the units have identifiable geophysical characteristics. Genetic names used by Fisher, Higgins, and Zietz [1979] have been dropped in favor of locality names used by Crowley [1976a].

1.3.1 Baltimore Gneiss

The Baltimore Gneiss is a mineralogically uniform granitic gneiss with layered, migmatized, or augen facies.

The Baltimore Gneiss has geophysical properties that are uniform throughout the study area regardless of facies. It has a low, relatively uniform density (2.683 g/cc - see Fig. 1-3) and a very low magnetic

This Report	Fisher and others, 1979	Crowley, 1976
-Wissahickon Group	-Wissahickon Group of Crowley (1976)	-Wissahickon Group
--(not encountered)	--Diamictite (undiff.)	--Sykesville Fm. ---gneiss mem. ---schist mem.
--Oella Fm. ---(included with the Baltimore Mafic Complex)	--Metagreywacke (undiff.)	--Oella Fm. ---Sweathouse Amphibolite Mem.
--(not encountered)	--Metagreywacke	--Piney Run Fm.
--(not encountered)	--Quartzose Schist	--Pleasant Grove Schist
--Loch Raven Schist (undiff.)	--Pelitic Schist (undiff.)	--Loch Raven Schist ---Hydes Marble Mem. ---Rush Brook Mem.
-Cockeysville Fm. (undiff.)	-Cockeysville Marble (undiff.)	-Cockeysville Marble --massive meta-dolostone mem. --massive meta-limestone mem. --layered meta-limestone mem. --layered meta-dolostone mem. --layered marble mem. --phlogopitic meta-limestone mem.
-Setters Fm. --garnet schist mem. (undiff.)	-Setters Fm. --garnet schist mem. (undiff.)	-Setters Fm. --garnet schist mem. --quartzite mem. ---schist lens ---conglomerate lens --gneiss mem. ---quartzite lens

Table 1-2: Comparison of Stratigraphic Nomenclature

-Baltimore Gneiss (undiff.)	-Baltimore Gneiss (undiff.)	-Baltimore Gneiss
		--hornblende gneiss mem.
		--streaked-augen gneiss mem.
		--augen gneiss mem.
		--layered gneiss mem.
-Slaughterhouse Gneiss	-(not defined)	-Slaughterhouse Gneiss
-Baltimore Mafic Complex	-Metaigneous rocks (undiff.)	-Baltimore Mafic Complex
--Amphibolite (undiff.)		--Mt. Washington Amphibolite
		--Holofield Layered Ultramafite
		[--Sweathouse Amphibolite]
		--(miscellaneous other mafic units)
--Serpentine		--Serpentine

table 1-2, continued

Rock Unit	No. of Samples	Average Density g/cc	95% Confidence Interval	Standard Deviation
Cockeysville Fm.	31	2.845	2.820-2.870	0.069
Amphibolite	30	2.996	2.952-3.040	0.118
Serpentine	10	2.639	2.613-2.665	0.037
Baltimore Gneiss	40	2.683	2.672-2.694	0.035
Oella Fm.	15	2.750	2.717-2.783	0.060
Loch Raven Schist	16	2.912	2.869-2.955	0.081
Wissahickon (combined)	31	2.834	2.794-2.874	0.108
Setters Fm. (undivided)	10	2.628	2.612-2.644	0.022
Slaughterhouse Gneiss	5	2.606	2.593-2.619	0.011
Silicified Breccias	8	2.606	2.550-2.662	0.067
Vein Quartz	2	2.666		0.003

Table 1-3: Measured Whole Rock Densities

susceptibility [Bromery, 1968; Fisher and others, 1979].

1.3.2 Setters Formation

The Setters Formation forms a thin unit directly overlying the Baltimore Gneiss. It consists of micaceous quartzites interlayered with feldspathic schists and gneisses. Three members and three lenses are defined by Crowley [1976a]. The quartzites form ridges and therefore, the formation's structural trend is fairly well known.

Because the Setters Formation contains abundant quartz, a low density mineral (2.667 g/cc - see Table 1-3), it has a negative density contrast with respect to the Baltimore Gneiss (Setters density = 2.628 g/cc, Baltimore Gneiss density = 2.683 g/cc, density contrast is -0.055 g/cc). However, because the Setters Formation is a thin unit and its density is close to that of the Baltimore Gneiss, it is difficult to differentiate with gravity methods. Subdividing it for this geophysical investigation is unnecessary.

1.3.3 Cockeysville Formation

The Cockeysville Formation consists of impure, massive and layered marbles and meta-dolostones which have been divided into 4 members by Crowley [1976a]. The members of the Cockeysville Formation can not be distinguished by gravity and the Cockeysville was not divided for this investigation.

It is a dense rock with a fairly uniform density at about 2.845 g/cc. The Cockeysville serves as a good gravity marker, as it has a large density contrast with respect to the Baltimore Gneiss (0.162 g/cc) and it has a fairly large areal extent.

1.3.4 Wissahickon Group

The Wissahickon Group rocks in this area consist of amphibolite-grade pelitic and psammitic schists and gneisses. Because of its great lithologic variability, the Wissahickon is very difficult to study using gravity modeling techniques. Its density ranges from 2.995 for pelitic schists to 2.717 for psammitic gneisses.

The end-member units in the Wissahickon are the Oella Formation (psammitic schists and gneisses) and Loch Raven Schist (pelitic schists). Most of the lower Wissahickon in the study area is gradational between these two units.

1.3.5 Baltimore Mafic Complex

The Baltimore Mafic Complex consists mostly of layered amphibolites with lesser amounts of metamorphosed ultramafic rocks. The amphibolites have a uniformly high density (2.996 g/cc). Associated serpentinite bodies have a very low density (2.639 g/cc). This large density difference is fairly easy to model using gravity.

Crowley's [1976a] Sweathouse Amphibolite Member of the Oella Formation has been included in the Baltimore Mafic Complex. Wherever Crowley has mapped this unit, it is always juxtaposed to amphibolites of the mafic complex. Crowley [1976a] defined the Sweathouse Member on the basis that it had some schist interlayered with the amphibolite. It was suggested by Muller [personal comm.] that this represents a tectonic melange that marks the fault zone between the mafic complex and the Oella Formation. The Sweathouse Member contains mostly amphibolites of identical compositions as the amphibolites of the Baltimore Mafic Complex. The Sweathouse has geophysical properties indistinguishable from the mafic complex and was included as part of the mafic complex in this study.

1.3.6 Slaughterhouse Gneiss

The Slaughterhouse Gneiss is a very uniform and massive quartz-rich gneiss. It is the least dense of all the rocks studied (2.606 g/cc), and it has a negative density contrast with respect to the Baltimore Gneiss (-0.077 g/cc). This results in an observable negative gravity anomaly at the surface.

1.4 Field Relations

Poor exposure prevented observation of most geologic contacts. The Baltimore Gneiss - Setters Formation contact is seen most often. The foliation of the gneiss is parallel to the layering in the Setters. The contact is often marked by an intense zone of cataclasis in the gneiss and feldspathization of the Setters [Muller, personal comm.]. While it is generally agreed by most workers that this contact marks an unconformity, field evidence suggests some movement has occurred at the contact zone.

As far as can be determined, the Setters Formation - Cockeysville Formation contact has never been observed in outcrop. However, the Cockeysville Formation - Wissahickon Group contact has been exposed in the Arundel Corp. Greenspring Avenue quarry. The contact is a gradational zone where layers of the Cockeysville become more micaceous and feldspathic as one gets nearer to the contact. Carbonate beds appear intermittently in the Wissahickon a short distance above the contact. At this exposure, it is clear that the contact is not a fault, but a conformable facies change.

The Slaughterhouse Gneiss - Baltimore Gneiss contact has been observed in saprolite at a construction site at Greenspring Avenue and Slaughterhouse Run. The contact is gradational, the Slaughterhouse Gneiss becoming more micaceous and more banded as it grades into layered Baltimore Gneiss.

The Baltimore Mafic Complex - Wissahickon contact (see page 21) is marked locally by Crowley's [1976a] Sweathouse Member which is probably a tectonic melange.

Within the mafic complex, the amphibolite - serpentine boundary has been observed in at least two instances. Along Falls Road at Copper Hill Rd. in the Bare Hills area, the contact is marked by a zone of talc schist[2]. A drill core made during the Baltimore subway construction also was marked with a zone of talc schist at the contact [Muller, personal comm.].

---

[2] This was mapped by Crowley [1975 and 1976b] as Oella Formation.

2. METHODS

2.1 The Gravity Method

By measuring minute lateral changes in the earth's gravitational field, anomalously dense rocks can be located in the subsurface. The earth's gravitational field can be mathematically described in terms of **equipotential surfaces** - a family of surfaces which tend to parallel the earth's topography. Every point on an equipotential surface has the same gravitational potential. In the gravity method, the gradient of this potential - the acceleration due to gravity - is measured and interpreted.

The gravity equipotential surface that intersects the ocean-atmosphere interface is known as the **geoid**. Because the oceans are fluid, they conform to the gravitational pull exerted upon them and to the effects of the earth's rotation. Therefore, sea level is the geoid. All deviations from the geoid are due to either the distance the observer is away from the center of the earth[3] (i.e. topography and the overall shape of the earth) or lateral inhomogeneities in the earth's mass.

---

[3] according to Newton's Laws, gravitational force varies inversely to the square of the distance

By comparing the theoretical model of the earth's gravitational field calculated from a laterally homogeneous earth to the observed gravity value at a given point corrected to sea level (i.e. the geoid), any differences are directly attributable to lateral density variations in the subsurface.

Corrections of the observed values are collectively termed **gravity reductions** and include instrument drift, reference field, earth tides, free-air, bouguer, and terrain corrections.

2.1.1 Instrument Drift

Modern portable gravity meters are subject to instrument drift over time. The instrument drift is determined by repeated measurements at the same location. A large number of repeated station occupations produces more accurate instrument drift determinations. Instrument drift is considered to be a linear function between each measurement with respect to time [Nettleton, 1976].

2.1.2 Gravity Reference Field

The earth is not a true sphere but rather an oblate spheroid. Its shape deviates somewhat from the shape of the geoid. Both the shape of the earth and the geoid vary proportionally with latitude. This is due to a systematic increase in the centrifugal acceleration as the distance from the earth's spin axis to the earth's surface increases from the poles to the equator. On the average, the acceleration at the equator is about 5300 mgal[4] larger than at the poles [Dobrin, 1976].

The **Gravity Reference Field** is a mathematical formula that predicts the earth's gravitional force at sea level (on the geoid) assuming a laterally homogeneous earth. It consists of two terms. The first term represents the gravity value of any point on the geoid, assuming a uniformly dense, non-spinning earth. The second term is a complex correction term which relates the earth's spin, the latitude of the observation, and the flattening of the poles.

After correcting for instrument drift and calibrating to points of known gravity (see Appendix A), the Gravity Reference Field is subtracted from the raw gravity values. In this study, the IGSN 71 formula [Woollard, 1979] was used to calculate the Gravity Reference Field.

---

[4] A milligal is the commonly used unit to express small values of acceleration. One mgal is equal to 0.00001 m/sec/sec.

2.1.3 Earth Tides

The earth yields plastically to tidal forces in much the same way as the oceans, though on a smaller scale. **Earth tides** are minute cyclical changes in the elevation of the earth due to this tidal attraction. These changes result in time related differences in the distance between the observer (i.e. gravity station) and the center of the earth [Melchior, 1978]. In the study area, earth tides resulted in as much as a 0.2 mgal difference in gravity values of a single station over the course of a day.

Longitude, time of day, and date are critical factors which are used to calculate earth tides as they are in ocean tide calculations. Earth tides are calculated by using Cartwright's methods [Cartwright and Tayler, 1971; Cartwright and Edden, 1973] .

2.1.4 Free-air Correction

Subtracting the Gravity Reference Field and the affects of earth tides from the raw gravity values yields data with variations due to topography and lateral density inhomogeneities. To remove the effect of elevation, an adjustment known as the **free-air correction** is made. Gravity decreases with increasing distance from the center of the earth. This means that a correction must be added to the gravity value observed at an elevation above sea level. The correction factor is 0.3086 mgal/m. Accurate elevation control is essential for this correction.

2.1.5 Bouguer Correction

While the free-air correction removes the effect of elevation, it does not take into account the gravitational attraction of the rock between the observation point and sea level (hence the name 'free-air'). This gravitational attraction is removed by subtracting the **bouguer correction.** The bouguer correction is made by assuming a horizontal slab of infinite extent exists between the observer and sea level. The two factors required of this correction are: 1) the elevation, and 2) a density value for the slab.

The latter factor is a matter of some concern. The bouguer density should be matched closely to the average density of the rocks that may exist between the observation elevation and sea level. Most workers use 2.67 g/cc for their bouguer density. This is the average density of the earth's continental crust as a whole and it closely approximates the average density of granite. This value is well suited for this study because the crystalline rocks are mostly granitic in gross mineralogy [Hopson, 1964].

It is important to point out that the bouguer anomalies that result from the bouguer correction may be caused by two effects: 1) deviations between the densities of rocks that actually exist in the slab and the assumed bouguer density; 2) all rocks below the slab [Ervin, 1977]. This point cannot be overemphasized.

In this study, gravity values were reduced to sea level. The gravity effects of the anomalous densities within the bouguer slab were removed in the modeling routines. Gravity modeling will only be for anomalous densities below sea level. This technique avoids the aforementioned problems of the bouguer slab [Nettleton, 1976].

The bouguer correction with a bouguer density of 2.67 is 0.1119 mgal/m.

2.1.6 Terrain Correction

The bouguer correction assumes a flat slab. On the whole, this is a good approximation of the earth's topography. However, in moderate relief terrains, this approximation is no longer valid. Deep valleys or high mountains will exert some influence upon the observed gravity and cause deviations from the assumed bouguer slab. To correct for this affect, a variety of methods can be used. One of the most widely used methods is the Hammer Charts [Hammer, 1939].

Bouguer corrections used in conjuction with terrain corrections produce **complete bouguer anomalies**; without the terrain corrections, **simple bouguer anomalies** are produced.

In this study the relief was low. The maximum elevation was about 210 meters and the minumum elevation was about 60 meters above sea level. The maximum relief encountered was in the vicinity of Brooklandville where there was a 14 degree slope in a distance of 600 meters. This would amount to a maximum terrain correction of about 0.1 mgal. The maximum slope encountered on or adjacent to any of the roads in the study area was 5 degrees at Falls Road and Seminary Avenue. A terrain correction in this case would be negligible. Because all gravity stations were occupied along roads and, in the case of maximum relief, the terrain correction would have amounted to less than 1% of the total amplitude of the regional gravity, it was felt that the relief was low enough in the study area not to warrant this correction.

2.2 Fieldwork

2.2.1 Elevation Control

Because elevation is such a critical component in gravity reductions, accurate elevation data were essential for this investigation. Fortunately such data (second-order benchmarks) were available from the Baltimore City and Baltimore County Dept. of Public Works at an accuracy of +/- 0.08 meters. The public works departments use these data for the accurate location of sewage and water pipelines in this urban area. Survey field crews operate year-round to collect or update the elevation data collections. Most of these pipelines lie buried beneath major roads and thus most elevation benchmarks were along these roads. In general, these data became sparse further from the Baltimore City limits particularly to the north and west of the study area.

In Baltimore City, most elevation points were marked with a brass screw driven into the concrete of a curb or sidewalk. Other points were marked with benchmark disks. All were easy to find. Elevation points were often about 250 meters apart and were generally located near road intersections.

Baltimore County elevation points were far more diverse both in location and in type of benchmark. Many bridges and headwalls contained benchmarks which consisted of squares or crosses chiseled in the concrete. Some locations had benchmark disks. In many cases, USC&G[5] benchmarks and azimuth stations were used. In general, though, most elevation markers consisted of some type of metal spike either driven into road macadam or driven into the ground. The metal spikes were quite difficult to locate since they were often buried under soil or asphalt. The areal density of elevation points was more variable than for Baltimore City points, but benchmarks were usually about 250 to 400 meters apart.

During the survey, the baseplate for the gravity meter stood within 0.05 meters of the elevation point. A baseplate was used at every station.

Sections of the Phoenix Dome traverse had to be surveyed because inadequate elevation control existed. A Berger Transit and a level rod were used to accurately determine these elevations.

2.2.2 Gravity Station Occupation

Data collection was organized in the following manner. Each field day represented a complete loop.

---

[5] United States Coast & Geodetic Survey - now the National Geodetic Survey

Specifically, the Baltimore Base[6] was measured as the first and the last station of the day. LaCoste and Romberg Gravity Meter No. G-111 and Texas Instruments Worden Gravity Meter, Educator Model No. 476 (one or both) were used to measure the gravity value of each station. The time of day was noted at every gravity reading and was accurate to within 5 minutes.

[6] See Appendix A for specifics on this station.

2.3 Density Measurements

Whole rock densities of 167 representative samples from 10 different lithologies were measured in order to establish constraints on gravity models. Samples were cut into cubes of approximately 15 cubic centimeters and were then washed thoroughly with water. After the samples were dry, they were soaked in carbon tetrachloride and ultrasonically cleaned. Following this preparation, each sample was measured using two Kraus-Jolly Balances[7]. The liquid medium used was carbon tetrachloride[8]. Carbon tetrachloride was used because: 1) it is not reactive with the rocks; 2) it is a non-polar substance that has a low surface tension, thus it can easily penetrate the pores of the sample; 3) it evaporates quickly, thus speeding the time of sample measurement. Air was driven out of rock pores ultrasonically. Measurements were accurate to within 5%. The porosity of the rock will not affect the density obtained by this method because liquid fills the rock interstices. This is a good approximation of gross rock

---

[7] See Hurlbut and Klein [1977] for a more complete description of whole rock density measuring techniques using the Kraus-Jolly Balance.

[8] density of which is 1.545 g/cc

density for rocks in the study area because rock porosity in metamorphic terrains is generally less than 1% [Dingman and others, 1954; Ellis, 1909; Uhl, 1979]. This would make porosity less than the error in the measurement. Table 1-3 lists the results from the density measurements.

2.4 Computer Analysis

2.4.1 Gravity Reductions

All gravity reductions were completed using a complex computer program at the National Geodetic Survey in Rockville, Maryland. Raw gravity meter readings (in instrument dial units without the drift removed), the date, time of day, latitude, longitude, and elevation for each station were entered into the program. The program isolated traverse loops and removed instrument drift. Instrument dial units were converted to milligal units based upon a scale factor for each gravity meter and upon a known absolute gravity base station. The scale factors could either be entered into the program or determined by the program.

In this study, the LaCoste-Romberg gravimeter G-111 was known to have a history of high reliability. Its scale factor was well established[9]. The scale factor of the Worden gravimeter was determined by comparison with the LaCoste-Romberg gravimeter.

Once instrument dial units were converted to milligals, a weighting factor was entered into the

---

[9] The National Geodetic Survey keeps history files on all gravity meters run through this computer program.

program. The LaCoste-Romberg gravimeter had an estimated reading error of +/- 0.005 mgal as compared to the estimated reading error of +/- 0.05 mgal for the Worden gravimeter. Because the LaCoste-Romberg gravimeter is a more precise instrument both in its low reading error and its history of high reliability, it was weighted more heavily in all subsequent calculations. In a sense, when both meters were used at a single station occupation, the LaCoste-Romberg gravity meter was the major contributing meter and the Worden meter was used as a check upon it[10].

The data reduction was completed with the calculation of the absolute gravity, free-air anomaly, and simple bouguer anomaly values (Appendix B).

2.4.2 Description of IMGRAM and Modeling Methods

Gravity modeling was achieved using an interactive two-dimensional potential fields modeling program developed exclusively for this study. Because the program models two-dimensional profiles, gravity points which lie on a line (linear traverses) were isolated from the data set. The linear distance of each station from

---

[10] The calculated error for each station measurement was approximately 0.030 mgal when both meters occupied the station, 0.032 mgal when the LaCoste-Romberg meter alone occupied the station, and 0.070 mgal when the Worden meter alone occupied the station.

an arbitrary point of origin was measured along a traverse. Locations of geologic contacts were measured. These data were entered into the program in preparation for modeling.

It must be noted that any potential field method will produce a nonunique model [Dobrin, 1976; Nettleton, 1976].

Figure 2-1 demonstrates the various gravity profiles produced by simple models. Model A in Figure 2-1 was used in Figure 2-2 to demonstrate modeling ambiguities. Figures 2-2A and 2-2B show two different circumstances - three bodies are at one depth but have different densities and three bodies are at different depths but have the same density. These two circumstances generate the same set of gravity profiles. Theoretically, greater depth bodies of the same density will produce profiles with both a longer wavelength and a lower amplitude while bodies of decreasing density at the same depth will produce profiles with the same wavelength but a lower amplitude. Usually, however, it is not possible to make distinctions based on wavelength unless the body's density is accurately known. Figure 2-2C demonstrates that infinite combinations of depth and shape can produce the same gravity profile. Together, Figures 2-1 and 2-2 illustrate that a modeled body has three attributes, density, shape, and depth.

Geologic constraints help select particular density, shape, and depth attributes for a model. Important constraints needed for gravity modeling are:

- Surface geologic contact control;
- Accurate subsurface density control;
- Strike and dip control;
- Subsurface geologic contact control (e.g. drill holes).

Of these, density may be the most difficult to determine because of variations of density within one lithology. The ideal case for gravity modeling would be individual rock units with a uniform density distribution and large density contrasts. In reality, this is seldom the case. Facies changes and inhomogeneities in rock densities may present obstacles to modeling.

The computer program used in gravity modeling was named IMGRAM which is an acronym for Interactive Magnetics and Gravity Reduction And Modeling.

IMGRAM was written in the BASIC programming language and is fully documented. In its present configuration, the program can be implemented on either a DEC 20 computer or a PDP 11 computer.

IMGRAM uses a forward-type method to create gravity models of the subsurface. It incorporates many different polygon modeling techniques [Talwani and others, 1959; Talwani, 1965; Nagy, 1966; McGrath and Hood, 1970; Nabighian, 1972; Nabighian, 1974; Bhattacharyya, 1978; Murthy and Rao, 1979]. In the modeling procedure, the shape of a subsurface body is approximated by an n-sided polygon. A density is assigned to the polygon. By entering the vertices of the polygon, a gravity profile is calculated. It is compared with the observed gravity profile and the shape of polygon can be altered to improve the fit between the observed data and the profile calculated from the polygon.

An important assumption is made in two-dimensional modeling calculations: A polygon represents a tabular three-dimensional body that extends infinitely perpendicular to the plane of the profile. In most cases this is a realistic approximation.

2.4.3 Three-Dimensional Techniques

Two techniques were developed to calculate three-dimensional models of the subsurface: automatic 3-D gravity modeling and anomaly map interpretation.

2.4.3.1 Three-Dimensional Gravity Modeling

Various methods have been devised to produce three-dimensional gravity models [Talwani and Ewing, 1960; Cordell and Henderson, 1968; Bhattacharyya and

Figure 2-1: Gravity Effects of Various Bodies

Gravity anomaly profiles calculated from simple two-dimensional polygonal bodies with a positive density contrast. A) A square; B) An infinite slab (gravity profile generated is a step function); and C) An infinite wedge. Note that the gravity effects of all these bodies were calculated assuming the bodies extend infinitely perpendicular to the page.

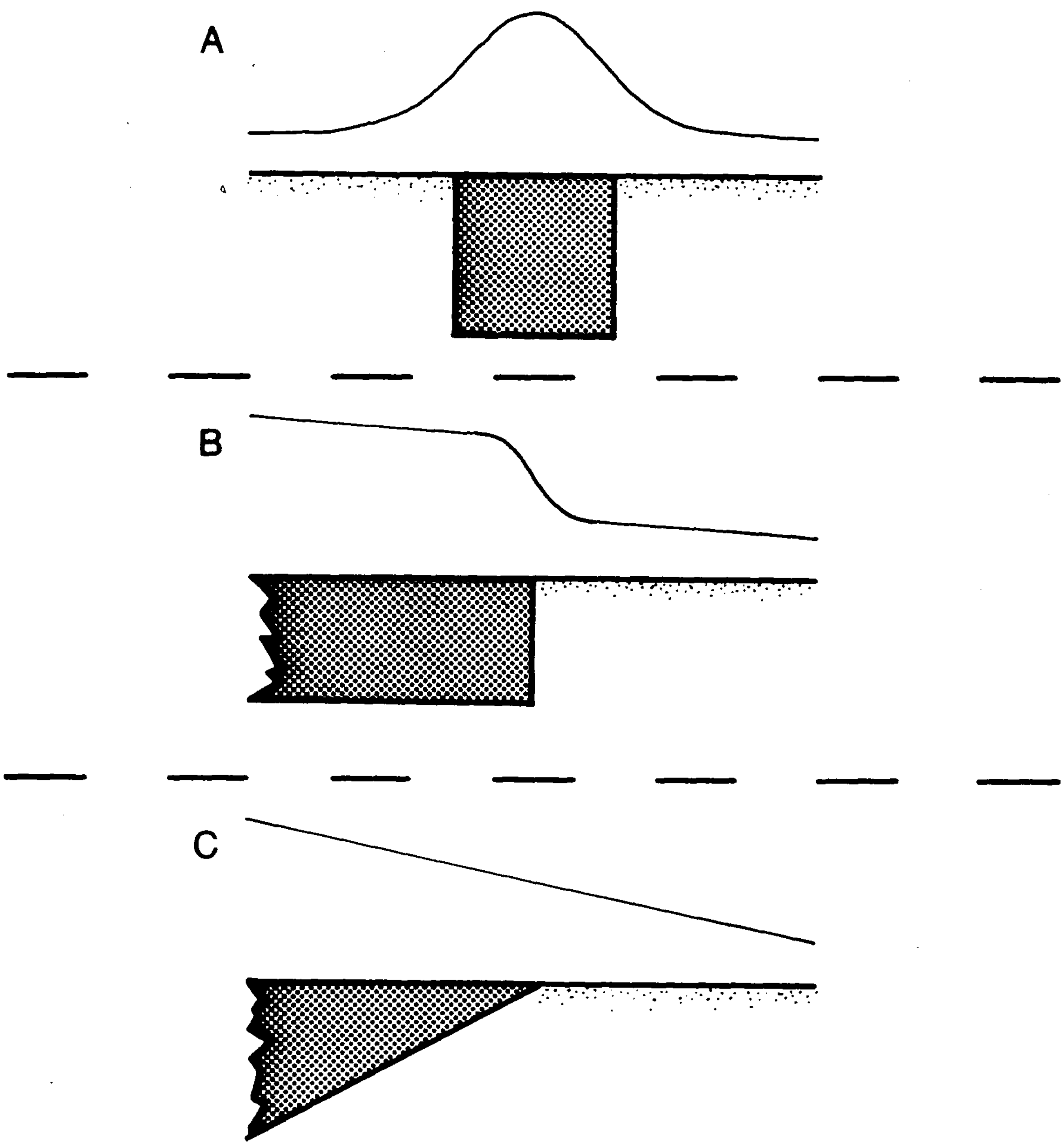
A
B
C

Figure 2-2: Gravity Interpretation Ambiguities

Interpretation ambiguities in the gravity anomaly profiles that result from different ways of modeling two-dimensional polygonal bodies with positive density contrasts. A) Varying the density contrast will produce differing gravity profiles from the same body. B) Varying the depth of the body while keeping the density and the shape constant will produce differing gravity profiles. C) Varying the shape and the depth of a body while keeping the density constant could generate the same gravity profiles. Note that all these gravity profiles were calculated assuming the bodies extend infinitely, in a tabular fashion, in the third dimension.

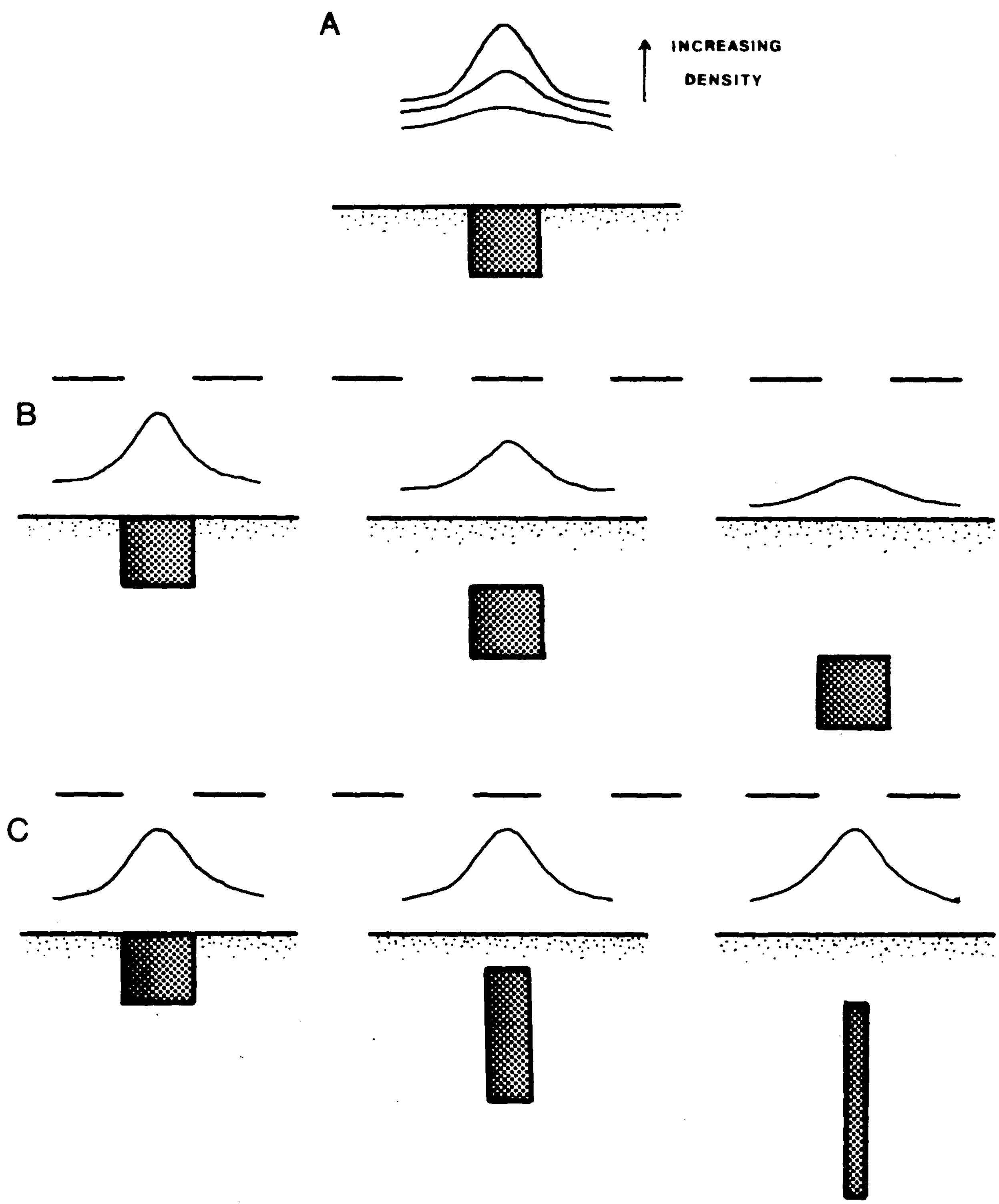
A
INCREASING
DENSITY
B
C

Navolio, 1975; Gerald and Debeglia, 1975]. Of these, the Talwani and Ewing [1960] is a forward-type routine, the others are inverse-type.

The Talwani and Ewing [1960] method requires that a model be entered into the program by first slicing the model into horizonal sheets and then by entering the vertices of the polygons defined on the horizontal surfaces. The thicknesses each sheet are then entered. A synthetic gravity map is calculated from the model.

This method can only operate on one body at a time. Further, it is a very tedious process to enter the shape of the model. For these reasons, the Talwani and Ewing [1960] approach was judged inappropriate for this investigation.

The other three-dimensional modeling methods [Cordell and Henderson, 1968; Bhattacharyya and Navolio, 1975; and Gerald and Debeglia, 1975] require that an observed gravity map be entered into the program and models of the subsurface are produced by iterative processes. Cordell and Henderson [1968] and Gerald and Debeglia [1975] use iterative techniques that generate models until a least-squares fit of a given correlation occurs. Bhattacharyya and Navolio [1975] use fourier transforms and deconvolution methods to calculate models that fit the observed gravity. The above three inverse-type modeling methods produce models that consist of vertical prisms floating on some type of surface at depth (analogous to various size blocks of wood floating in water).

The Cordell and Henderson [1968] method was attempted for the Chattolanee Dome gravity data. This method did not produce realistic geological results because only two lithologies could be represented in the model and the surface used to float the prisms could not be constrained for the Chattolanee Dome due to lack of subsurface data.

It was decided that three-dimensional subsurface structure in the study area could best be determined by utilizing two-dimensional profiles.

2.4.3.2 Anomaly Map Interpretation

The simple bouguer anomaly map for the Chattolanee Dome (Fig. 5-2) was used to interpret the subsurface structure. In this study, trend surface analysis was applied to the simple bouguer anomaly map for anomaly separation in order to isolate the sources of the gravity anomalies. [Davis, 1973; Till, 1974; Nettleton, 1976].

Trend surface analysis is a statistical method used to fit polynomial equation surfaces to the observed surface by a least-squares inversion. The more terms that are in the polynomial equation, the more complicated the trend surface is. A first-order trend surface is a flat plane, a second-order trend surface is a parabolic surface, and higher orders produce more complex trend surfaces. The object of the analysis is to discover the lowest order, statistically significant, trend surface that fits the mapped data.

The data that do not fit the trend surface (the residuals) are then examined separately. Presumably, the trend surface represents the regional, large scale signals in the data while the residuals represent local phenomena.

3. ANALYSIS OF DATA

3.1 General Comment on Linear Traverses

Gravity models of the subsurface are nonunique, therefore a special effort must be made to constrain the geophysics with the geology. The general philosophy used in all the models was to keep each model simple. The simple-shaped bodies that produced good profile matches were preferred over more complex-shaped bodies. This philosophy was used because complex models loose their significance due to the error limits of the gravity and density values, and the structural control. All traverse models were initiated using quadrilateral bodies and were systematically refined to produce the models which follow. Many of the models were extended beyond the length of the traverse in order to eliminate edge effects.

In general, at depths greater than 2500 meters, loss of resolution in the modeling method permits only the vaguest understanding of the structure. This limit depends upon many factors, particularly the density contrasts involved, the structural complexity, and the fact that the gravitational force decreases with the square of the distance.

3.2 Chattolanee Dome

3.2.1 Bouguer Gravity Map

During the summer of 1980, 431 gravity stations were occupied in the field area. Of these, 6 station values were discarded as erroneous (due to either misreading of instruments or inaccurately surveyed elevations), the values of 368 stations in a net pattern over a 160 square kilometer area were contoured to make the bouguer anomaly map over the Chattolanee Dome (Fig. 5-2), and 57 values come from a traverse over the Phoenix Dome. A listing of the 425 stations values is found in Appendix B.

The bouguer anomaly map displays the same trends that Bromery [1967b, 1968] reported. However, the station density in this study was far greater and thus the gravity map shows more detail[11].

In general, the bouguer anomaly map (Fig. 5-2) indicates a trough-like depression in the gravity field which has an axis that trends about N80W. Closer inspection of the map reveals that there is a linear 'wrinkle' on or near the trough axis that trends

[11] At any given location that was occupied both in this study and by Bromery, anomaly values differ by a few mgals. This is probably due to the Gravity Reference Field used in each study. Bromery used the now obsolete 1930 International Gravity Formula.

approximately N70W. This gravity lineament was even more intriguing since it trends through several local structural features noted by Crowley [1976b; 1977; and others, 1975].

A small fault was mapped by Crowley [1976b; and others, 1975] in the vicinity of the small town of Chattolanee in the north central part of the Chattolanee Dome. The trend of this fault was assumed to be N10W. A field check of this feature revealed that there is a small (unmapped) silicified breccia zone associated with the fault and this outcrop trends about N70W.

Along this N70W trend to the southwest, a slight topographic high occurs between the fault at Chattolanee and a fault mapped at the intersection of Old Court Road and Greenspring Avenue. A field check of this fault revealed the existence of another silicified breccia zone striking approximately N70W. Silicified breccia appears to grade into a quartz vein as the fault trends into the Baltimore Gneiss to the northwest (this may be one of the breccia zones noted by Broedel [1937]). Perhaps the topographic high between the two faults is caused by a vein of quartz that links the two faults.

It appears that the gravity lineament may indicate a high-angle west-northwest striking fault.

3.2.2 Geologic Map

Based upon data obtained in this investigation, a revised geologic map (Fig. 5-1) and a geologic column (Fig. 3-1) of the Chattolanee Dome were produced. The map represents a new interpretation of the geology based upon the geophysics.

A different stratigraphic grouping was used for modeling purposes (Table 1-2). Crowley's Sweathouse Amphibolite Member of the Oella Formation was included with the amphibolites of the Baltimore Mafic Complex (see page 21 for further explanation). Because of this new grouping, the southern contact of the Bare Hills serpentinite body is considered part of the Baltimore Mafic Complex as well (see page 23).

The eastern extent of the Chattolanee Dome is fault bounded based upon gravity models (see page 69).

The Greenspring Ave. - Old Court Rd. Fault and the fault at Chattolanee were reoriented parallel to the linear trends in the gravity along which occur the silicified fault breccias. The fault near the intersection of Old Court Rd. and Lightfoot Drive (southwest of the Greenspring Ave.- Old Court Rd. fault) was also reoriented to N70W based upon aerial photographic evidence.

The reentrant of Cockeysville Marble at Owings Mills was eliminated based upon a boring drilled near Reisterstown Rd. and Painters Mill Rd. in Owings Mills. The boring revealed schist bedrock [Muller, personal comm.] rather than Cockeysville [Crowley, 1976b and 1977].

The Wissahickon contacts at the southwestern section of the Chattolanee Dome (near Mount Wilson) were modified, based upon new reconnaissance mapping.

Figure 3-1: Generalized Geologic Column
of the rock units in the
vicinity of the Chattolanee Dome

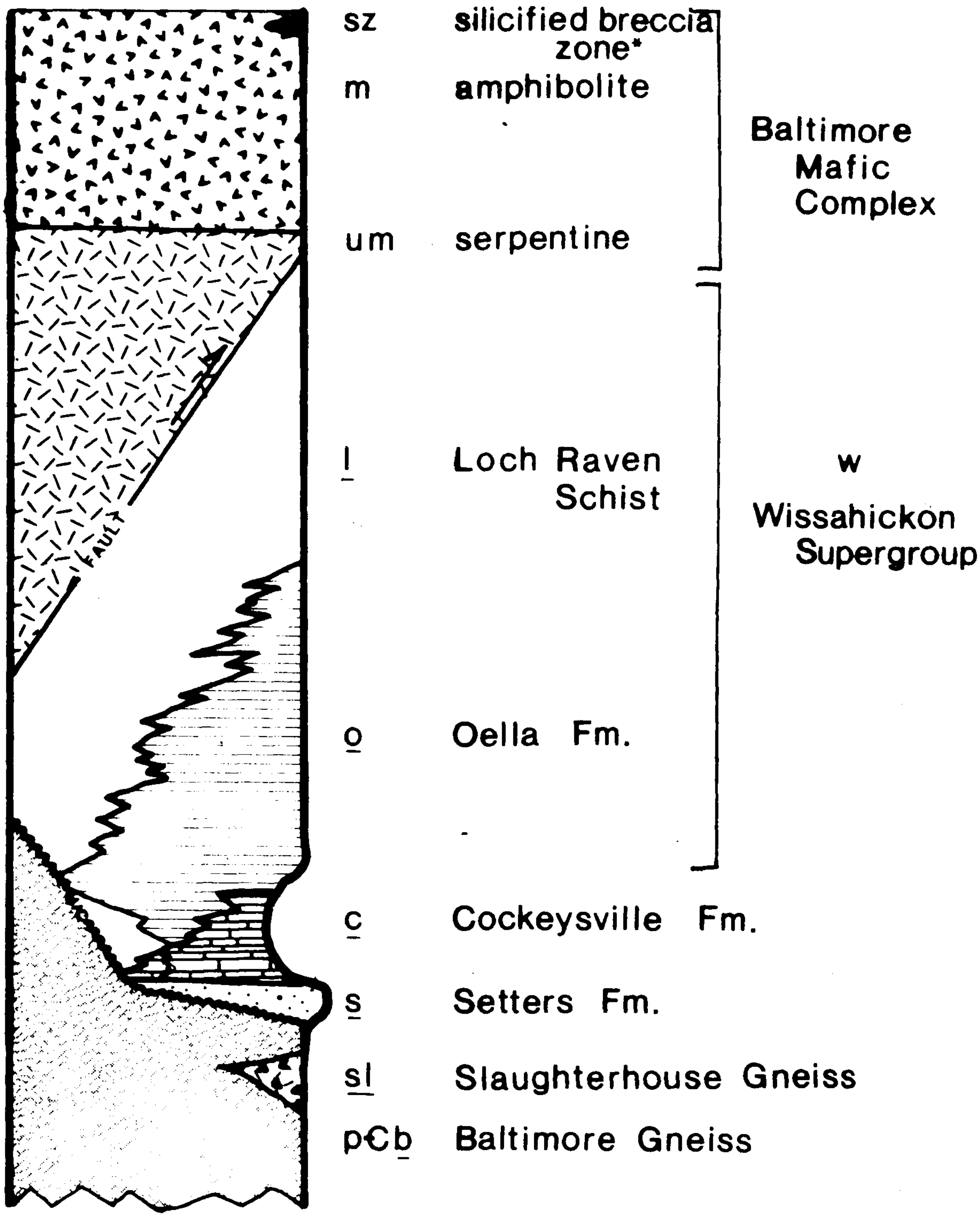

*OCCURS THROUGHOUT THE COLUMN

3.2.3 Trend Surface Analysis

A trend surface map was produced from the gravity data (Fig. 5-3). The best fit surface was obtained at 94% correlation between the observed map values and the calculated trend surface, using a second-order polynomial (a quadratic equation). The surface, in essence, was a smoothed gravity anomaly map. A low order trend surface at a high correlation indicates that the gravity anomalies were caused by a large, regional mass which has a gravity anomaly that overwhelms any smaller, more local variations in density inhomogeneities. It also suggests that the large regional event represents a relatively simple body. Residuals from this trend surface were small (averaging about 0.6 mgals) and were unmappable. These residuals probably represent random errors in the data rather than local events.

Examination of the 2nd order trend surface map revealed the following:

1. The shape of the trend surface matches closely the shape of the bouguer gravity. This is to be expected.

2. The trend surface forms a trough with the trough axis roughly parallel to the long axis of the Chattolanee Dome in the east and angles northward in the west.

3. The shape of the trend surface indicates that there is a wedge of high density material thickening westward under the dome. This is evidenced by the dip of the trough axis.

4. The trough, itself, is probably due to the low density material that makes up the core of the Chattolanee Dome (i.e. Baltimore Gneiss).

3.2.4 North-South Gravity Traverses

Three north-south gravity traverses - the Reisterstown Road Traverse, the Stevenson Road Traverse, and the Greenspring Avenue Traverse - are roughly parallel to each other and are approximately perpendicular to the long axis (east to west) of the Chattolanee Dome (Fig. 5-4). The Reisterstown Road Traverse was the westernmost model completed for the Chattolanee Dome. It runs southeast to northwest and it crosses the dome axis at about a 45 degree angle. The Stevenson Road Traverse crosses the Chattolanee Dome directly perpendicular to the long axis of the dome. The Greenspring Avenue Traverse is roughly parallel and east of the Stevenson Road Traverse. All three traverses cross the same general structure and lithologies, however, on the southern side of the Chattolanee Dome, the Cockeysville Formation is locally absent. The Slaughterhouse Gneiss is crossed only by the Greenspring Avenue Traverse.

The models for these three traverses (Figs. 3-2, 3-3, and 3-4) were calculated. As indicated by the trend surface analysis (page 55), a wedge of higher density rock occurs underneath the dome. Models calculated without the higher density rock beneath the dome produced profiles with lower gravity values than observed. Two major ambiguities exist when this wedge of rock is modeled: 1) The lithology (i.e. the density) of the wedge is uncertain. The wedge was assumed to contain Wissahickon lithologies because the Wissahickon is the most extensive high density rock unit in the study area. 2) The shape, depth, and thickness of the wedge cannot be determined (see Fig. 2-2C). This is because no surface or subsurface control exists. The wedge appears to thin to the east. This is apparent from the bouguer gravity map (Fig. 5-2) and the 2nd order trend surface map (Fig. 5-3) of the Chattolanee Dome. These two maps show a regional trough that dips to the east.

The three models across the dome indicate that the Baltimore Mafic Complex overthrusts the Wissahickon on a surface that dips about 45 degrees to the south. This is very clear from the model calculations and it is well constrained since the density contrast between the Baltimore Mafic Complex amphibolites and the Wissahickon rocks is large (0.084 to 0.246 g/cc). Structures under the mafic complex are less clear, especially to the south where the complex thickens. The steep observed gravity gradient over the mafic complex overwhelms signals from structures below the complex.

The Setters Fm., the Cockeysville Fm., and the Wissahickon Group rocks all appear to mantle the

Baltimore Gneiss at a rather steep dip. The dip (apparent dip) is shallower north of the dome in the Reisterstown Road Traverse (Fig. 3-2).

Based on the modeling, the Slaughterhouse Gneiss (Fig. 3-4) cannot be any thicker than 200 meters, due to its large negative density contrast with respect to the Baltimore Gneiss (-0.077 g/cc).

3.2.5 Falls Road I Traverse

The Falls Road I Traverse runs northward from Mount Washington to Brooklandville in the valley that separates the Chattolanee Dome from the Towson Dome (see Fig. 5-4).

According to the model (Fig. 3-5), the valley is floored by a thin sequence of metasediments (no thicker than 700 meters). The Loch Raven and Oella rocks thicken and dip to the south. This is in accord with the geologic control which indicates that a syncline with a plunge axis to the south occurs in the valley [Mathews and Miller, 1905; Crowley and others, 1975]

The mafic complex overthrust contact (at about a 30 degree angle) can be clearly delineated in this model. The Bare Hills serpentinite body is clearly related to the Baltimore Mafic Complex and it seems to lie along the overthrust. The density contrast between serpentine and amphibolite is very large (0.358 g/cc) resulting in a high confidence for this relationship.

Figure 3-2: Gravity Model of the Reisterstown Rd. Traverse

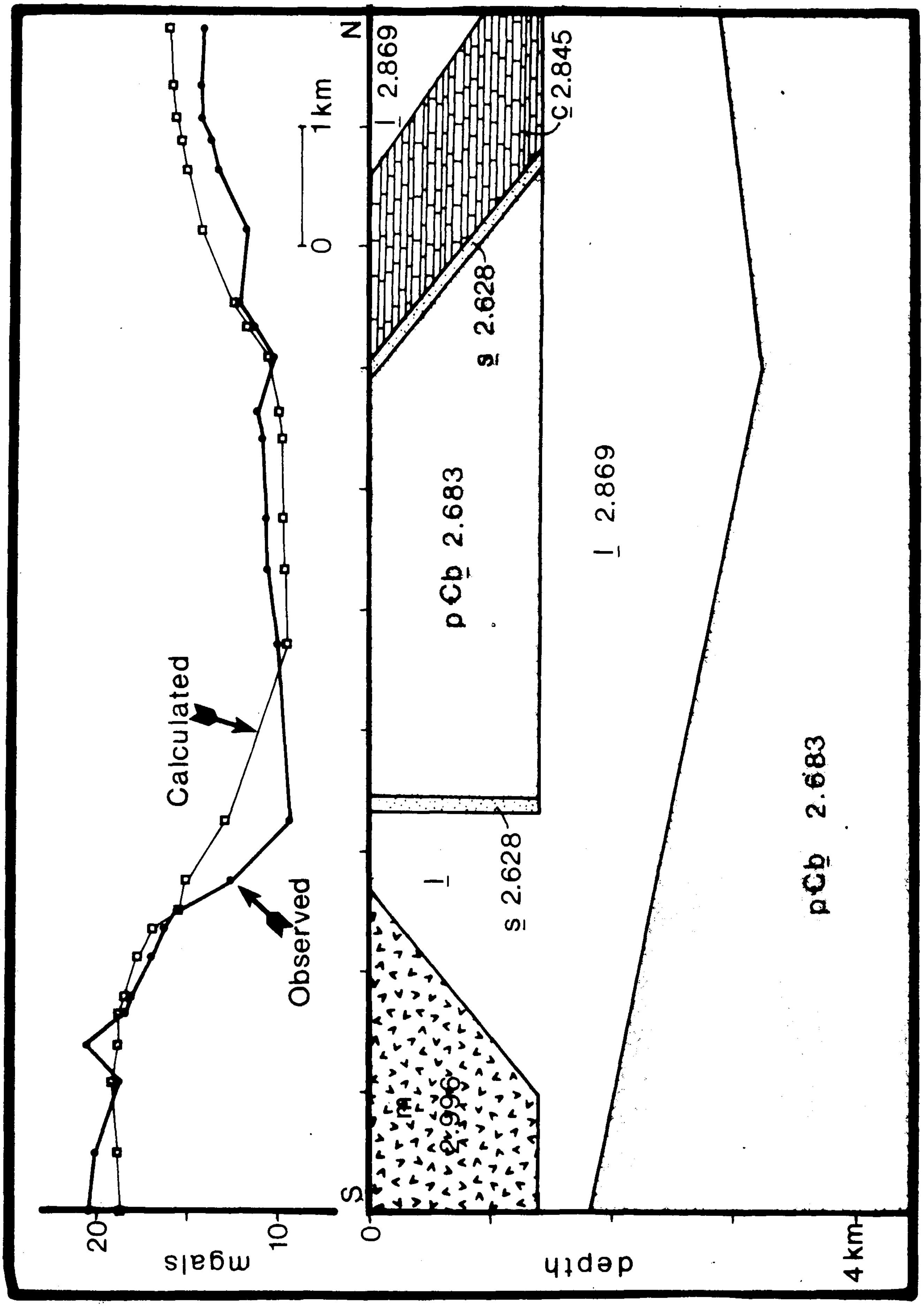
Calculated
Observed
mgals
20
10
depth
0
4 km
S
N
0
1 km
m 2.996
l
s 2.628
pЄb 2.683
l 2.869
s 2.628
c 2.845
l 2.869
pЄb 2.683

Figure 3-3: Gravity Model of the Stevenson Rd.
Traverse

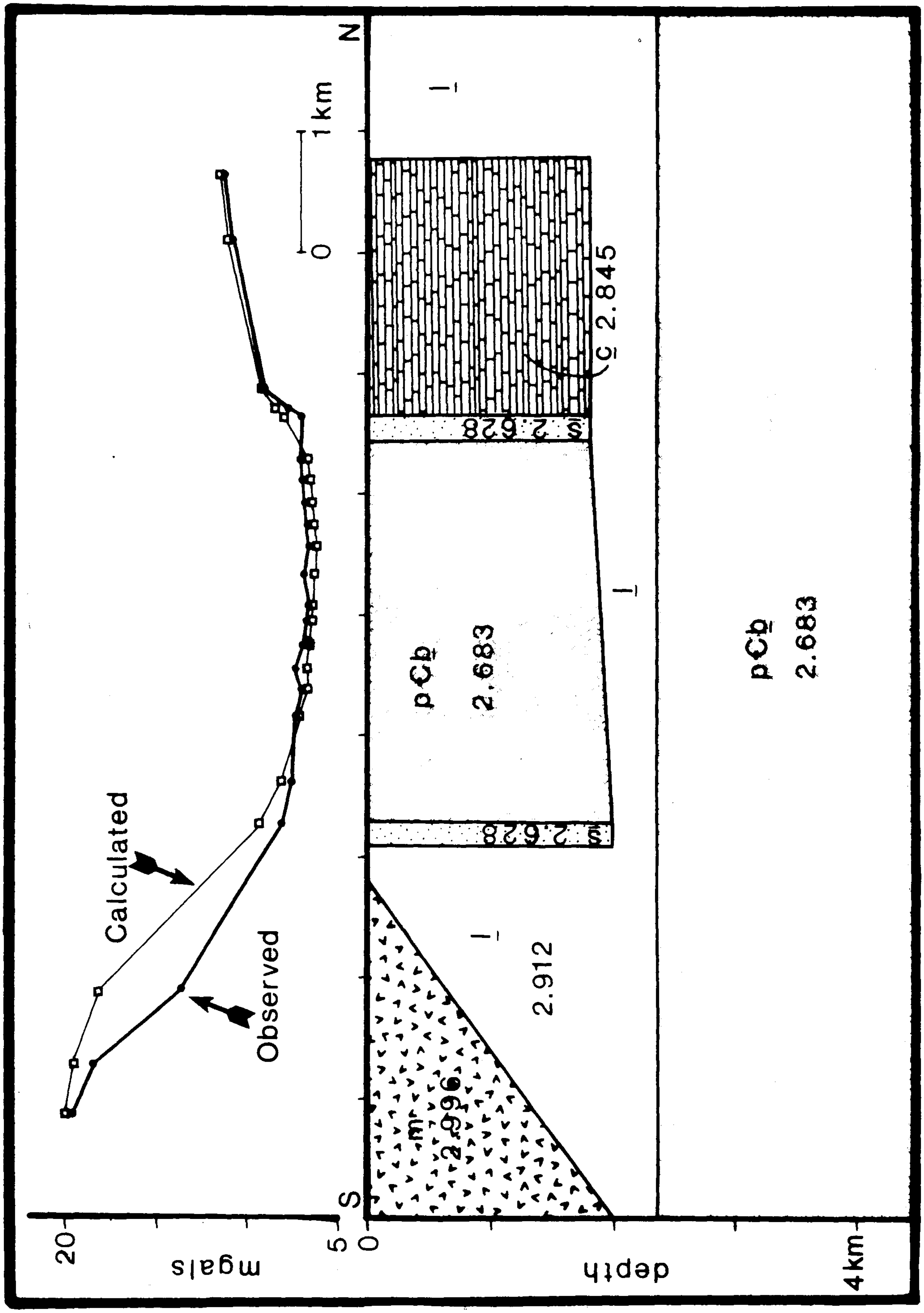

Calculated
Observed
mgals
20
5
0
depth
4 km
S
N
0
1 km
m 2.996
l 2.912
s 2.628
pCb 2.683
s 2.628
c 2.845
l
l
pCb 2.683

Figure 3-4: Gravity Model of the Greenspring Ave. Traverse

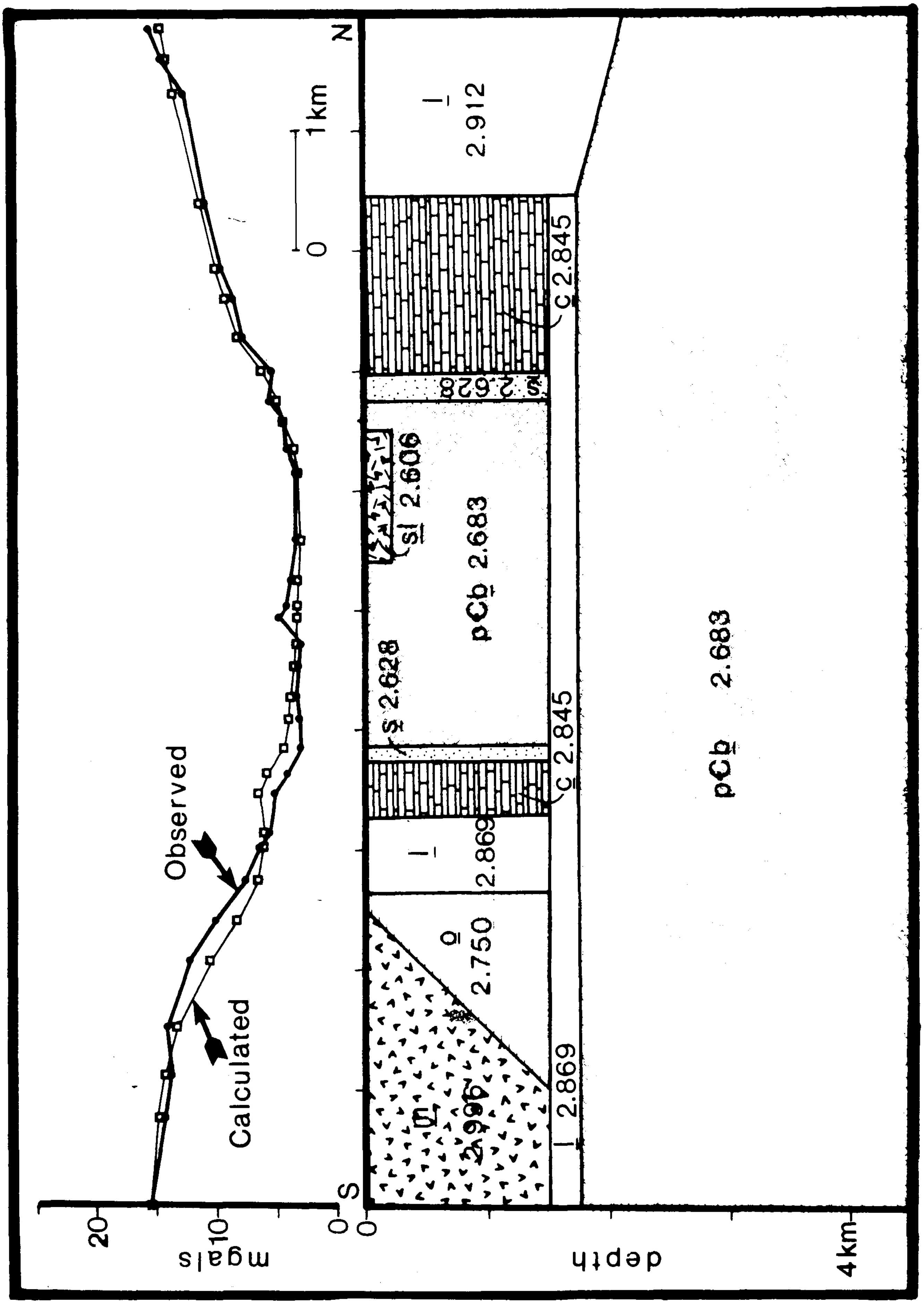

mgals
20
10
0
S
N
Observed
Calculated
0
1km
depth
4km
2.996
Ω 2.750
2.869
Ⅰ 2.869
c 2.845
s 2.628
sl 2.606
pЄb 2.683
s 2.628
c 2.845
Ⅰ 2.912
pЄb 2.683

Figure 3-5: Gravity Model of the Falls Rd. I Traverse

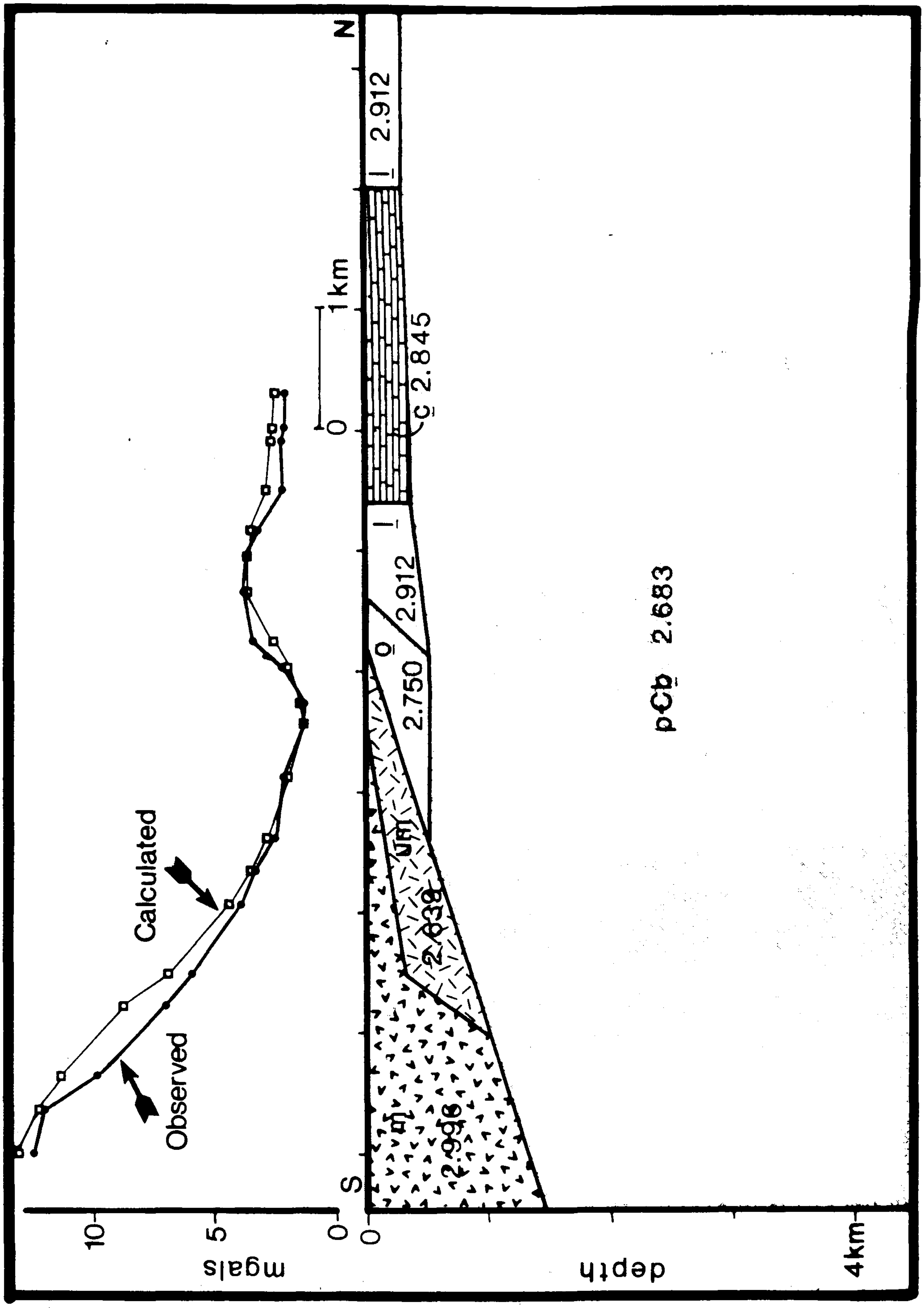
Calculated
Observed
mgals
10
5
0
depth
0
4km
S
N
0
1km
2.912
2.845
2.912
2.750
2.683

3.2.6 Keyser Road Traverse

The Keyser Road Traverse trends east-west and is approximately parallel to the long axis of the Chattolanee Dome. This traverse crosses from the Chattolanee dome into the valley between the Chattolanee and the Towson Domes (Fig. 5-4).

The gradient of the observed gravity (Fig. 3-6) is similar to the gravity effects of a wedge (Fig. 2-1C). This is further verification that a westward-thickening wedge of high density rock underlies the Chattolanee Dome. However, the shape, density, and depth of the wedge cannot be constrained for reasons previously discussed (see page 58). In this model, a Wissahickon lithology (density) is assumed.

Again, the Slaughterhouse Gneiss cannot be modeled any thicker than 200 meters because of its large negative density contrast with the Baltimore Gneiss. The Slaughterhouse Gneiss appears to form only a thin sheet in the Baltimore Gneiss.

The valley between the Chattolanee and Towson Domes can be modeled as a syclinal structure, in accordance with the structural control.

Crowley's map [Crowley, 1976b; Crowley and others, 1975] shows the eastern end of the Chattolanee Dome truncated by an unconformity. While there is no good exposure of this contact, it could also be interpreted as a fault since a relatively thick section of Setters appears to be missing and the contact is suspiciously linear.

The model indicates that the latter interpretation may be correct.

3.2.7 Ruxton Fault Traverse

The Ruxton Fault was first recognized by Mathews and Miller [1905] as a N-S fault which truncates the western end of the Towson Dome. They suggested that the fault was a low-angle thrust fault with a dip to the east. Mathews and Miller do not provide a clear explanation why they interpret the fault as eastward dipping. Broedel [1937] believed that the Ruxton Fault was a high-angle normal fault. This was based upon the attitude of the silicified breccias near Lake Roland. A traverse was made across the fault to attempt to determine its attitude (Fig. 5-4).

Despite the apparent deviations between the observed gravity and the gravity calculated from the model of this traverse, the two gravity profiles are in close agreement (Fig. 3-7). The apparent deviations are due to an enlargement of the gravity scale.

The eastern section of the Ruxton Fault Traverse which is over the Towson Dome displays the same

Figure 3-6: Gravity Model of the Keyser Rd. Traverse

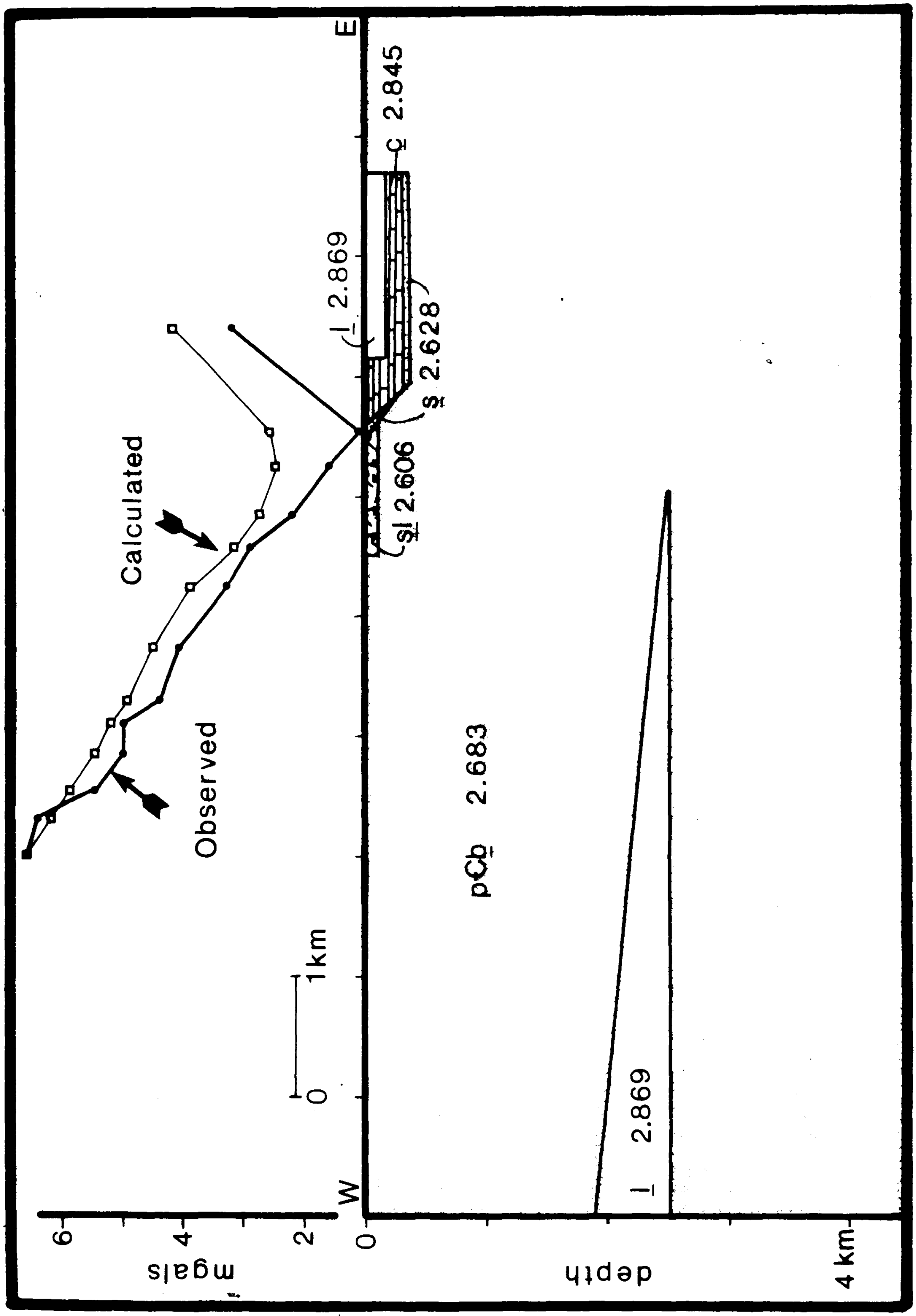

mgals
6
4
2
0
depth
4 km
W
E
0
1 km
Calculated
Observed
pC̲b̲ 2.683
l̲ 2.869
2.869
l̲
c̲ 2.845
s̲ 2.628
s̲l̲ 2.606

relationship as in Fig. 2-1C. The model, therefore, must have a wedge of higher density rock underlying the Towson Dome. This high density rock is probably Cockeysville since this is the same rock that underlies the valley between the Chattolanee and the Towson Domes. The Ruxton Fault is best modeled as a vertical fault which truncates the Cockeysville wedge. An alternative approach would be to model the upper surface of the Cockeysville wedge under the Towson Dome reaching the surface as the Ruxton Fault, however a poor match results between the observed data and the calculated values in this case. The upper surface of the Cockeysville wedge must occur deeper than 100 meters below sea level.

Models of the Ruxton Fault may have difficulties due to rock bodies outside the plane of the traverse affecting the observed gravity, however, geological arguments also support a high angle fault. The Ruxton Fault in map view remains a linear feature as it crosses variations in the topography. If it were a low angle fault, its trace would be more irregular.

As demonstrated in the Falls Road I Traverse and the Keyser Road Traverse, the valley between the Chattolanee and Towson Domes is floored by metasedimentary rocks no thicker than 700 meters. Furthermore, the Ruxton Fault Traverse model clearly displays the synclinal structure of the valley. It appears that the syncline is overturned to the east.

Except for the thin metasedimentary cover in the valley between the two domes, Baltimore Gneiss (or any other granitic rock with a similar density) can be modeled as extending downward infinitely. Realistically, however, structures at depths greater than about 6 km. cannot be distinguished in this model.

3.2.8 Miscellaneous Traverses

Other traverses were modeled but are not presented because they did not compare in quality to the above traverses. In general, they either had 1) irresolvable ambiguities, 2) bodies from out of the plane of the profile affecting the observed gravity, or 3) could not be modeled with simple or geologically reasonable bodies. These miscellaneous traverses were:

- Two traverses along Falls Rd. which connected the Falls Rd. I Traverse to the south with the Phoenix Dome Traverse in the north: These could not be modeled due to poor subsurface contact control and due to bodies out of the plane of the profile affecting the observed gravity.

- A traverse along Lyons Mill Rd. from Deer Park Rd. to Painters Mill Rd.: This traverse crossed the western nose of the Chattolanee Dome. It simply did not produce geologically meaningful results. This was probably due to bodies out of the plane of the profile.

- A traverse along Painters Mill Rd. from Winands

Figure 3-7: Gravity Model of the Ruxton Fault Traverse

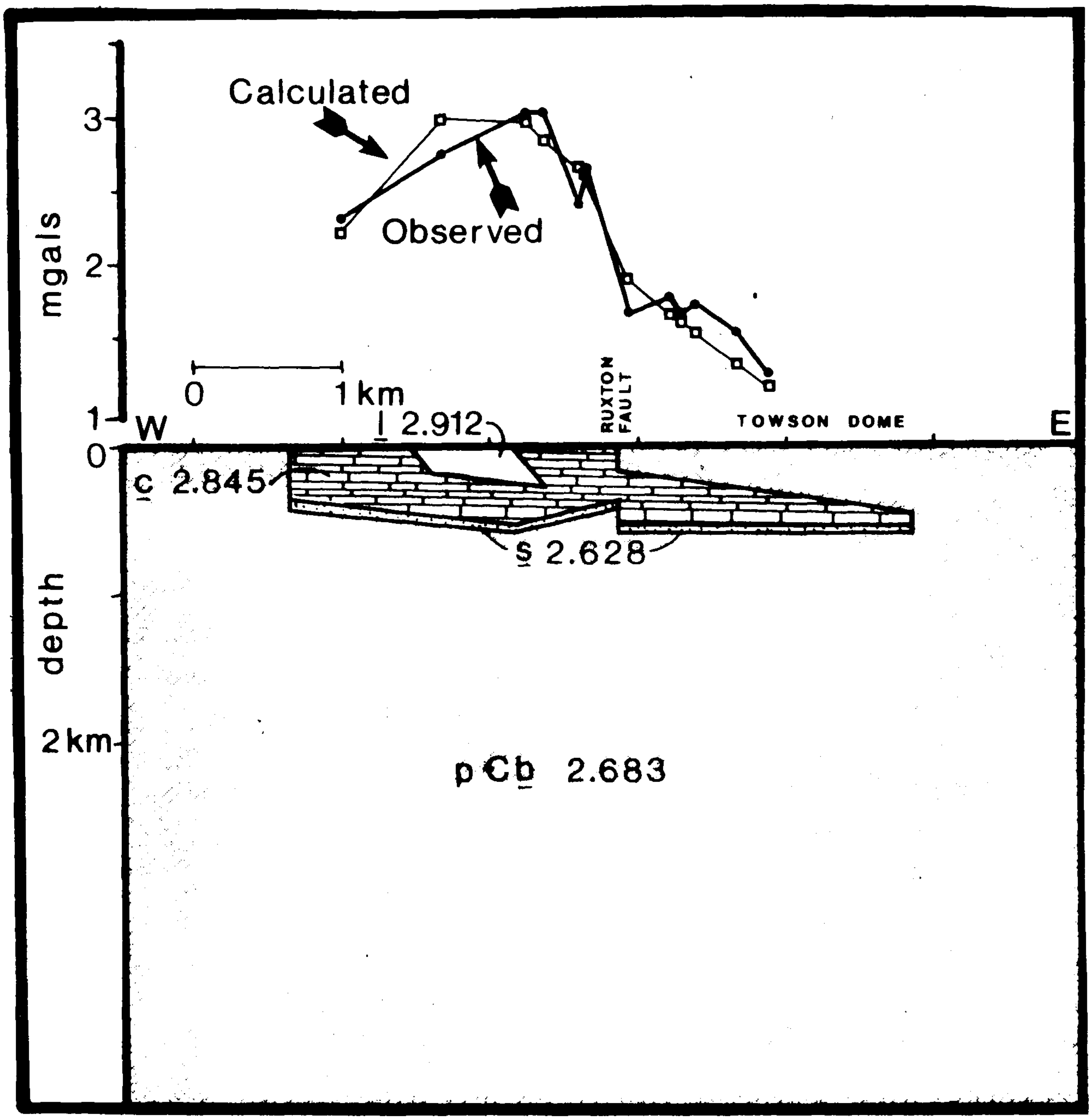

Calculated
Observed
mgals
3
2
1
0
1 km
W
l 2.912
RUXTON FAULT
TOWSON DOME
E
c 2.845
s 2.628
depth
2 km
pCb 2.683

Rd. to Reisterstown Rd.: This traverse was approximately north-south at the west end of the dome. The traverse did not produce meaningful results probably due to bodies out of the plane of the profile and due to poor subsurface contact control.

In general, traverses in the western half of the Chattolanee Dome were of poorer quality than those of the eastern half. This was because there was better station density and geologic controls in the eastern section.

3.3 Phoenix Dome Traverse

The Phoenix Dome is approximately 10 kilometers north of the Chattolanee Dome. The structure of the Phoenix Dome has been interpreted as a rooted dome [Broedel, 1937] and the bottom limb of a rootless nappe [Crowley, 1976a and b; Fisher and others, 1979]. Remapping of the Phoenix Dome is currently in progress [Muller, in prep.].

The gravity traverse was made along Falls Rd. from Miller Rd. to Coopersville. The geology in the area is quite complicated (Fig. 5-5). The rocks along the traverse all dip to the north at a fairly steep angle. Exceptions to this trend are the rocks at the southern side of the dome in Worthington Valley which dip steeply to the south [Muller, personal comm.]. Another exception to this trend occurs east of Falls Rd. just south of Butler. The rocks dip to this south locally in this area, probably because they are locally overturned [Muller, personal comm.]. The Cockeysville Formation is repeated four times along Falls Road northward from Shawan to Coopersville. Further complications arise due to lithologic changes along strike of the Setters Formation [Fisher, 1971].

A simplified version of Muller's geologic map of the Hereford Quadrangle [in prep.] contains the most up-to-date structural control for this traverse (Fig. 5-5). Four different interpretations of the subsurface structure of the Phoenix Dome can be derived based upon these data (Fig. 3-8). These four interpretations assume that folding (rather than faulting) is the chief large-scale style of deformation. Faulting appears insignificant in this section of the Phoenix Dome; field evidence for large faults is lacking and where faults do occur on a local scale, displacements seem small.

The general strategy used in determining the subsurface structure of the Phoenix Dome was to input each of the four different models to see which model produced the best fit with the observed gravity. High resolution modeling was not attempted since it was felt that not enough constraints were available, particularly density control.

3.3.1 Model 1

Model 1 is that of a rooted dome with a syncline on the roof of the dome. This model produced a very poor match (Fig. 3-9). The main problem with this model is that there is too much low density Baltimore Gneiss present in the core of the dome. This produces a gravity profile that is lower than the observed profile. Increasing the density of the Baltimore Gneiss within the density error limits did not significantly improve the

Figure 3-8: Diagram of Possible Structures of the Phoenix Dome

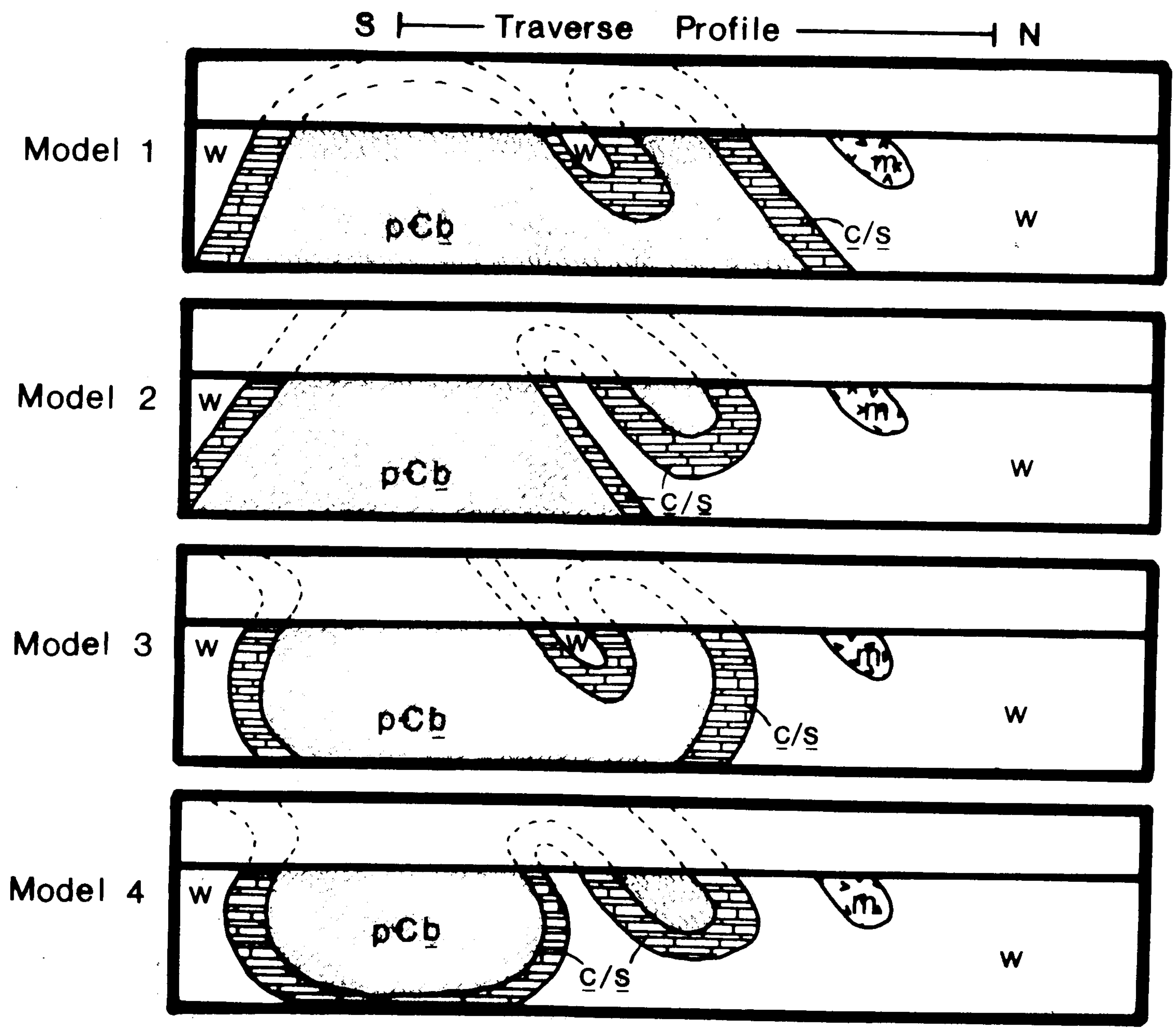
S
Traverse Profile
N
Model 1
Model 2
Model 3
Model 4
w
pC̶b
c/s
m

Figure 3-9: Gravity Model of the Phoenix Dome
Traverse-Model 1

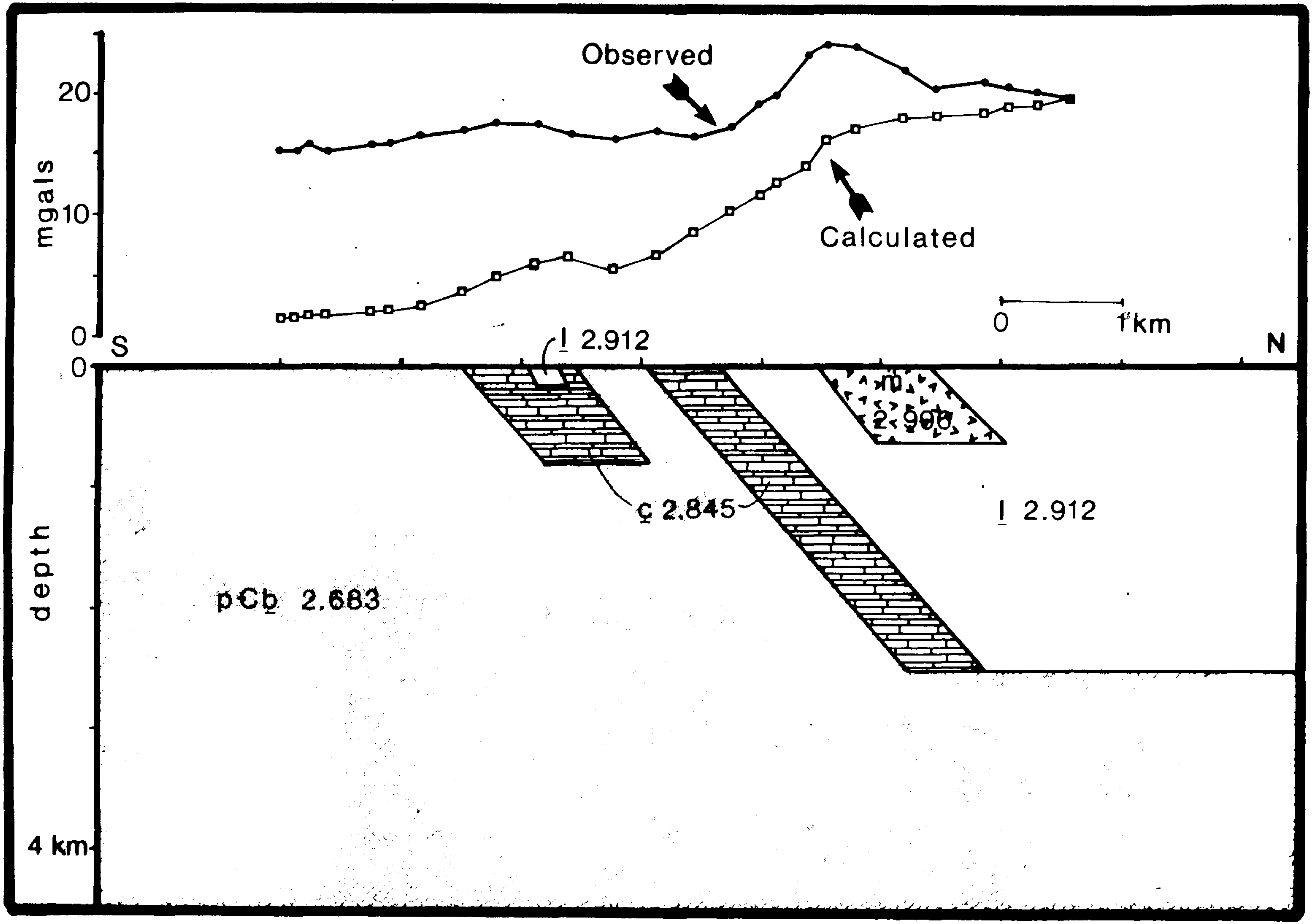

Observed
Calculated
mgals
20
10
0
S
N
0
1 km
depth
4 km
I 2.912
c 2.845
I 2.912
pCb 2.683

fit.

3.3.2 Model 2

Model 2 is a rooted, overturned nappe. It produces another poor match between the calculated and observed data for precisely the same reasons as was the case in Model 1 (Fig. 3-10). A better match was achieved, however, over the inlier zone. The low density mass Baltimore Gneiss in the southern end of the traverse again causes a much lower gravity than was observed.

The structure of the Phoenix Dome does not appear to be rooted, as demonstrated by the poor fit of the gravity data to profiles calculated from Models 1 and 2. For this reason, rootless structures (Models 3 and 4) were tried. Rootless structures imply that a body of higher density material exists under the low density Baltimore Gneiss. This high density mass was assumed to be one of the Wissahickon units, specifically the Loch Raven Schist. This assumption is based upon Bromery's [1967a and 1968] data that suggest that a material with a high magnetic susceptibility exists beneath the dome. The Loch Raven Schist fits both these density and the magnetic constraints.

Figure 3-10: Gravity Model of the Phoenix Dome Traverse-Model 2

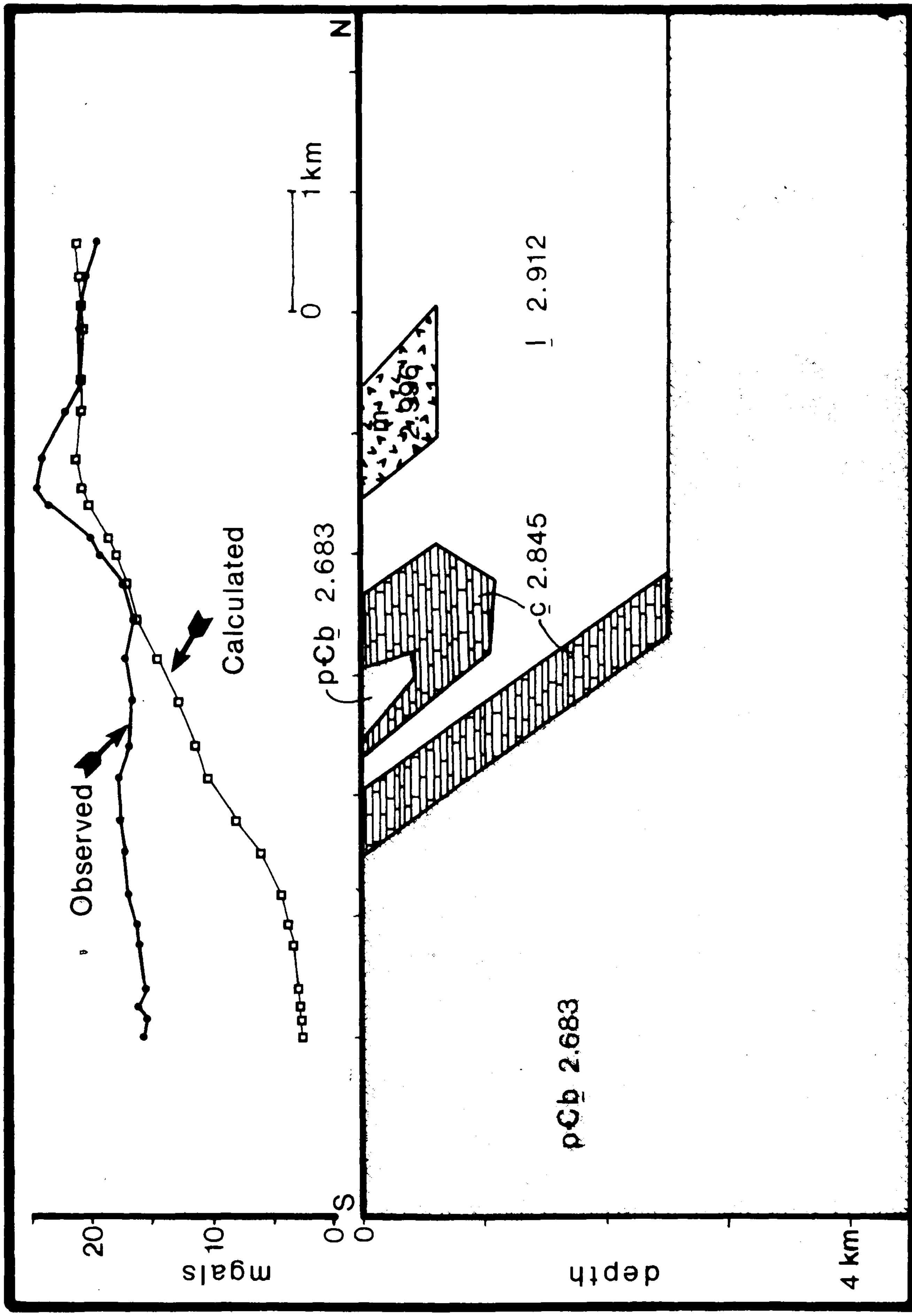
Observed
Calculated
1 km
0
N
S
pЄb 2.683
c 2.845
l 2.912
2.996
mgals
20
10
0
depth
4 km

3.3.3 Model 3

Model 3 represents the top limb of a rootless nappe. The gravity profile produced fits the observed gravity fairly well. The bottom limb of this structure has to occur rather deep so that Baltimore Gneiss can completely surround the inlier. This results in a lack of mass (too much Baltimore Gneiss) at the southern end of the traverse and a large excess of mass (too much Loch Raven Schist) at the northern end of the traverse. Even if the bottom limb of the structure is brought up to a depth of 1.5 km. - the shallowest it can be made and still fit the geological constraints - the situation remains the same.

3.3.4 Model 4

Model 4 represents a bottom limb of a rootless nappe. It produced the best fit among all the models (Fig. 3-12). This model demonstrates that the western end of the Phoenix Dome is best interpreted as a rootless structure.

Figure 3-11: Gravity Model of the Phoenix Dome Traverse-Model 3

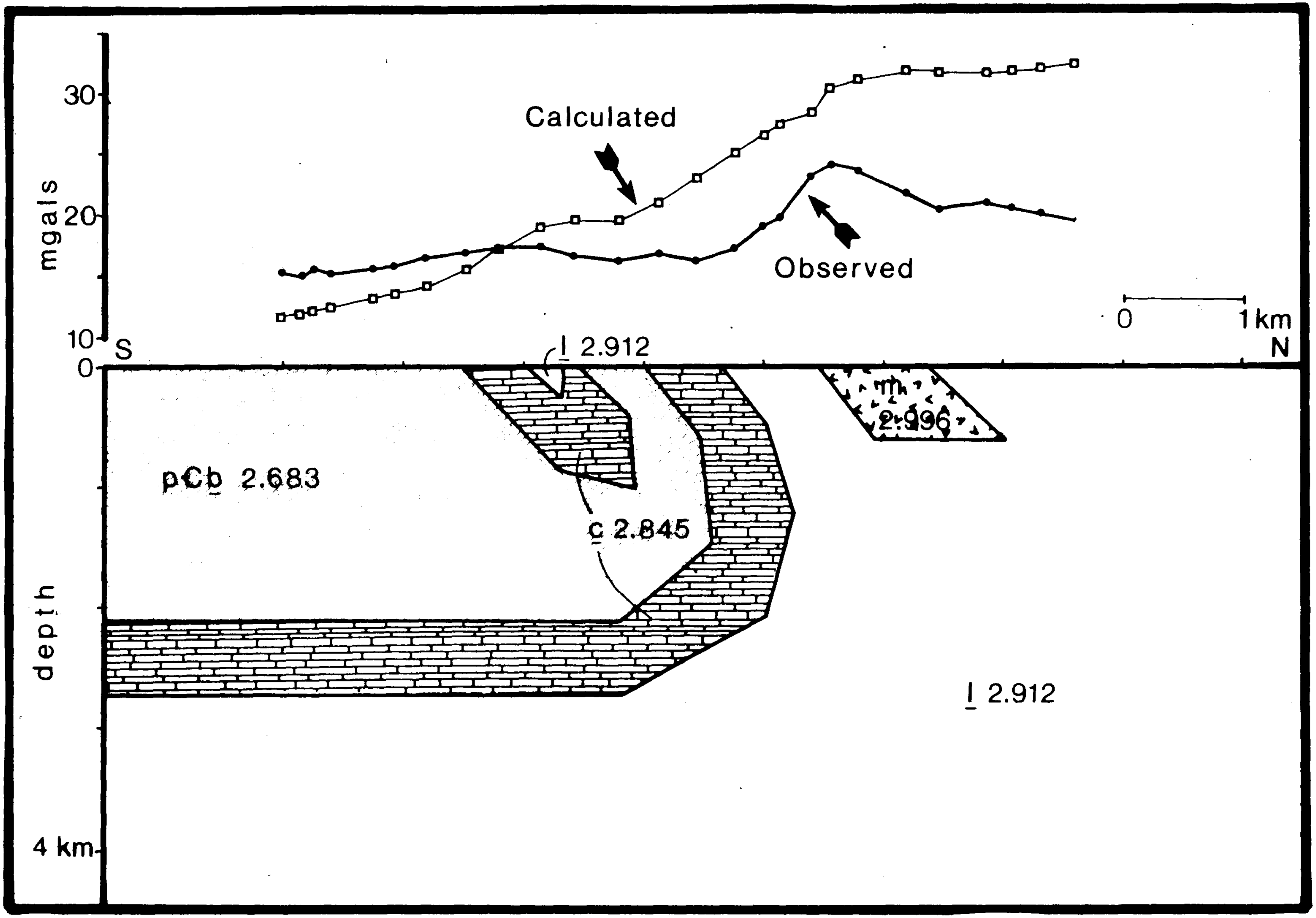

mgals
30
20
10
Calculated
Observed
0
1km
S
N
0
depth
4 km
l 2.912
pCb 2.683
c 2.845
m
2.996
l 2.912

Figure 3-12: Gravity Model of the Phoenix Dome Traverse-Model 4

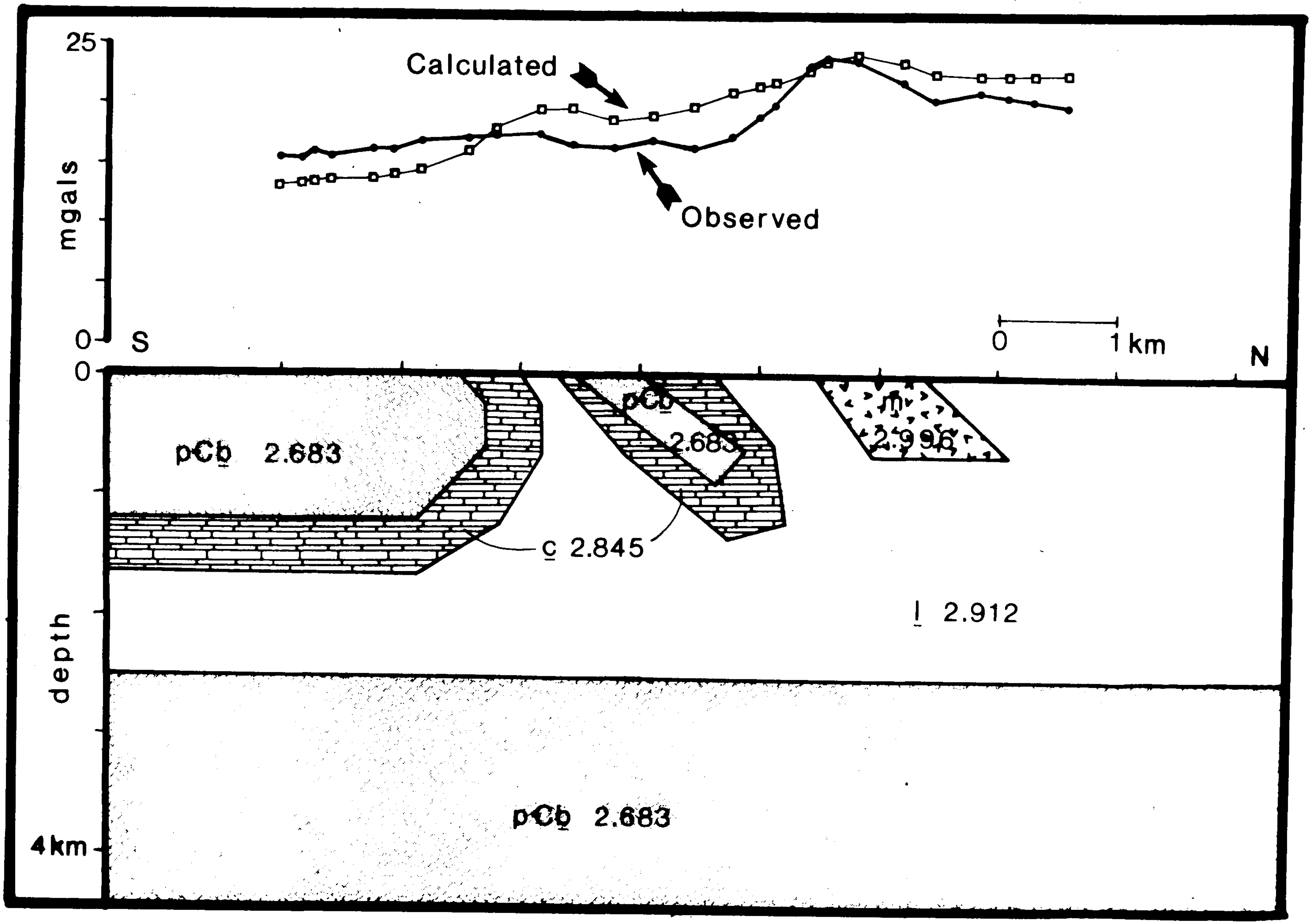

25
mgals
0
Calculated
Observed
S
N
0
1 km
0
depth
4 km
pCb 2.683
pCb
2.683
m
2.996
c 2.845
l 2.912
pCb 2.683

4. DISCUSSION

Some specific conclusions can be drawn concerning the subsurface structure of the Chattolanee Dome, the Phoenix Dome, and the Towson Dome.

The Phoenix Dome appears to be a nappe-like structure. Assuming no major faults are present, the structure in the western end of the dome is probably that of a bottom limb of a rootless nappe. The long axis of the Phoenix Dome trends approximately N70E. The nappe movement was most likely perpendicular to this trend and the gravity models indicate a root zone to the south.

The location of the root zone for the Phoenix Dome may be the Chattolanee Dome. If this is the case then the kidney-shaped outcrop of Cockeysville north of the Chattolanee Dome (known as "The Caves"; see Fig. 5-1) is not an anticline as Crowley [1976a; 1977; and others, 1975] suggests but rather a syncline comprising of a thin sliver of marble from the overturned bottom limb of the Phoenix Nappe (Fig. 4-1A).

It is also possible that there is no structural tie between the Phoenix Dome and the Chattolanee Dome. In this case (Fig. 4-1B), the Phoenix Dome may be rooted to the south under the Chattolanee Dome and the Chattolanee Dome is stacked on top of the Phoenix Nappe. Unfortunately, neither Fig. 4-1A nor Fig. 4-1B can be resolved with the geophysical data because of poor results along Falls Road (see page 73). Structural data is also ambiguous and can support many interpretations [Muller, personal comm.]. The Chattolanee Dome is indeed anticlinal at or near the surface. It appears to be rooted to the east with the root zone beneath the valley between the Chattolanee Dome and the Towson Dome. The western end of the Chattolanee Dome is underlain by a wedge of metasediments. This wedge could be either fold related or fault related (Fig. 4-2). The geophysical evidence is inconclusive. It seems that other thrust faults would be parallel to the wedge if indeed the wedge is due to faulting. The westward thickening wedge of Cockeysville underlying the Towson Dome may signify a parallel, imbricate fault.

If an episode of large-scale, low-angle imbricate faulting has occurred in the Baltimore Gneiss Dome terrain, some of these faults must intersect the surface and should be seen in the geology. In the case of the Chattolanee Dome, a fault trace should occur in Wissahickon rocks at the western end of the dome if this theory is correct. Field work in the southwestern end of the Chattolanee Dome near Mount Wilson located no faults however, exposure is very limited.

Another explanation for the wedge-shaped bodies

Figure 4-1: Hypothetical Southeast-Northwest Profile Through the Chattolanee and Phoenix Domes

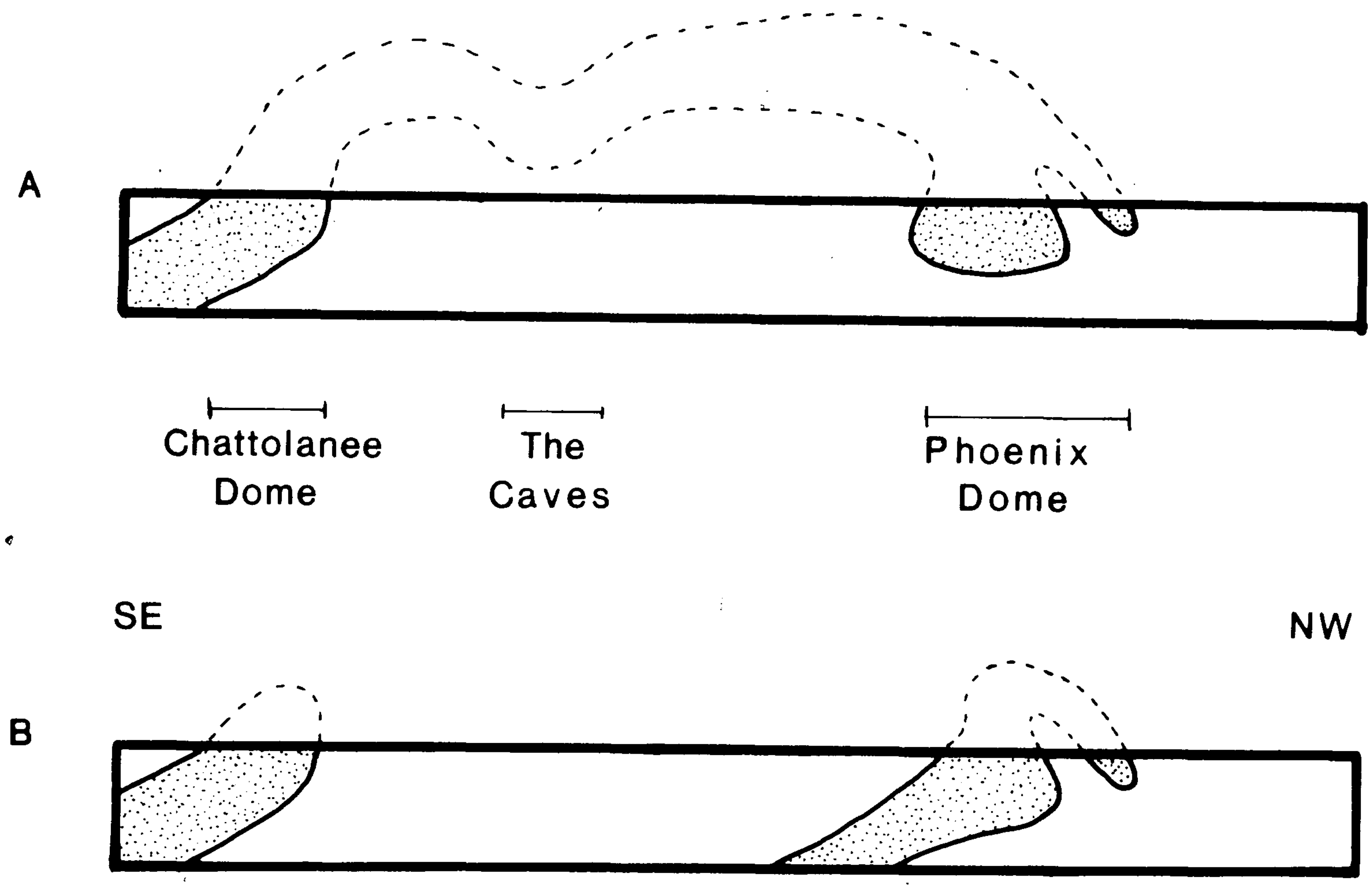
A
Chattolanee
Dome
The
Caves
Phoenix
Dome
SE
NW
B

under the Chattolanee and the Towson Domes is that the bodies represent overturned limbs of nappes (see Fig. 4-2B). Bromery [1968] noted that the Baltimore Gneiss Domes, and in particular the Chattolanee and Towson Domes, are associated with flat, negative magnetic anomalies. Fisher and others [1979] determined that the magnetic anomalies could not be explained in terms of the magnetic properties of the Baltimore Gneiss. The Baltimore Gneiss has a very low magnetic susceptibility and a random normal remanent magnetization. Further, the Setters and Cockeysville Formations have similarly low magnetic susceptibilities. Wissahickon rocks have a relatively high susceptibility and are associated with nearly all the magnetic anomalies in the study area. A possible explanation for the negative magnetic anomaly over the Chattolanee Dome is that overturned Wissahickon rocks underlie the Baltimore Gneiss at depth. This would tend to support the interpretation seen in Fig. 4-2B.

The Baltimore Mafic Complex overthrust may have been the mechanism responsible for napping. The mafic complex seems to be thrust northwestward. Perhaps it bulldozed the more plastic Baltimore Gneiss and Glenarm metasediments ahead of the thrust causing the nappes. Relatively hot high density mafic rocks on top of low density pelitic and psammitic metasedimentary rocks could have heated the metasedimentary rocks and caused them to deform plastically. The metasedimentary rocks will want to rise diapirically because of the gravitational instability in this inverted density relationship.

A summary interpretation of the subsurface structure of the Chattolanee Dome can be seen in Figure 4-3.

Figure 4-2: Hypothetical East-West Profile Through The Chattolanee Dome

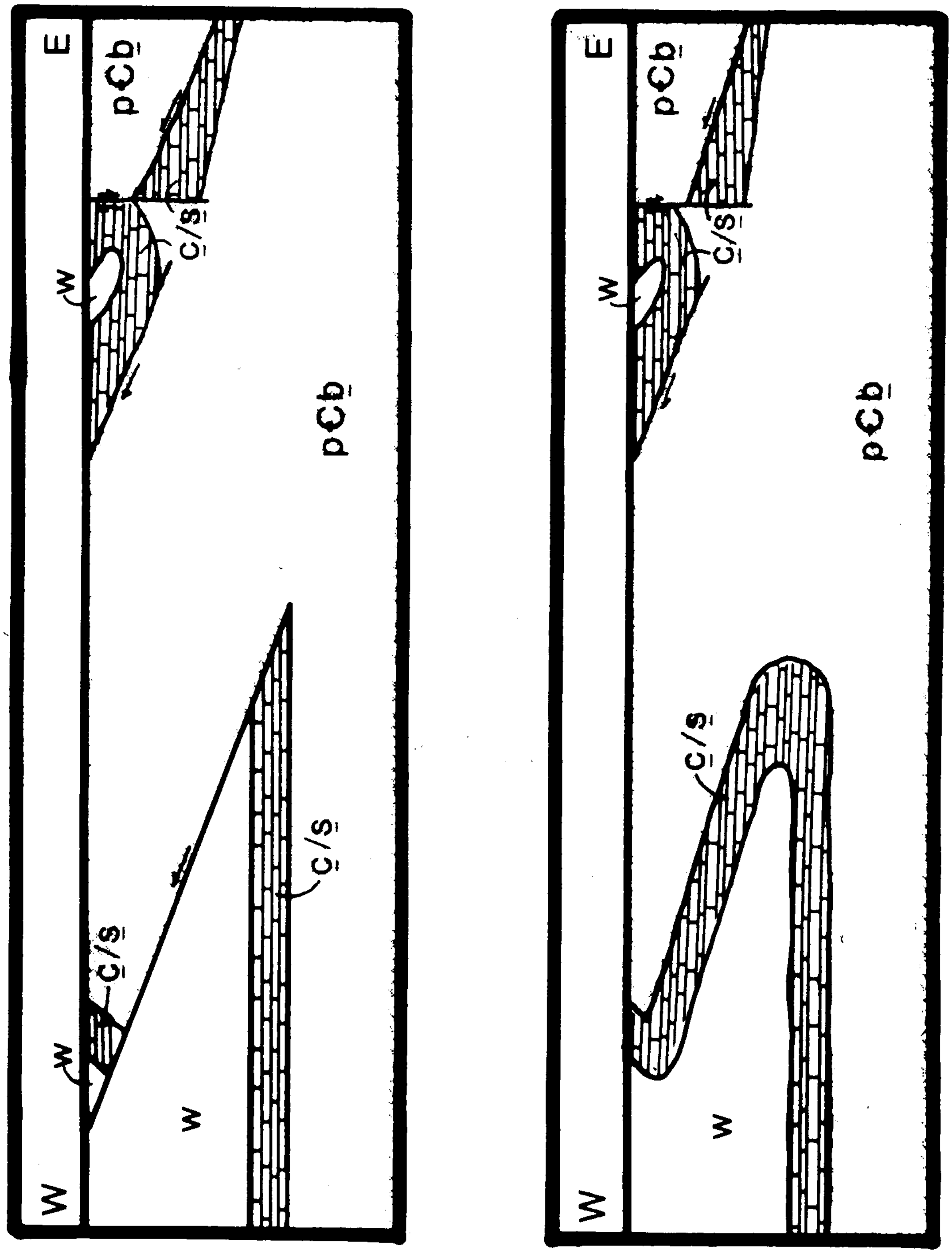

A
B

Figure 4-3: Block Diagram of the Chattolanee Dome

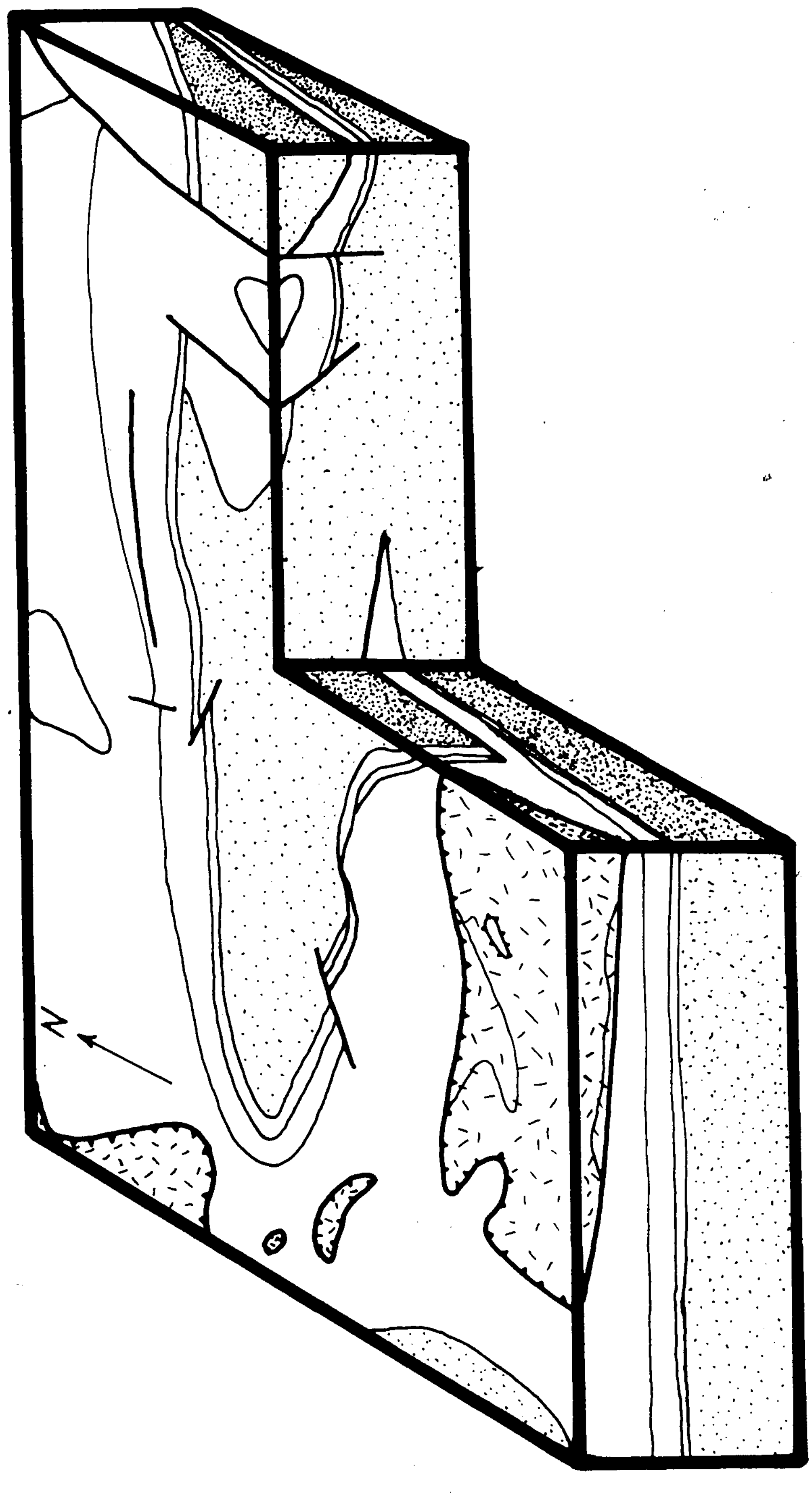
N

4.1 Tectonic Scheme

It seems clear from the geophysical evidence that the structure of the Baltimore Gneiss Domes, more specifically the Chattolanee, Towson, and Phoenix Domes, are not as simple as Eskola [1949] believed. Eskola thought that the gneiss domes form from mobilization and migmatization due to diapiric rising. He reasoned that the basement gneisses reach some critical depth at very high temperature and the gneiss was migmatized and behaved as a fluid with no strength. Because the gneiss is a low density rock, it rises diapirically. This is similar to diapiric salt doming. The structural history based on the large-scale imbricate faulting hypothesis is deduced as:

1. Extreme ductile deformation forming nappes.
2. Imbricate thrusting of the whole package.
3. Thrusting of the Baltimore Mafic Complex.
4. Late-stage normal faulting (isostatic rebound ?). These faults were fairly shallow since fault breccias are still preserved.

The structural history based on the folding hypothesis is deduced as:

1. Thrusting of the Baltimore Mafic Complex accompanied by extreme ductile deformation, forming nappes.
2. Late-stage normal faulting.

The second scenario is preferred over the first since it had a build-in mechanism for napping. The overall mechanism that formed the Baltimore Gneiss Domes was probably a complex type of crustal shortening. This crustal shortening event was possibly a continental-continental collision, perhaps Taconic in age, as age dates of the latest metamorphism suggests [Higgins, 1972].

4.2 Recommendations for Further Work

1. More detailed subsurface data is necessary in order to verify these interpretations. Drill coring and seismic profiles would be highly valuable.

2. Paleomagnetic work, particularly on the meta-igneous rocks, may provide information such as delineation of various tectonic blocks and paleolatitudes.

3. This high-density gravity survey could be extended to provide more information concerning the other domes adjacent to the Chattolanee Dome.

4. Petrofabric analysis of the silicified breccias may provide a clue as to the fault movements.

5. More fold analysis is necessary in order to determine different fold styles and orientations. This type of analysis may provide new data concerning stress directions.

REFERENCES

Bhattacharyya, B. K., 1978, Computer modeling in gravity and magnetic interpretation: **Geophysics**, v. 43, p. 912-929.

Bhattacharyya, B. K. and Navolio, M., 1975, Digital convolution for computing gravity and magnetic anomalies due to arbitrary bodies: **Geophysics**, v. 40, p. 981-992.

Broedel, C. H., 1937, The structure of the gneiss domes near Baltimore, Maryland: **Maryland Geological Survey**, v. 13, p. 149-187.

Bromery, R., 1967a, **Aeromagnetic map of Baltimore County and Baltimore City, Maryland**: U. S. Geol. Survey, Geophysical Investigations Map GP-613, Scale 1:62,500.

Bromery, R., 1967b, **Simple bouguer gravity map of Baltimore County and Baltimore City, Maryland**: U. S. Geol. Survey, Geophysical Investigations Map GP-614, Scale 1:62,500.

Bromery, R., 1967c, Structural and lithologic information interpreted from an aeromagnetic and gravity survey of Baltimore County, Maryland: **Geological Society of America, Special Paper Number 115**, p. 252-253, Abstract only.

Bromery, R., 1968, **Geological interpretation of aeromagnetic and gravity surveys of the northeastern end of the Baltimore - Washington Anticlinorium, Hartford, Baltimore, and part of Carroll County, Maryland** [Ph.D. Thesis]: Johns Hopkins University, Unpublished, 124 p.

Cartwright, D. E. and Edden, A. C., 1973, Corrected Tables of Tidal Harmonics: **Geophys. Jour. Royal Astr. Soc.**, v. 33, p. 253-264.

Cartwright, D. E. and Tayler, R. J., 1971, New Computations of the Tide-generating Potential: **Geophys. Jour. Royal Astr. Soc.**, v. 23, p. 45-74.

Choquette, P. W., 1957, **Petrology and structure of the Cockeysville Formation near Baltimore, Maryland** [Ph.D. Thesis]: Johns Hopkins University, Unpublished.

Choquette, P. W., 1960, Petrology and structure of the Cockeysville Formation (pre-Silurian) near Baltimore, Maryland: **Geol. Soc. America Bull.**, v. 71, p. 1027-1052.

Cleaves, E. T., Edwards, J., Jr., Glaser, J. D., compilers, 1968, **Geological Map of Maryland:** Maryland Geological Survey, Scale 1:250,000.

Cloos, E. and Anderson, J. L., 1950, **The geology of Bear Island, Potomac River, Maryland:** Johns Hopkins Univ. Studies in Geology No. 6, Part 2.

Cohen, C. J., 1937, Structure of the metamorphosed gabbro complex at Baltimore: **Maryland Geological Survey**, v. 13, p. 215-236.

Cordell, L. and Henderson, R., 1968, Iterative three - dimensional solution of gravity anomaly data using a digital computer: **Geophysics**, v. 33, p. 596-601.

Crowley, W. P., 1976a, **The geology of the crystalline rocks near Baltimore and its bearing on the evolution of the Eastern Maryland Piedmont:** Maryland Geological Survey, Report of Investigations No. 27, 40 p.

Crowley, W. P., 1976b, **Geologic Map of Baltimore County and Baltimore City:** Maryland Geological Survey, Scale 1:62,500.

Crowley, W. P., 1977, **Geologic map of the Reisterstown Quadrangle, Maryland:** Maryland Geological Survey, Scale 1:24,000.

Crowley, W. P. and Cleaves, E. T., 1974, **Geologic Map of the Towson Quadrangle, Maryland:** Maryland Geological Survey, Scale 1:24,000.

Crowley, W. P., Higgins, M. W., Bastian, T., and Olsen, S., 1971, **New interpretations of the Eastern Piedmont geology of Maryland or Granite and Gabbro or Greywacke and Greenstone:** Maryland Geological Survey, Guidebook No. 2, 43 p.

Crowley, W. P. and Reinhardt, J., 1979, **Geologic map of the Baltimore West Quadrangle:** Maryland Geological Survey, Scale 1:24,000.

Crowley, W. P. and Reinhardt, J., 1980, **Geologic map of**

the Ellicott City Quadrangle, Maryland: Maryland Geological Survey, Scale 1:24,000.

Crowley, W. P., Reinhardt, J., and Cleaves, E. T., 1975, **Geologic map of the Cockeysville Quadrangle, Maryland:** Maryland Geological Survey, Scale 1:24,000.

Crowley, W. P., Reinhardt, J., and Cleaves, E. T., 1976, **Geologic Map of the White Marsh Quadrangle, Maryland:** Maryland Geological Survey, Scale 1:24,000.

Daniels, D., in preparation, **Simple Bouguer Gravity Map of Maryland:** U. S. Geol. Survey, Scale 1:250,000.

Davis, J. C., 1973, **Statistics and Data Analysis in Geology:** New York, N. Y., John Wiley & Sons, Inc., 550 p.

Dingman, R. J., Meyer, G., and Martin, R. O. R., 1954, **The Water Resources of Howard and Montgomery Counties, Maryland:** Md. Dept. of Geology, Mines, and Water Resources, Bull. no. 14, 260 p.

Dobrin, M. B., 1976, **Introduction to Geophysical Prospecting,** Third Edition: New York, McGraw-Hill Book Co., 630 p.

Edwards, J., Jr. and Hansen, H. J., 1979, **New data bearing on the structural significance of the upper Chesapeake Bay magnetic anomaly:** Maryland Geological Survey, Report of Investigations No. 30, 44 p.

Ellis, E. E., 1909, A Study of the Occurrence of Water in Crystalline Rocks, in Gregory, H. E., **Underground Water Resources of Connecticut:** U. S. Geol. Survey Water Supply Paper 232, p. 54-101.

Ervin, C. P., 1977, Short Note: Theory of the bouguer anomaly: **Geophysics**, v. 42, p. 1468.

Eskola, P. E., 1949, The problem of mantled gneiss domes: **Quarterly Jour. Geological Soc. London**, v. 104, p. 461-476.

Fisher, G. W., 1963, **The petrology and structure of the crystalline rocks along the Potomac River, near Washington, D. C.** [Ph.D. Thesis]: Johns Hopkins University, Unpublished.

Fisher, G. W., 1970, The metamorphosed sedimentary rocks along the Potomac River near Washington, D.C., **in** Fisher, G. W., Pettijohn, F. J., Reed, J. C., and Weaver, K. N., (eds.), **Studies in Appalachian Geology: Central and Southern**: New York, Wiley - Interscience, p. 299-315.

Fisher, G. W., 1978, **Geologic Map of the New Windsor Quadrangle, Maryland**: U. S. Geol. Survey Misc. Invest. Series Map I-1037, Scale 1:24,000.

Fisher, G. W., 1971a, Kyanite-, staurolite-, and garnet-bearing schists in the Setters Formation, Maryland Piedmont: **Geol. Soc. America Bull.**, v. 82, p. 229-232.

Fisher, G. W., 1971b, **The Piedmont crystalline rocks at Bear Island, Potomac River, Maryland**: Maryland Geological Survey, Guidebook No. 4, 32 p.

Fisher, G. W., Higgins, M. W., and Zeitz, I., 1979, **Geological interpretations of aeromagnetic maps of the crystalline rocks in the Appalachians, Northern Virginia to New Jersey**: Maryland Geological Survey, Report of Investigations No. 32, 43 p.

Gerard, A. and Debeglia, N., 1975, Automatic three - dimensional modeling for interpretation of gravity or magnetic anomalies: **Geophysics**, v. 40, p. 1014-1034.

Hammer, S., 1939, Terrain corrections for an inclined plane in gravity computations: **Geophysics**, v. 4, p. 184-194.

Hansen, H. J., 1974, Interpretation of Chesapeake Bay aeromagnetic anomalies: Comment: **Geology**, v. 2, p. 449-450.

Herz, N., 1950, **The petrology of the Baltimore Gabbro and the Baltimore - Patapsco Aqueduct** [Ph.D. Thesis]: Johns Hopkins University, Unpublished.

Herz, N., 1951, Petrology of the Baltimore Gabbro: **Geol. Soc. America Bull.**, v. 62, p. 979-1016.

Higgins, M. W., 1972, Age, origin, regional relations, and nomenclature of the Glenarm Series, Central Appalachian Piedmont: a reinterpretation: **Geol. Soc. America Bull.**, v. 83, p. 989-1026.

Higgins, M. W. and Fisher, G. W., 1971, A further revision of the stratigraphic nomenclature of the Wissahickon Formation in Maryland: **Geol. Soc. America Bull.**, v. 82, p. 769-774.

Higgins, M. W., Fisher, G. W., and Zietz, I., 1973, Aeromagnetic discovery of a Baltimore Gneiss Dome in the Piedmont of Northwestern Delaware and Southeastern Pennsylvania: **Geology**, v. 1, p. 41-43.

Higgins, M. W., Zietz, I., and Fisher, G. W., 1974a, Interpretations of aeromagnetic anomalies bearing on the origin of Upper Chesapeake Bay and river course changes in the central Atlantic Seaboard region: Speculations: **Geology**, v. 2, p. 73-76.

Higgins, M. W., Zietz, I., and Fisher, G. W., 1974b, Interpretation of Chesapeake Bay aeromagnetic anomalies: Reply: **Geology**, v. 2, p. 450.

Hopson, C. A., 1964, The crystalline rocks of Howard and Montgomery Counties, **in The geology of Howard and Montgomery Counties**: Maryland Geological Survey, p. 27-215.

Hurlbut, C. S. and Klein, C., 1977, **Manual of Mineralogy (after James D. Dana)**, 19th edition: New York, N. Y., John Wiley & Sons, Inc., 532 p.

Knopf, E. B. and Jonas, A. I., 1923, Stratigraphy of the crystalline schists of Pennsylvania and Maryland: **Am. Jour. Science, 5th series**, v. 5, p. 40-62.

Knopf, E. B. and Jonas, A. I., 1925, **Map of Baltimore County and Baltimore City showing the geological formations**: Maryland Geological Survey, Scale 1:62,500.

Knopf, E. B. and Jonas, A. I., 1929, The geology of the crystalline rocks of Baltimore County, **in Baltimore County**: Maryland Geological Survey, p. 97-199.

Mathews, E. B., 1904, The structure of the Piedmont Plateau as shown in Maryland: **Am. Jour. Science, 4th series**, v. 17, p. 141-159.

Mathews, E. B., 1925, **Map of Baltimore County and Baltimore City showing the geological formations**: Maryland Geological Survey, Scale 1:62,500.

Mathews, E. B., 1933, **Map of Maryland showing the geological formations:** Maryland Geological Survey, Scale 1:380,160.

Mathews, E. B. and Miller, W. J., 1905, Cockeysville Marble: **Geol. Soc. America Bull.**, v. 65, p. 347-366.

McGrath, P. H. and Hood, P. J., 1970, The dipping dike case: a computer curve - matching method of magnetic interpretation: **Geophysics**, v. 35, p. 831-848.

Melchior, P., 1978, **The Tides of the Planet Earth:** Oxford, England, Pergamon Press, 609 p.

Miller, W. J., 1905, **The crystalline limestones of Baltimore County, Maryland** [Ph.D. Thesis]: Johns Hopkins University, Unpublished.

Muller, P. D., in preparation, **Geologic Map of the Hereford Quadrangle, Maryland:** Maryland Geological Survey, Scale 1:24,000.

Murthy, I. V. and Rao, D. B., 1979, Gravity anomalies of two - dimensional bodies of irregular cross - section with density contrast varying with depth: **Geophysics**, v. 44, p. 1525-1530.

Nabighian, M. N., 1972, The analytical signal of two - dimensional magnetic bodies with polygonal cross - section: its properties and use for automated anomaly interpretation: **Geophysics**, v. 37, p. 507-517.

Nabighian, M. N., 1974, Additional comments on the analytical signal of two - dimensional magnetic bodies with polygonal cross - section: **Geophysics**, v. 39, p. 85-92.

Nagy, D., 1966, The gravitational attraction of a right rectangular prism: **Geophysics**, v. 21, p. 362-371.

Nettleton, L. L., 1976, **Gravity and magnetics in oil prospecting:** New York, McGraw-Hill Book Co., 464 p.

Olsen, S. N., 1972, **Petrology of the Baltimore Gneiss** [Ph.D. Thesis]: Johns Hopkins University, Unpublished, 295 p.

Olsen, S. N., 1977, Origin of the Baltimore Gneiss migmatites at Piney Creek, Maryland: **Geol. Soc.**

America Bull., v. 88, p. 1089-1101.

Reed, J. C., Jr. and Jolly, J., 1963, **Crystalline rocks of the Potomac River Gorge near Washington, D. C.:** U. S. Geol. Survey Prof. Paper 414-H, 16 p.

Southwick, D. L., 1969, Crystalline rocks of Hartford County, **in The Geology of Hartford County, Maryland:** Maryland Geological Survey, p. 1-76.

Southwick, D. L. and Fisher, G. W., 1967, **Revision of Stratigraphic Nomenclature of the Glenarm Series in Maryland:** Maryland Geological Survey, Report of Investigation No. 6, 19 p.

Talwani, M., 1965, Computation with the help of a digital computer of magnetic anomalies caused by bodies of arbitrary shape: **Geophysics**, v. 30, p. 797-817.

Talwani, M. and Ewing, M., 1960, Rapid computation of gravitational attraction of three - dimensional bodies of arbitrary shape: **Geophysics**, v. 25, p. 203-225.

Talwani, M., Worzel, J. L., and Landisman, M., 1959, Rapid gravity computations for two - dimensional bodies with application to the Mendocino submarine fracture zone: **Jour. Geophys. Research**, v. 64, p. 49-51.

Till, R., 1974, **Statistical Methods for the Earth Scientist, an introduction:** London, England, Macmillan Press, 154 p.

Tilton, G. R., Davis, G. L., Wetherill, G. W., Aldrich, L. T., Jager, E., 1959, Mineral ages in the Maryland Piedmont: **Carnegie Inst. Wash. Yearbook 58**, p. 171-174.

Tilton, G. R., Doe, B. R., and Hopson, C. A., 1970, Zircon age measurements in the Maryland Piedmont, with special reference to Baltimore Gneiss problems, **in** Fisher, G. W., Pettijohn, F. J., Reed, J. C., Jr., and Weaver, K. N. (eds.), **Studies in Appalachian Geology: Central and Southern:** New York, Wiley - Interscience, p. 429-434.

Tilton, G. R., Wetherill, G. W., Davis, G. L., and Hopson, C. A., 1958, Ages of minerals from the Baltimore Gneiss near Baltimore, Maryland: **Geol.**

Soc. America Bull., v. 69, p. 1469-1474.

Uhl, V. W., 1979, Occurrence of Groundwater in the Satpura Hills Region of Central India: **Jour. Hydrology**, v. 41, p. 123-141.

Wagner, M. E. and Crawford, M. L., 1975, Polymetamorphism of the Precambrian Baltimore Gneiss in Southeastern Pennsylvania: **Am. Jour. Science**, v. 275, p. 653-682.

Wetherill, G. W., Davis, G. L., and Lee-Hu, C., 1968, Rb-Sr measurements on whole rocks and separated minerals from the Baltimore Gneiss, Maryland: **Geol. Soc. America Bull.**, v. 79, p. 757-762.

Wetherill, G. W., Tilton, G. R., Davis, G. L., Hart, S. R., and Hopson, C. A., 1966, Age measurements in the Maryland Piedmont: **Jour. Geophys. Research**, v. 71, p. 2139-2155.

Williams, G. H., 1886, **The gabbros and associated hornblende rocks occurring in the neighborhood of Baltimore, Maryland**: U. S. Geol. Survey Bull. 28, 78 p.

Williams, G. H., 1891, The petrography and structure of the Piedmont Plateau in Maryland: **Geol. Soc. America Bull.**, v. 2, p. 301-322.

Williams, G. H., 1892, **Guide to Baltimore with an account of the geology of its environs (includes geologic map)**: Baltimore, J. Murphy & Co., American Institute of Mining Engineers, Guidebook prepared by local committee, 139 p.

Woollard, G. P., 1979, The new gravity system - changes in international gravity base values and anomaly values: **Geophysics**, v. 44, p. 1352-1366.

Zietz, I., Gilbert, F. P., and Kirby, J. R., Jr., 1978, **Aeromagnetic Map of Maryland**: U. S. Geol. Survey Geophys. Invest. Map GP-923, Scale 1:250,000.

Zietz, I., Gilbert, F. P., and Kirby, J. R., Jr., 1980, **Aeromagnetic Map of Delaware, Maryland, Pennsylvania, West Virginia, and parts of New Jersey, and New York**: U. S. Geol. Survey Geophys. Invest. Map GP-927, Scale 1:1,000,000.

APPENDICES

APPENDIX A: Gravity Base Station Descriptions

Explanation: Since portable gravity meters can measure only relative differences in the earth's gravitational field, they must be calibrated to stations which have accurately determined absolute gravity. These stations are collectively known as gravity base stations. Most gravity base stations are established by ties with other previously established base stations using portable gravity meters. All gravity base stations are ultimately tied to stations where the absolute gravity was determined by an accelerometer. These stations are known as first-order gravity stations.

The following is a descriptive listing of base stations used in this study. These stations are on file with the Gravity and Astronomy Division of the National Geodetic Survey (a branch of the National Ocean Survey - NOAA).

Existing Stations Used

=> NBS-2

Location:	Room 129, Bldg. 202 National Bureau of Standards Gaithersburg, Maryland
Description:	The station is a brass plate set in the southwest corner of manhole slab, near the door to corridor. This is a first-order station.
Latitude:	39 07.85 N
Longitude:	77 13.20 W
Elevation:	131 m. (approx.)
g:	980101.37 mgals
Established:	Nov. 1965 [Tate, 1966], revised 1979

=> Harrisburg

Location:	Harrisburg, Pennsylvania
Description:	The station is at the Capital City Airport. It is at the southwest corner of the Smith Aircraft Corp. hangar, the hangar west of the building closest to the control tower. The site is below the "Office Entrance" sign. A USC&GS BM disk is on the south face of the building at the same corner.
Latitude:	40 13.3 N
Longitude:	76 51.3 W
Elevation:	102.570 m.
g:	980119.72 mgals
Established:	Nov. 1967

=> Pottsville

Location:	Pottsville, Pennsylvania
Description:	The station is located in the town of Pottsville, at the Civil War Monument on Market Street. It is on a concrete base on the south side of the west monument. A USC&GS disk is 0.6 meters above the site.
Latitude:	40 41.0 N
Longitude:	76 11.9 W
Elevation:	200.318 m.
g:	980133.13 mgals
Established:	Nov. 1967

=> Scranton

Location:	Scranton, Pennsylvania
Description:	The station is at the Scranton - Wilkes-Barre Airport. It is at the terminal building, 3 meters east of the southeast corner, on the ground in a corner formed by the intersection of two fences.
Latitude:	41 20.5 N
Longitude:	75 43.5 W
Elevation:	280.0 m.
g:	980209.86 mgals
Established:	Nov. 1967

Stations Established for this Survey

=> Baltimore Base

Location:	Baltimore, Maryland
Description:	The station is located in Glenmar, Maryland, 1 km. south of Stevenson, Maryland and 1 km. north of Exit 21 of Interstate 695. It consists of a brass plate set in concrete marked "Gravity Base Station". The station monument is adjacent to the concrete curb on the south side of Elm Hollow Court.
Latitude:	39 24.02 N
Longitude:	76 42.68 W
Elevation:	162.80 m.
g:	980090.148 mgals
Established:	Aug. 1980

=> Lehigh Base

Location:	Bethlehem, Pennsylvania
Description:	The station is at Williams Hall, Lehigh University. It is at the east entrance to the building. A brass screw is driven into the southwest corner of the concrete, at the outside entranceway.
Latitude:	40 36.40 N
Longitude:	75 21.92 W
Elevation:	107.85 m.
g:	980137.769 mgals
Established:	Sept. 1980

APPENDIX B: Measured Gravity Station Values

Explanation: The following is a list of gravity station values measured from May to September 1980. The headings are as follows:

Stat.	Codenumber for the gravity station
Lat.	The latitude of the station in degrees and minutes (north of the Equator)
Long.	The longitude of the station in degrees and minutes (west of the Prime Meridian
Elev.	The elevation of the station in meters above sea level
Absol. g	The gravitational acceleration at the station in mgals
F. A.	The free-air anomaly in mgals
B. A.	The bouguer anomaly in mgals

Stat.	Lat.	Long.	Elev.	Absol. g	F. A.	B. A.
		* * * Chattolanee Dome Net * * *				
1G1	39 25.20	76 41.40	100.52	980107.133	20.750	9.501
1G3	39 25.40	76 40.80	106.92	980106.283	21.580	9.615
1G4	39 25.40	76 41.20	104.86	980107.438	22.098	10.364
1G5	39 25.50	76 41.50	111.47	980106.625	23.177	10.703
1G6	39 25.90	76 41.90	171.52	980097.281	31.773	12.579
1G8	39 25.40	76 41.80	115.92	980105.638	23.711	10.740
1G9	39 25.10	76 41.40	102.60	980105.642	20.048	8.567
1G10	39 24.90	76 41.40	90.82	980106.902	17.968	7.806
1G11	39 24.80	76 41.30	97.03	980102.901	16.031	5.174
1G12	39 24.60	76 41.20	121.41	980096.926	17.875	4.290
1G13	39 24.50	76 41.20	131.68	980094.385	18.652	3.917
2G1	39 25.10	76 40.20	89.45	980106.924	17.273	7.263
2G2	39 25.20	76 40.20	93.28	980107.238	18.619	8.182
2G3	39 25.30	76 40.50	97.13	980106.955	19.379	8.509
2G4	39 25.50	76 40.30	99.23	980106.535	19.308	8.205
2G5	39 25.60	76 40.30	109.14	980106.678	22.362	10.149
2G6	39 25.90	76 40.50	156.68	980099.879	29.792	12.259
2G8	39 26.10	76 40.90	172.02	980097.928	32.279	13.030
2G9	39 26.00	76 42.60	165.48	980098.225	30.704	12.187

Stat.	Lat.	Long.	Elev.	Absol. g	F. A.	B. A.
2G10	39 25.30	76 42.60	107.42	980107.885	23.482	11.462
2G11	39 25.20	76 42.70	105.12	980107.874	22.911	11.148
2G12	39 25.00	76 42.70	105.16	980107.394	22.739	10.972
2G13	39 25.00	76 42.90	109.98	980106.547	23.379	11.072
2G14	39 24.70	76 42.90	99.83	980106.211	20.353	9.182
2G15	39 24.60	76 42.80	104.15	980103.886	19.509	7.855
2G16	39 24.60	76 42.80	111.97	980101.701	19.738	7.209
2G17	39 24.50	76 42.70	140.62	980095.944	22.969	7.234
3G1	39 24.80	76 43.30	110.68	980105.775	23.117	10.732
3G2	39 24.90	76 43.10	111.26	980106.344	23.718	11.268
3G3	39 26.20	76 40.90	168.44	980099.468	32.566	13.718
3G4	39 26.50	76 41.00	180.71	980097.430	33.872	13.650
3G5	39 26.70	76 41.10	178.62	980098.319	33.818	13.831
3G6	39 26.80	76 41.10	188.37	980097.100	35.461	14.382
3G7	39 26.90	76 41.50	189.16	980097.008	35.466	14.298
3G8	39 26.80	76 42.10	183.45	980098.872	35.713	15.185
3G9	39 26.80	76 42.50	189.89	980097.423	36.253	15.004
3G10	39 26.70	76 42.80	185.79	980097.948	35.660	14.870
3G11	39 26.70	76 43.10	197.70	980095.625	37.014	14.891
3G12	39 26.80	76 43.20	191.53	980096.749	36.084	14.652
3G13	39 26.50	76 42.90	200.83	980094.249	36.900	14.426
3G14	39 26.20	76 42.60	192.47	980095.301	35.813	14.276
3G15	39 26.10	76 42.40	179.90	980096.973	33.756	13.625
3G16	39 26.90	76 43.40	191.44	980097.411	36.571	15.149
3G17	39 26.50	76 43.80	145.30	980103.854	29.368	13.108
3G18	39 26.30	76 44.00	137.42	980105.711	29.088	13.711
3G19	39 26.20	76 44.10	136.76	980104.898	28.220	12.916
4G1	39 25.00	76 40.10	88.31	980105.783	15.926	6.045
4G2	39 24.90	76 40.10	84.33	980104.238	13.300	3.864
4G3	39 24.70	76 40.10	88.93	980101.598	12.378	2.426
4G4	39 24.50	76 40.10	97.29	980098.309	11.964	1.077
4G5	39 24.30	76 40.10	101.57	980098.374	13.645	2.279
4G6	39 24.10	76 40.10	92.68	980099.762	12.585	2.214
4G7	39 24.00	76 40.00	80.53	980102.120	11.343	2.331
4G8	39 23.90	76 40.00	78.27	980102.502	11.173	2.415
4G9	39 23.80	76 39.80	76.75	980103.524	11.874	3.286
4G10	39 23.60	76 39.80	74.87	980104.153	12.221	3.842
4G11	39 23.50	76 39.70	72.77	980104.498	12.065	3.922
4G12	39 23.30	76 39.60	76.18	980103.160	12.074	3.549
4G13	39 23.10	76 39.60	89.15	980099.054	12.265	2.290
4G14	39 23.10	76 39.90	100.84	980098.060	14.880	3.596
4G15	39 22.80	76 39.10	90.01	980098.464	12.387	2.314
4G16	39 22.60	76 39.10	65.87	980103.315	10.083	2.712
4G17	39 22.40	76 39.00	68.81	980103.251	11.221	3.522
4G18	39 23.90	76 40.10	80.09	980101.921	11.156	2.193

Stat.	Lat.	Long.	Elev.	Absol. g	F. A.	B. A.
4G19	39 24.10	76 39.60	97.84	980099.280	13.695	2.747
5G1	39 23.40	76 42.80	167.26	980089.082	25.955	7.239
5G2	39 23.50	76 42.80	167.27	980089.508	26.236	7.519
5G3	39 23.60	76 42.70	165.12	980089.669	25.587	7.110
5G4	39 23.70	76 42.80	158.36	980091.023	24.706	6.986
5G5	39 23.90	76 42.80	163.12	980090.493	25.350	7.097
5G6	39 24.10	76 42.80	156.84	980091.561	24.184	6.634
5G7	39 24.40	76 42.70	143.74	980094.977	23.114	7.029
5G8	39 24.30	76 42.50	147.73	980093.436	22.951	6.420
5G9	39 24.30	76 42.30	151.88	980091.753	22.550	5.555
5G10	39 24.30	76 41.90	156.11	980090.394	22.497	5.028
5G11	39 24.20	76 41.80	156.32	980089.581	21.897	4.404
5G12	39 24.10	76 41.10	120.68	980095.349	16.813	3.309
6G1	39 24.00	76 41.20	117.64	980096.269	16.944	3.779
6G2	39 23.80	76 41.30	124.34	980094.996	18.033	4.120
6G3	39 23.20	76 41.30	133.72	980092.895	19.714	4.751
6G4	39 23.80	76 41.50	138.41	980092.362	19.742	4.254
6G6	39 23.70	76 43.30	150.08	980094.359	25.488	8.694
6G7	39 23.70	76 42.90	166.43	980089.774	25.948	7.324
6G8	39 23.90	76 42.40	148.51	980092.714	23.062	6.444
6G9	39 24.00	76 42.30	146.57	980092.487	22.089	5.687
6G10	39 24.10	76 42.50	157.08	980090.744	23.441	5.864
6G11	39 24.10	76 42.00	149.55	980091.147	21.520	4.785
6G12	39 24.00	76 41.70	150.70	980090.621	21.498	4.634
6G13	39 23.90	76 41.80	138.15	980093.209	20.360	4.901
6G14	39 23.70	76 41.20	143.10	980090.118	19.092	3.079
6G15	39 23.60	76 41.40	154.03	980088.360	20.855	3.619
6G16	39 23.50	76 41.60	156.75	980088.336	21.817	4.277
6G17	39 23.20	76 42.30	159.47	980089.321	24.087	6.242
6G18	39 23.10	76 42.40	145.03	980092.424	22.883	6.653
6G19	39 23.00	76 42.40	138.20	980093.499	21.996	6.531
6G20	39 22.90	76 42.70	150.03	980092.099	24.394	7.605
6G21	39 22.80	76 42.90	156.02	980091.291	25.584	8.125
6G22	39 23.00	76 42.90	159.41	980090.629	25.671	7.833
7G1	39 24.00	76 42.10	147.42	980091.867	21.731	5.234
7G2	39 23.50	76 41.10	124.23	980093.877	17.324	3.422
7G3	39 23.40	76 41.10	112.36	980095.737	15.668	3.095
7G4	39 23.30	76 41.20	111.22	980095.755	15.483	3.037
7G5	39 23.20	76 41.10	103.22	980098.359	15.767	4.216
7G6	39 23.10	76 41.20	106.79	980098.334	16.991	5.041
7G7	39 22.90	76 41.20	117.33	980096.445	18.649	5.520
7G8	39 22.80	76 40.50	130.31	980095.650	22.010	7.427
7G9	39 22.90	76 40.50	130.09	980094.747	20.890	6.332
7G10	39 23.00	76 40.50	121.08	980095.866	19.079	5.531
7G11	39 23.10	76 40.30	112.58	980097.122	17.566	4.968
7G12	39 23.00	76 40.70	104.45	980098.557	16.638	4.951

Stat.	Lat.	Long.	Elev.	Absol. g	F. A.	B. A.
7G13	39 23.70	76 40.80	153.45	980087.451	19.620	2.448
7G14	39 23.80	76 40.70	139.28	980089.898	17.545	1.960
7G15	39 23.80	76 40.60	130.39	980091.423	16.326	1.736
7G16	39 23.90	76 40.50	117.74	980093.957	14.811	1.635
7G17	39 23.80	76 40.40	97.75	980097.177	12.009	1.071
7G18	39 24.00	76 41.00	109.44	980097.021	15.164	2.918
8G1	39 22.70	76 40.60	134.42	980096.221	23.995	8.954
8G2	39 22.50	76 40.70	130.00	980098.064	24.771	10.224
8G3	39 22.50	76 41.00	128.36	980098.212	24.411	10.048
8G4	39 22.70	76 41.10	136.68	980094.324	22.795	7.500
8G5	39 22.60	76 41.30	131.99	980096.725	23.896	9.127
8G6	39 22.60	76 41.50	137.14	980095.730	24.492	9.146
8G7	39 22.70	76 41.60	141.97	980094.139	24.243	8.357
8G8	39 22.80	76 41.60	122.99	980096.669	20.769	7.006
8G9	39 22.80	76 41.80	127.10	980096.127	21.495	7.272
8G10	39 22.80	76 42.00	129.02	980095.584	21.545	7.107
8G11	39 22.70	76 42.20	139.99	980094.444	23.938	8.273
8G12	39 22.10	76 41.70	147.01	980093.402	25.948	9.498
8G13	39 22.60	76 42.00	146.03	980094.790	26.294	9.953
8G14	39 22.50	76 42.30	145.19	980095.308	26.701	10.454
8G15	39 22.50	76 42.40	147.76	980095.223	27.410	10.875
9G1	39 22.30	76 39.20	65.84	980104.276	11.477	4.110
9G2	39 22.00	76 39.10	60.48	980104.165	10.157	3.389
9G3	39 21.70	76 39.30	97.47	980099.793	17.642	6.735
9G4	39 21.90	76 39.40	100.88	980099.858	18.464	7.176
9G5	39 22.00	76 39.60	75.80	980106.752	17.472	8.989
9G6	39 22.30	76 39.60	87.23	980102.858	16.659	6.899
10G1	39 21.30	76 39.80	117.37	980101.209	25.790	12.657
10G2	39 21.60	76 39.60	115.80	980099.255	22.910	9.952
10G3	39 22.00	76 39.30	65.31	980105.892	13.373	6.065
10G4	39 22.20	76 39.90	109.63	980101.094	21.956	9.689
10G5	39 22.00	76 40.00	82.32	980106.970	19.700	10.489
10G6	39 21.80	76 39.90	111.33	980101.873	23.852	11.394
10G7	39 21.60	76 39.80	123.84	980099.647	25.782	11.924
10G8	39 21.50	76 39.80	134.49	980097.642	27.212	12.163
10G9	39 21.70	76 40.10	122.77	980101.109	26.767	13.028
10G10	39 21.90	76 40.50	103.73	980106.100	25.587	13.979
10G11	39 22.20	76 40.70	119.57	980102.190	26.121	12.741
10G12	39 22.20	76 40.10	107.68	980102.654	22.917	10.867
11G1	39 22.00	76 39.00	92.51	980102.313	18.187	7.835
11G2	39 21.80	76 40.40	97.24	980107.009	24.640	13.759
11G3	39 21.80	76 40.50	99.62	980107.050	25.415	14.268
11G4	39 21.70	76 40.30	123.24	980101.832	27.633	13.843
11G5	39 20.40	76 40.20	136.39	980098.814	30.595	15.333
11G6	39 22.00	76 40.80	117.45	980103.796	27.368	14.225
11G7	39 22.30	76 40.70	116.82	980101.902	24.836	11.763

Stat.	Lat.	Long.	Elev.	Absol. g	F. A.	B. A.
11G8	39 22.30	76 40.60	119.57	980101.190	24.972	11.592
11G9	39 22.30	76 40.90	121.26	980101.492	25.795	12.227
11G10	39 22.00	76 40.10	133.89	980101.972	30.617	15.635
11G11	39 21.90	76 40.80	128.34	980102.608	29.690	15.328
11G12	39 21.80	76 41.10	123.04	980104.918	30.511	16.742
11G13	39 21.60	76 41.40	125.71	980105.770	32.481	18.414
11G14	39 21.40	76 41.50	138.28	980103.843	34.731	19.257
11G15	39 21.40	76 41.10	133.06	980105.211	34.487	19.598
11G16	39 21.60	76 41.20	122.23	980106.156	31.793	18.116
11G17	39 21.70	76 40.80	103.22	980107.723	27.346	15.796
11G18	39 21.50	76 40.80	117.05	980105.384	29.570	16.473
11G19	39 21.30	76 41.10	136.03	980103.764	34.106	18.883
11G20	39 21.30	76 40.50	136.18	980100.147	30.534	15.295
12G1	39 21.90	76 40.10	118.80	980101.369	25.505	12.211
12G2	39 21.90	76 41.40	117.63	980106.787	30.564	17.400
12G3	39 21.60	76 41.60	136.97	980104.347	34.535	19.208
12G4	39 21.40	76 42.20	136.78	980105.306	35.731	20.425
12G5	39 21.20	76 42.40	135.14	980107.095	37.309	22.186
12G6	39 21.60	76 42.30	142.04	980103.641	35.392	19.498
12G7	39 21.60	76 42.40	144.27	980103.906	36.345	20.202
12G8	39 21.70	76 42.20	138.20	980104.437	34.856	19.391
12G9	39 21.80	76 42.50	145.13	980103.044	35.454	19.214
12G11	39 21.80	76 42.10	133.34	980104.954	33.725	18.804
12G12	39 21.60	76 41.80	134.46	980105.525	34.937	19.891
12G13	39 21.70	76 41.80	133.55	980104.836	33.819	18.875
12G14	39 21.90	76 41.60	122.76	980105.633	30.990	17.254
14G1	39 22.30	76 41.60	136.48	980098.989	27.990	12.718
14G2	39 22.20	76 41.10	127.53	980101.092	27.478	13.207
14G3	39 22.20	76 41.20	129.79	980100.999	28.084	13.560
14G4	39 22.20	76 41.40	135.17	980100.799	29.543	14.418
14G5	39 22.20	76 41.70	136.18	980101.143	30.199	14.961
14G6	39 22.00	76 41.90	132.17	980103.001	31.116	16.326
14G7	39 22.20	76 41.90	136.28	980101.257	30.346	15.095
14G8	39 22.10	76 42.00	136.50	980102.143	31.445	16.171
14G9	39 22.00	76 42.10	130.79	980105.104	32.791	18.156
14G10	39 22.10	76 42.40	136.40	980102.502	31.773	16.510
14G11	39 22.10	76 42.50	139.64	980102.180	32.451	16.825
14G12	39 22.00	76 42.40	137.53	980103.360	33.128	17.738
18G1	39 24.20	76 42.80	151.80	980092.772	23.692	6.705
18G2	39 24.30	76 42.70	157.30	980091.766	24.234	6.633
18G3	39 24.30	76 42.10	147.71	980092.066	21.576	5.047
18G4	39 24.10	76 41.50	148.98	980090.611	20.808	4.137
18G5	39 24.40	76 41.10	146.22	980091.052	19.954	3.592
18G6	39 24.20	76 41.20	111.41	980099.739	18.195	5.728
18G7	39 25.40	76 42.40	119.36	980105.695	24.830	11.473
18G8	39 25.40	76 41.00	105.89	980106.829	21.807	9.958

Stat.	Lat.	Long.	Elev.	Absol. g	F. A.	B. A.
18G9	39 25.50	76 40.30	110.13	980105.605	21.745	9.421
18G10	39 25.70	76 40.40	119.05	980104.606	23.201	9.880
18G11	39 26.00	76 40.60	167.85	980097.768	30.980	12.197
18G12	39 26.80	76 41.80	186.28	980097.953	35.670	14.824
18G13	39 26.10	76 42.20	168.03	980098.851	31.971	13.168
18G14	39 23.80	76 42.70	157.43	980091.102	24.350	6.734
18G15	39 23.60	76 42.30	152.33	980090.878	22.849	5.803
18G16	39 23.70	76 42.20	148.18	980091.749	22.290	5.709
19G1	39 23.30	76 42.80	161.35	980090.287	25.483	7.428
19G2	39 23.30	76 42.60	161.11	980090.005	25.129	7.101
19G3	39 23.10	76 42.50	152.42	980091.393	24.130	7.074
19G4	39 23.30	76 42.10	166.12	980087.457	24.126	5.537
19G5	39 23.50	76 41.70	160.84	980087.787	22.533	4.534
19G6	39 23.90	76 40.80	130.22	980091.955	16.659	2.087
19G7	39 24.00	76 40.80	115.12	980095.265	15.160	2.278
19G8	39 23.90	76 40.20	83.31	980100.467	10.696	1.373
19G9	39 23.60	76 41.20	141.64	980090.650	19.322	3.473
19G10	39 23.10	76 41.00	111.99	980096.923	17.183	4.652
19G11	39 23.20	76 40.70	119.53	980095.141	17.581	4.206
19G12	39 23.20	76 40.50	133.41	980092.782	19.507	4.578
20G1	39 23.30	76 43.30	159.37	980091.152	25.738	7.905
20G2	39 23.00	76 43.10	153.42	980092.230	25.424	8.256
20G3	39 22.80	76 41.10	124.41	980095.979	20.515	6.594
20G4	39 23.00	76 39.40	108.90	980094.155	13.610	1.424
20G5	39 23.00	76 39.50	103.87	980095.113	13.017	1.394
20G6	39 24.10	76 39.20	84.38	980102.202	12.462	3.021
20G7	39 24.10	76 39.20	77.69	980103.505	11.702	3.009
20G8	39 24.10	76 39.00	73.52	980103.747	10.658	2.431
20G9	39 24.00	76 38.90	72.30	980104.094	10.775	2.685
20G10	39 24.10	76 38.70	80.18	980101.697	10.664	1.692
20G11	39 24.10	76 38.50	86.71	980100.491	11.473	1.770
20G12	39 24.10	76 38.50	90.13	980099.727	11.765	1.679
20G13	39 24.20	76 38.40	96.92	980098.606	12.590	1.745
20G14	39 24.20	76 38.20	112.67	980095.313	14.158	1.550
20G15	39 24.20	76 38.10	109.20	980095.710	13.483	1.264
21G1	39 22.40	76 42.60	141.25	980099.085	29.412	13.605
21G2	39 22.20	76 43.00	144.39	980101.141	32.729	16.573
21G3	39 22.00	76 43.00	147.75	980101.792	34.716	18.182
21G4	39 22.00	76 42.90	147.05	980102.228	34.934	18.479
21G5	39 22.10	76 42.80	149.96	980100.532	33.989	17.208
21G6	39 22.00	76 42.70	148.46	980101.525	34.667	18.054
21G7	39 21.90	76 42.80	147.70	980104.113	37.168	20.640
21G8	39 21.90	76 43.00	148.40	980103.318	36.589	19.983
21G9	39 21.70	76 43.20	143.67	980105.651	37.758	21.681
21G10	39 21.50	76 43.10	147.60	980105.452	39.067	22.551
21G11	39 21.40	76 43.00	139.36	980106.976	38.197	22.602

Stat.	Lat.	Long.	Elev.	Absol. g	F. A.	B. A.
21G12	39 21.40	76 42.80	135.61	980107.058	37.121	21.946
21G13	39 22.00	76 43.30	146.59	980103.796	36.361	19.957
21G14	39 21.90	76 43.20	143.75	980105.127	36.964	20.878
22G1	39 23.40	76 43.30	165.33	980089.891	26.168	7.668
22G2	39 23.60	76 43.50	150.83	980094.007	25.515	8.637
22G3	39 23.70	76 43.60	141.94	980096.038	24.653	8.770
22G4	39 23.90	76 43.60	132.62	980098.122	23.567	8.726
22G5	39 24.00	76 43.70	130.01	980099.818	24.309	9.761
22G6	39 24.20	76 43.70	117.11	980101.533	21.747	8.643
22G7	39 24.40	76 43.80	111.20	980103.373	21.469	9.026
22G8	39 26.50	76 43.70	157.99	980102.117	31.544	13.866
22G9	39 22.60	76 43.20	151.95	980094.485	27.817	10.814
22G10	39 22.50	76 43.30	157.42	980095.081	30.247	12.632
23G1	39 22.70	76 43.40	157.17	980091.515	26.311	8.723
23G2	39 22.30	76 43.80	149.86	980099.323	32.452	15.683
23G3	39 22.30	76 43.70	148.00	980100.039	32.594	16.033
23G4	39 22.20	76 43.60	147.92	980100.943	33.623	17.070
23G5	39 24.70	76 43.50	113.32	980105.463	23.768	11.088
23G6	39 24.70	76 43.80	120.05	980104.382	24.765	11.331
23G7	39 24.50	76 44.60	121.63	980103.384	24.549	10.939
23G8	39 24.40	76 44.60	123.98	980102.245	24.284	10.411
23G9	39 24.30	76 44.60	132.05	980100.954	25.633	10.856
23G10	39 24.30	76 44.80	134.36	980100.177	25.566	10.531
23G11	39 24.30	76 44.90	136.35	980099.937	25.940	10.683
23G12	39 24.40	76 45.30	132.61	980102.279	26.981	12.142
23G13	39 25.10	76 45.60	166.19	980097.864	31.895	13.298
23G14	39 25.20	76 45.30	181.44	980094.972	33.561	13.258
23G15	39 25.40	76 45.00	189.78	980094.106	34.972	13.735
23G16	39 25.50	76 44.80	192.20	980094.001	35.465	13.958
23G17	39 25.70	76 44.60	191.99	980094.474	35.577	14.093
23G18	39 25.80	76 44.50	184.57	980096.043	34.709	14.056
23G19	39 25.80	76 44.30	181.10	980096.761	34.356	14.091
23G20	39 26.00	76 44.20	181.88	980096.472	34.013	13.661
24G1	39 26.50	76 44.30	144.93	980105.592	30.992	14.773
24G2	39 26.80	76 44.80	155.07	980104.167	32.253	14.900
24G3	39 26.90	76 45.50	192.74	980098.921	38.482	16.914
24G4	39 26.50	76 46.10	208.94	980094.264	39.416	16.036
24G5	39 26.30	76 46.20	185.94	980098.022	36.374	15.567
24G6	39 26.20	76 46.10	178.62	980098.906	35.145	15.157
24G7	39 26.00	76 46.10	174.35	980098.963	34.181	14.671
24G8	39 25.60	76 45.90	174.54	980097.834	33.702	14.170
24G9	39 25.20	76 45.90	190.55	980093.968	35.366	14.044
24G10	39 25.00	76 46.20	160.29	980099.501	31.859	13.922
24G11	39 24.80	76 46.30	153.39	980100.498	31.022	13.857
24G12	39 24.80	76 46.30	159.71	980098.800	31.273	13.402
24G13	39 24.60	76 46.00	152.64	980098.471	29.058	11.978

Stat.	Lat.		Long.		Elev.	Absol. g	F. A.	B. A.
24G14	39	24.40	76	45.70	137.31	980101.570	27.723	12.358
24G15	39	24.30	76	45.60	136.17	980100.684	26.632	11.395
24G16	39	24.20	76	45.40	144.74	980097.838	26.580	10.383
24G17	39	24.00	76	45.20	157.13	980096.051	28.911	11.328
24G18	39	24.00	76	45.10	155.51	980096.182	28.543	11.141
25G1	39	23.70	76	44.80	165.73	980093.402	29.360	10.814
25G2	39	23.50	76	44.60	160.51	980093.923	28.565	10.604
25G3	39	23.30	76	44.30	165.84	980092.303	28.886	10.329
25G4	39	23.40	76	44.70	149.21	980096.506	27.811	11.114
25G5	39	23.30	76	44.80	163.36	980094.059	29.877	11.597
25G6	39	23.30	76	45.10	151.06	980097.077	29.099	12.196
25G7	39	23.10	76	45.20	136.19	980100.124	27.853	12.614
25G8	39	23.00	76	45.40	128.30	980104.306	29.749	15.392
25G9	39	23.00	76	45.60	126.56	980104.081	28.986	14.824
25G10	39	22.90	76	45.70	137.26	980103.282	31.635	16.276
25G11	39	22.90	76	45.80	152.89	980101.286	34.464	17.356
26G1	39	23.70	76	45.20	160.09	980095.439	29.656	11.742
26G2	39	23.60	76	45.60	156.17	980097.016	30.172	12.696
26G3	39	23.50	76	45.70	148.71	980098.568	29.569	12.928
26G4	39	23.50	76	45.80	141.26	980100.195	28.896	13.089
26G5	39	23.50	76	46.10	136.57	980101.885	29.140	13.858
26G6	39	23.50	76	46.40	136.69	980102.751	30.042	14.747
26G7	39	23.40	76	46.70	138.95	980102.968	31.104	15.556
26G8	39	23.50	76	47.20	162.67	980098.365	33.676	15.472
26G9	39	23.30	76	47.20	144.67	980102.105	32.156	15.967
26G10	39	22.90	76	47.40	180.03	980098.627	40.179	20.034
26G11	39	22.80	76	47.00	172.91	980100.214	39.719	20.370
26G12	39	23.50	76	47.30	176.71	980095.538	35.181	15.407
26G13	39	23.70	76	47.40	169.38	980097.332	34.415	15.462
26G14	39	23.90	76	47.20	158.55	980098.773	32.220	14.478
27G1	39	24.10	76	47.10	153.13	980099.769	31.246	14.112
27G2	39	24.10	76	47.00	142.00	980101.298	29.340	13.451
27G3	39	24.30	76	46.70	135.50	980101.436	27.178	12.015
27G4	39	24.50	76	46.70	136.11	980102.270	27.905	12.674
27G5	39	24.80	76	46.50	142.29	980102.457	29.554	13.632
27G6	39	24.90	76	46.50	151.74	980101.560	31.425	14.446
27G7	39	25.00	76	46.60	158.91	980100.380	32.312	14.530
27G8	39	25.20	76	46.90	151.32	980101.930	31.223	14.291
27G9	39	25.40	76	47.10	151.99	980102.589	31.793	14.786
27G10	39	25.60	76	47.50	178.25	980098.105	35.117	15.170
27G11	39	25.90	76	47.70	180.18	980099.462	36.627	16.465
27G12	39	25.70	76	47.80	200.29	980094.695	38.360	15.948
27G13	39	25.70	76	48.00	204.22	980093.879	38.758	15.905
27G14	39	25.70	76	48.20	213.04	980092.692	40.291	16.452
27G15	39	25.70	76	48.40	203.00	980094.883	39.383	16.668
28G1	39	23.60	76	47.70	174.56	980096.295	35.126	15.593

Stat.	Lat.	Long.	Elev.	Absol. g	F. A.	B. A.
28G2	39 23.60	76 48.00	172.05	980096.706	34.763	15.510
28G3	39 23.60	76 48.50	181.61	980094.740	35.748	15.425
28G4	39 23.40	76 48.80	173.38	980096.899	35.661	16.260
28G5	39 23.40	76 49.10	183.27	980096.537	38.352	17.844
28G6	39 23.50	76 49.40	187.51	980096.157	39.132	18.150
28G7	39 23.40	76 49.60	191.10	980095.328	39.559	18.175
28G8	39 25.80	76 48.50	193.78	980095.553	37.061	15.378
28G9	39 24.70	76 48.70	157.41	980102.581	34.494	16.879
28G10	39 24.50	76 49.00	161.45	980101.827	35.280	17.214
28G11	39 24.60	76 48.10	153.33	980102.167	32.969	15.811
29G1	39 24.80	76 46.90	140.33	980103.609	30.104	14.400
29G2	39 23.00	76 47.70	174.73	980099.872	39.644	20.091
29G3	39 22.00	76 46.40	154.23	980106.979	41.902	24.643
29G4	39 22.10	76 46.00	147.17	980109.202	41.799	25.330
29G5	39 22.00	76 45.70	153.87	980106.153	40.963	23.746
29G6	39 22.00	76 45.40	153.95	980104.314	39.149	21.922
29G7	39 22.10	76 45.20	142.38	980106.088	37.205	21.273
29G8	39 22.20	76 45.00	138.56	980106.038	35.829	20.324
29G9	39 22.20	76 44.90	143.23	980104.777	36.009	19.982
29G10	39 22.20	76 44.60	136.47	980107.110	36.257	20.986
29G11	39 22.40	76 44.40	124.25	980106.710	31.788	17.885
29G12	39 22.50	76 44.30	130.55	980102.118	28.994	14.385
29G13	39 22.60	76 43.80	156.52	980094.281	29.023	11.509
29G14	39 22.70	76 43.50	160.88	980091.522	27.460	9.458
30G1	39 21.70	76 44.20	143.74	980108.536	40.666	24.581
30G2	39 21.60	76 44.40	134.67	980110.469	39.946	24.876
30G3	39 21.60	76 44.70	119.06	980114.268	38.928	25.605
Base	39 24.00	76 42.70	162.80	980090.148	24.758	6.541

Stat.	Lat.	Long.	Elev.	Absol. g	F. A.	B. A.
		* * * Phoenix Dome Traverse * * *				
17G8	39 26.90	76 41.10	186.99	980096.840	34.626	13.702
17G7	39 27.10	76 41.20	170.86	980100.015	32.527	13.408
17G6	39 27.30	76 41.40	149.34	980104.354	29.929	13.219
17G5	39 27.40	76 41.50	132.29	980106.992	27.159	12.356
17G4	39 27.40	76 41.70	142.65	980105.526	28.890	12.928
17G3	39 27.60	76 41.90	180.02	980099.807	34.408	14.263
17G2	39 27.70	76 42.00	174.18	980101.319	33.969	14.479
17G1	39 27.90	76 42.00	185.21	980100.673	36.431	15.706
13G1	39 28.10	76 42.10	178.98	980101.916	35.457	15.429
13G2	39 28.20	76 42.10	182.59	980101.180	35.686	15.254
13G3	39 28.30	76 42.20	190.26	980099.919	36.645	15.355
13G4	39 28.40	76 42.30	196.35	980099.364	37.819	15.848
13G5	39 28.50	76 42.40	194.59	980100.146	37.912	16.138
13G6	39 28.60	76 42.50	204.22	980098.340	38.929	16.077
13G7	39 28.70	76 42.50	200.29	980099.343	38.572	16.159
13G8	39 28.90	76 42.50	193.25	980100.944	37.704	16.080
13G9	39 29.10	76 42.50	180.01	980103.113	35.492	15.349
13G10	39 29.40	76 42.50	176.98	980103.553	34.554	14.749
13G11	39 29.50	76 42.60	159.36	980105.917	31.330	13.498
13G12	39 29.60	76 42.60	150.15	980107.507	29.930	13.129
13G13	39 29.60	76 42.50	133.86	980111.088	28.485	13.506
13G14	39 29.70	76 42.50	134.45	980111.586	29.018	13.973
13G15	39 29.80	76 42.50	135.69	980111.089	28.756	13.572
13G16	39 30.10	76 42.70	157.44	980107.887	31.819	14.202
13G17	39 30.30	76 42.70	173.04	980105.101	33.553	14.190
15G18	39 30.50	76 42.80	157.46	980108.910	32.260	14.639
15G19	39 30.60	76 42.90	155.85	980109.622	32.325	14.886
15G20	39 30.70	76 42.90	145.73	980112.602	32.034	15.727
15G21	39 30.80	76 42.90	131.46	980115.400	30.282	15.571
15G22	39 30.90	76 43.00	119.64	980118.254	29.339	15.951
15G23	39 31.00	76 43.10	114.03	980119.107	28.312	15.553
15G24	39 31.10	76 43.10	113.68	980119.245	28.195	15.474
15G25	39 31.10	76 43.20	113.95	980119.552	28.584	15.834
15G26	39 31.20	76 43.20	123.23	980117.491	29.239	15.450
15G27	39 31.40	76 43.30	109.85	980120.788	28.112	15.820
15G28	39 31.50	76 43.30	118.77	980119.658	29.588	16.297
15G29	39 31.60	76 43.40	114.87	980121.236	29.815	16.961
15G30	39 31.70	76 43.50	98.25	980125.002	28.301	17.307
15G31	39 31.90	76 43.60	103.04	980124.626	29.107	17.577
15G32	39 32.00	76 43.70	109.18	980123.804	30.034	17.817
16G33	39 32.20	76 43.70	102.64	980124.350	28.264	16.779
16G34	39 32.30	76 43.90	105.39	980123.717	28.334	16.540

Stat.	Lat.	Long.	Elev.	Absol. g	F. A.	B. A.
16G35	39 32.50	76 44.00	109.66	980123.872	29.508	17.238
16G36	39 32.60	76 44.20	107.49	980123.866	28.685	16.657
16G37	39 32.70	76 44.30	120.24	980122.604	31.210	17.755
16G38	39 32.80	76 44.40	131.37	980122.133	34.026	19.326
16G39	39 32.90	76 44.50	127.25	980123.711	34.186	19.946
16G40	39 33.00	76 44.60	134.96	980123.848	36.552	21.451
16G41	39 33.20	76 44.70	139.60	980125.377	39.219	23.597
16G42	39 33.30	76 44.70	142.41	980125.823	40.382	24.447
16G44	39 33.50	76 44.80	149.45	980124.342	40.779	24.055
16G45	39 33.60	76 44.80	167.23	980119.201	40.976	22.263
16G46	39 33.70	76 44.90	178.81	980115.562	40.763	20.754
16G47	39 33.90	76 45.00	190.71	980114.019	42.596	21.256
16G48	39 34.00	76 45.00	187.89	980114.305	41.864	20.839
16G49	39 34.10	76 45.20	163.55	980118.936	38.837	20.535
16G50	39 34.30	76 45.20	149.43	980121.216	36.464	19.742

APPENDIX C: Gravity Stations and their Hub Numbers

Explanation: Hubs are reference numbers used to locate surveyed elevation points. Documentation of these points are kept on file at the Baltimore County Department of Public Works Survey Office and at the Baltimore City Department of Public Works Field Section. In this list, Baltimore County hubs are not marked with asterisks while Baltimore City hubs are marked with a single asterisk (*). A double asterisk (**) indicates those hubs surveyed by the author. These elevation points are located by a brass screw with a galvanized cap driven into the road macadam.

Stat.	Hub	Stat.	Hub	Stat.	Hub	Stat.	Hub
1G1	11180	2G9	11208	3G10	8290	4G9	3121
1G3	11220	2G10	13103A	3G11	4459	4G10	3922
1G4	11218	2G11	13103B	3G12	4460	4G11	11992
1G5	11213	2G12	13104	3G13	8314	4G12	3925
1G6	11209	2G13	3204	3G14	11204	4G13	7009
1G8	13098A	2G14	13147A	3G15	11205	4G14	7250
1G9	11181	2G15	13148	3G16	8295	4G15	7003
1G10	11182	2G16	1514A	3G17	8307A	4G16	12438
1G11	11183	2G17	1512	3G18	8309	4G17	9337
1G12	11185A	3G1	13109	3G19	8310	4G18	12033
1G13	11186	3G2	13108	4G1	7153	4G19	4860A
2G1	7154A	3G3	884	4G2	866B	5G1	5685
2G2	7156	3G4	11231	4G3	866	5G2	7144
2G3	11221	3G5	886	4G4	7151	5G3	5681
2G4	7157	3G6	887	4G5	7150	5G4	9240
2G5	11743	3G7	8279	4G6	7149A	5G5	9256
2G6	11229	3G8	8283	4G7	7012	5G6	8436
2G8	882	3G9	8286	4G8	7010	5G7	11420

Stat.	Hub	Stat.	Hub	Stat.	Hub	Stat.	Hub
5G8	8242	8G1	1978A	11G12	*7878	18G11	879
5G9	8240	8G2	4740	11G13	*6005	18G12	8280
5G10	8236	8G3	4738A	11G14	*5864	18G13	11207
5G11	9254	8G4	4736	11G15	*5961	18G14	9241
5G12	2483A	8G5	6939	11G16	*6002	18G15	11487
6G1	7128	8G6	6940	11G17	*7875	18G16	11488C
6G2	7130	8G7	12950	11G18	*7008	19G1	8615
6G3	8079	8G8	5439	11G19	*6999	19G2	8616
6G4	7134	8G9	12946A	11G20	*5940	19G3	8617
6G6	12225A	8G10	5437	12G1	*7256	19G4	6930
6G7	12223	8G11	12942A	12G2	*7871	19G5	1378
6G8	9244	8G12	12951A	12G3	*6110	19G6	7120
6G9	9246	8G13	6946A	12G4	*623	19G7	7122
6G10	11491	8G14	2272A	12G5	*7669	19G8	7115
6G11	9252	8G15	14035	12G6	*6842	19G9	8081
6G12	8442	9G1	*8123	12G7	*6828	19G10	10612
6G13	8441	9G2	*8298	12G8	*6839	19G11	10613
6G14	11235	9G3	*5943	12G9	*6844	19G12	10614
6G15	1380	9G4	*602	12G11	*6837	20G1	4842
6G16	1379	9G5	*5969	12G12	*7002	20G2	4841
6G17	1373	9G6	*561	12G13	*6127	20G3	8088
6G18	1371	10G1	*7992	12G14	*7458	20G4	7055
6G19	1369	10G2	*558	14G1	*7859	20G5	7006
6G20	1366	10G3	*8011	14G2	*7854	20G6	4856A
6G21	1364	10G4	*7053	14G3	*7843	20G7	4856
6G22	2266	10G5	*7045	14G4	*7842	20G8	4855A
7G1	8439	10G6	*5955	14G5	*7841	20G9	4853A
7G2	8082	10G7	*5954	14G6	*6852	20G10	4446
7G3	8083	10G8	*5942	14G7	*6853	20G11	4444
7G4	8084	10G9	*7257	14G8	*6851	20G12	4443
7G5	8085	10G10	*7850	14G9	*6850	20G13	4442
7G6	8086	10G11	*7857	14G10	*6855	20G14	4439
7G7	8087	10G12	*8001	14G11	*6835	20G15	4438A
7G8	7253	11G1	*5975	14G12	*5869	21G1	9939
7G9	7254	11G2	*570	18G1	8437	21G2	9843A
7G10	2004	11G3	*7870	18G2	8244	21G3	9911B
7G11	2005A	11G4	*568	18G3	8238	21G4	6321
7G12	1988A	11G5	*566	18G4	8231	21G5	12816
7G13	12036	11G6	*7848	18G5	11187A	21G6	12817
7G14	1386	11G7	*7461	18G6	11184	21G7	9911
7G15	12035	11G8	*7465	18G7	13101	21G8	9912
7G16	7118A	11G9	*7846	18G8	11219	21G9	9834A
7G17	7116A	11G10	*7851	18G9	11228	21G10	9832A
7G18	7127	11G11	*5989	18G10	11226	21G11	9829A

Stat.	Hub	Stat.	Hub	Stat.	Hub	Stat.	Hub
21G12	9827A	24G12	12747A	27G13	12593B	13G6	10284
21G13	9839A	24G13	12748A	27G14	12593	13G7	11417
21G14	9837A	24G14	8433	27G15	5548A	13G8	12811
22G1	5900	24G15	2156B	28G1	6479A	13G9	11608A
22G2	13158A	24G16	13127C	28G2	6482A	13G10	11610
22G3	13157	24G17	2160A	28G3	6486A	13G11	11612
22G4	13155	24G18	14010	28G4	12379	13G12	11613A
22G5	13154	25G1	2166A	28G5	12378A	13G13	4936
22G6	13151A	25G2	2167	28G6	6492	13G14	4470
22G7	4842	25G3	2170	28G7	6494	13G15	12862
22G8	8306	25G4	10876A	28G8	5585A	13G16	12864
22G9	10037	25G5	10877	28G9	12595	13G17	12865
22G10	10035	25G6	10888A	28G10	3334A	15G18	12867A
23G1	8203A	25G7	10902	28G11	5593	15G19	12868
23G2	10032	25G8	8649	29G1	9047	15G20	12869
23G3	10033A	25G9	10905	29G2	11034B	15G21	12870
23G4	2187	25G10	10906	29G3	3634	15G22	12871
23G5	13110	25G11	10907	29G4	11040A	15G23	12872
23G6	4848	26G1	10966	29G5	8987	15G24	12872A
23G7	13123A	26G2	2274	29G6	3636A	15G25	12873
23G8	13124A	26G3	10963	29G7	10971	15G26	12874
23G9	13125	26G4	10962	29G8	5625	15G27	12875A
23G10	13126	26G5	10961	29G9	5627	15G28	12876
23G11	13127A	26G6	10960	29G10	5630	15G29	12878
23G12	5389	26G7	10957	29G11	10026A	15G30	12879A
23G13	8336	26G8	11027	29G12	8428	15G31	12880
23G14	8334A	26G9	29955	29G13	8209	15G32	12881
23G15	8330A	26G10	14019	29G14	8204A	16G33	12882A
23G16	8328	26G11	7885A	30G1	5139	16G34	13045
23G17	8325	26G12	5298	30G2	5138	16G35	13044
23G18	8323	26G13	6478	30G3	5137	16G36	**
23G19	8322	26G14	11631A	17G8	8277	16G37	13042
23G20	8321	27G1	11631B	17G7	**	16G38	**
24G1	9542	27G2	11633A	17G6	**	16G39	**
24G2	9547	27G3	11635A	17G5	**	16G40	**
24G3	12665	27G4	11635B	17G4	**	16G41	**
24G4	5946	27G5	9050	17G3	**	16G42	**
24G5	5943	27G6	8535	17G2	**	16G44	**
24G6	5941	27G7	8534	17G1	**	16G45	**
24G7	5939	27G8	8533	13G1	10289	16G46	**
24G8	5937	27G9	14021	13G2	10288A	16G47	**
24G9	8477	27G10	9023	13G3	10287	16G48	**
24G10	8481	27G11	2124B	13G4	10286	16G49	**
24G11	11637	27G12	12593C	13G5	10283A	16G50	**

APPENDIX D: Oversize Figures

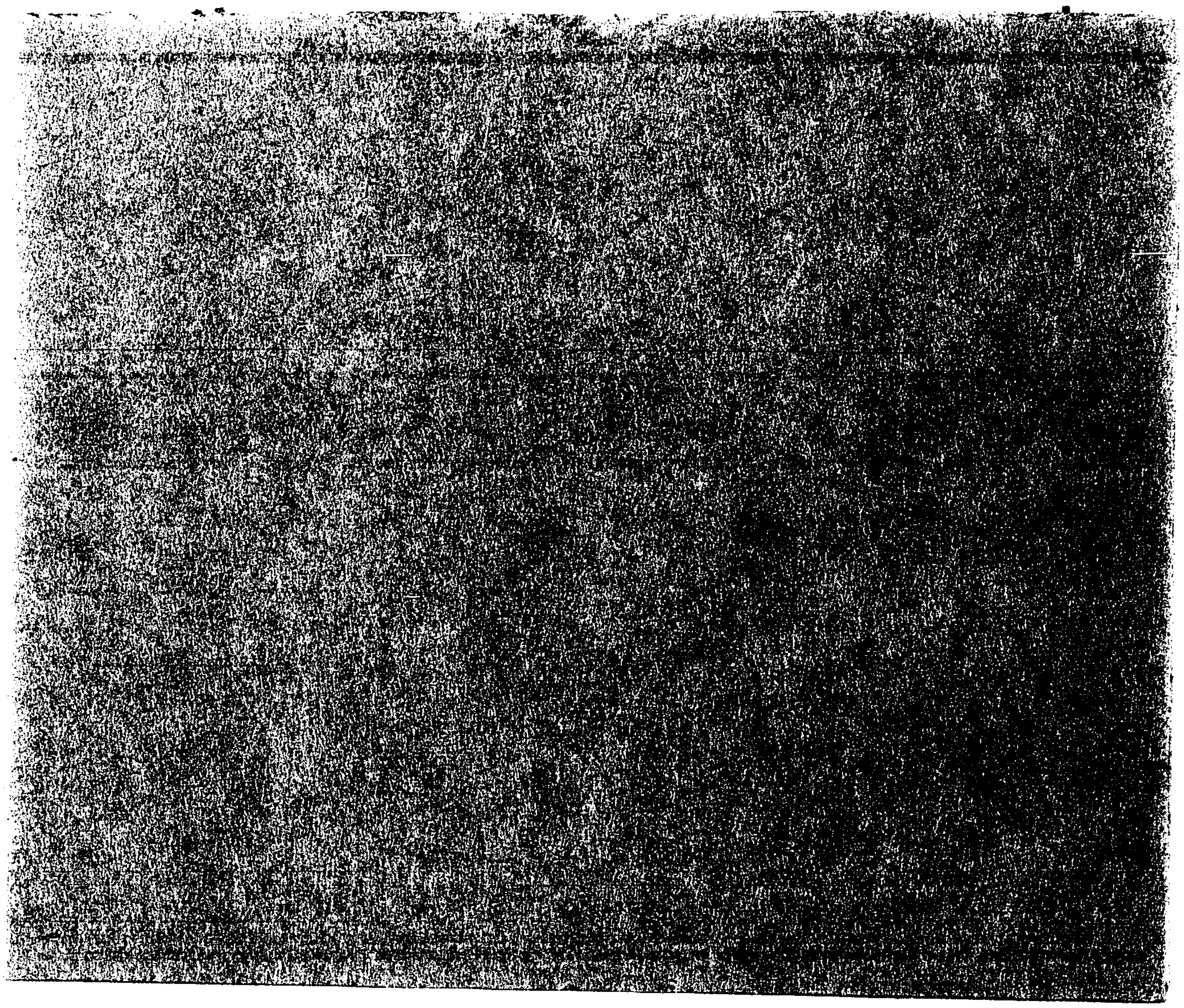

Figure 5-1: Geologic Map of the Chattolanee Dome

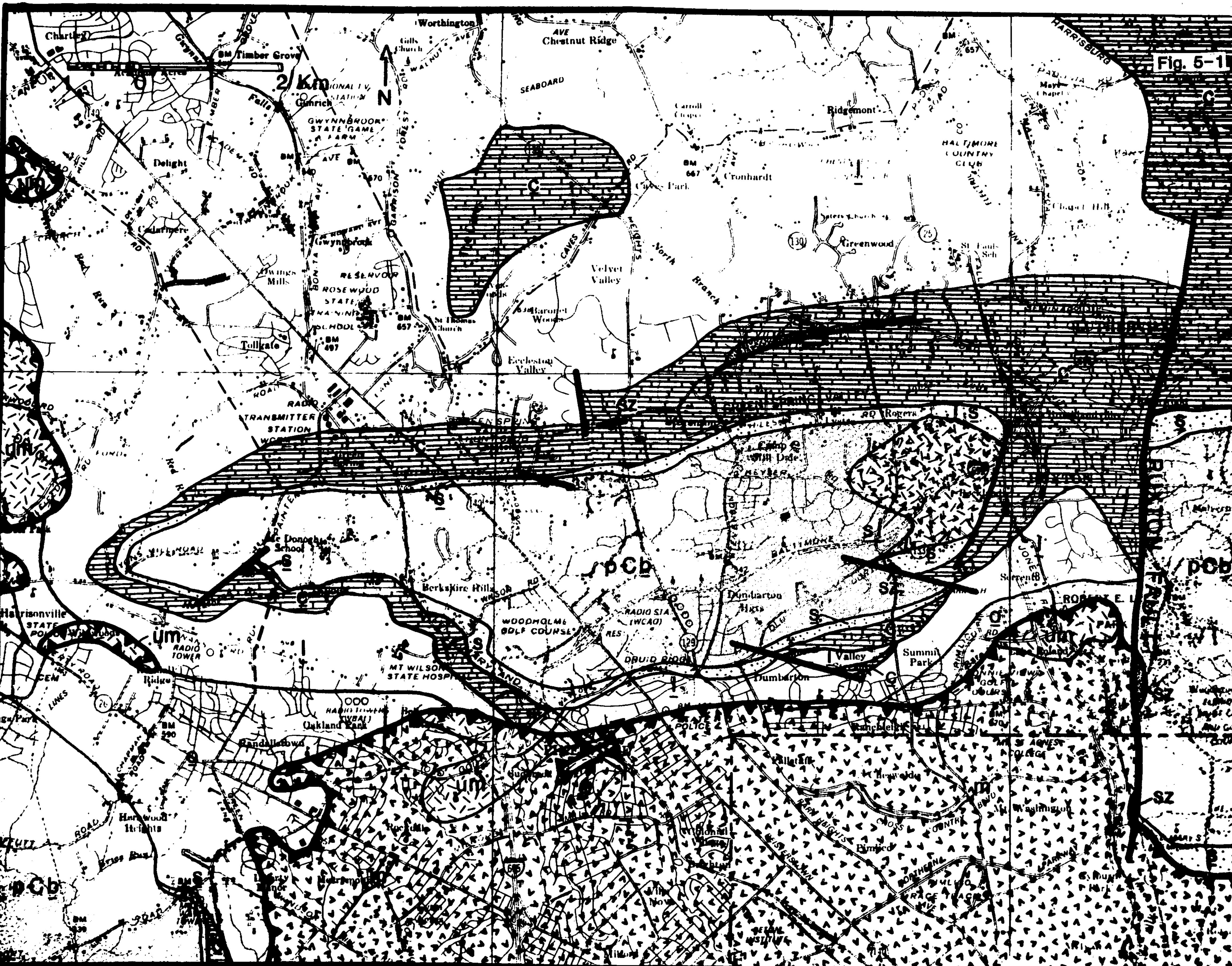

2 Km
N
Worthington
Chestnut Ridge
Timber Grove
Delight
Gwynnbrook
Owings Mills
Tollgate
Velvet Valley
Eccleston Valley
Cronhardt
Greenwood
Ridgemont
SEABOARD
BALTIMORE COUNTRY CLUB
ROSEWOOD STATE TRAINING SCHOOL
RADIO TRANSMITTER STATION
GWYNNBROOK STATE GAME FARM
Berkshire Hills
WOODHOLME GOLF COURSE
MT WILSON STATE HOSPITAL
RADIO TOWER
Randallstown
Oakland Park
Harwood Heights
Dumbarton
Summit Park
Valley
Pimlico
Mt Washington
HARRISBURG
C
pCb
um
S
SZ

Fig. 5-1

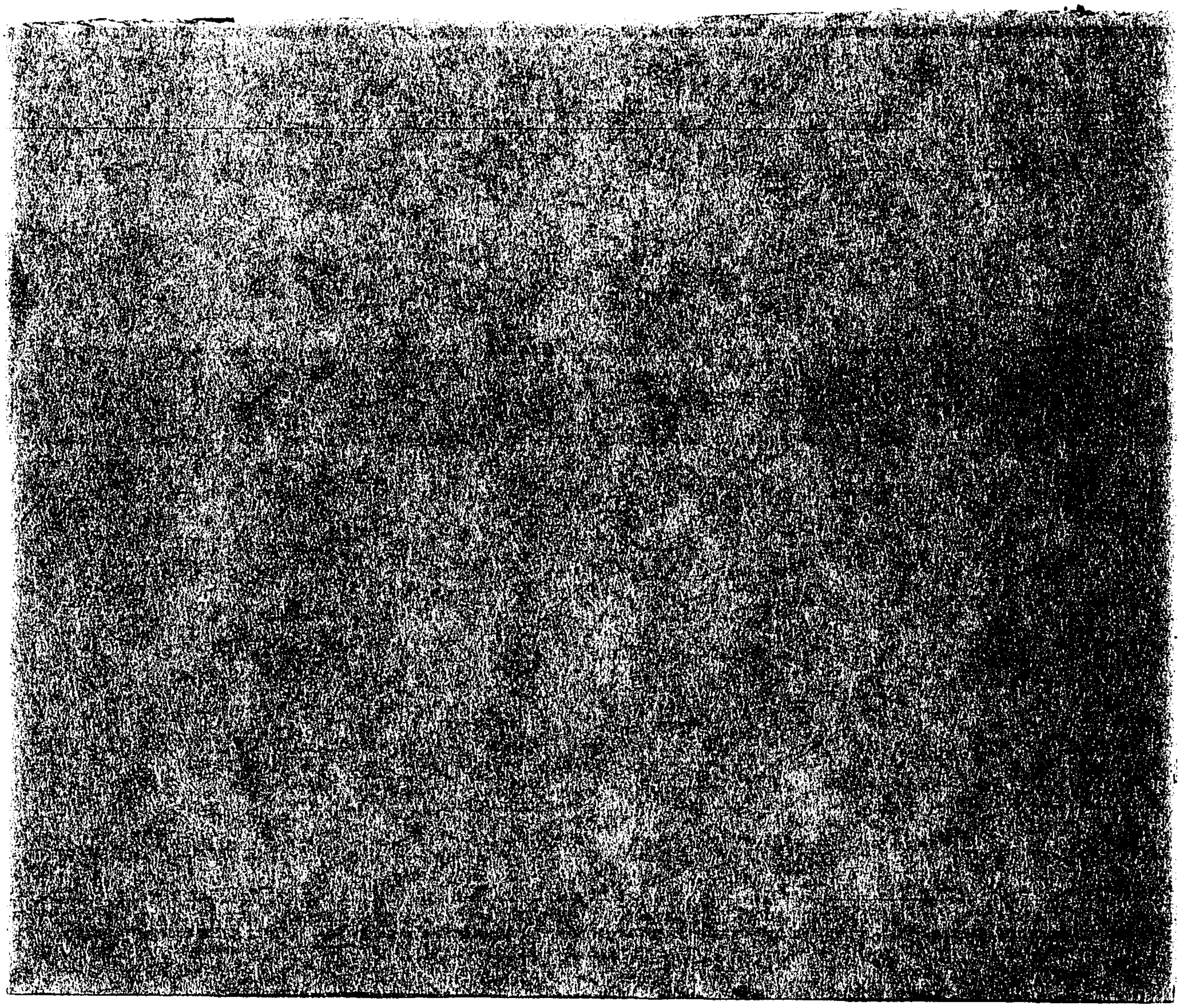

Figure 5-2: Simple Bouguer Gravity Map of the Chattolanee Dome

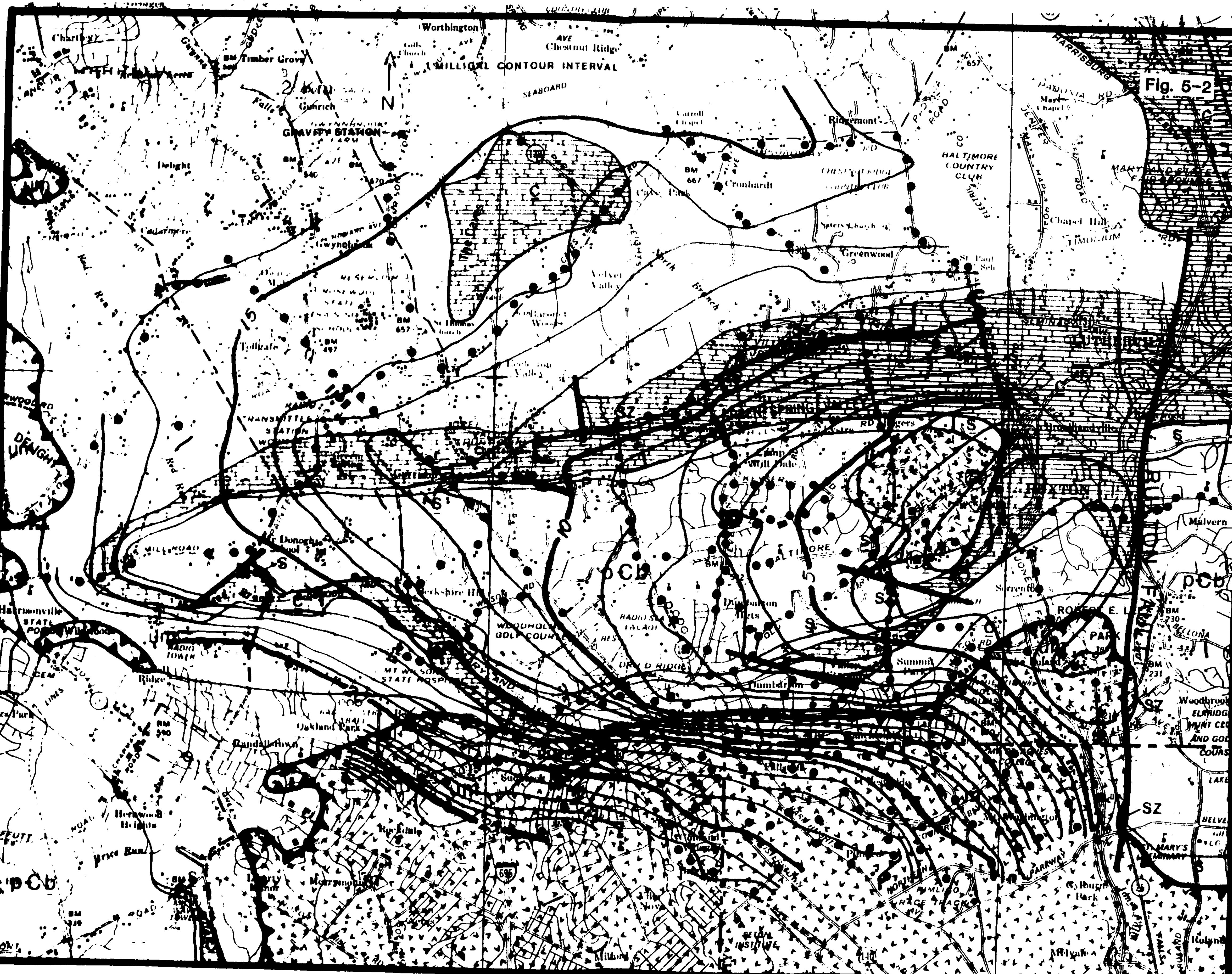
1 MILLIGAL CONTOUR INTERVAL
N
GRAVITY STATION
Worthington
Chestnut Ridge
Timber Grove
Delight
Ridgemont
HALTIMORE COUNTRY CLUB
Greenwood
Cronhardt
Velvet Valley
Chapel Hill
TIMONIUM
GREEN SPRING VALLEY
BROOKLANDVILLE
RUXTON
Malvern
Sorrento
ROBERT E. LEE PARK
WOODHOLME GOLF COURSE
MT WILSON STATE HOSPITAL
Dumbarton
Summit Park
Oakland Park
Randallstown
Herwood Heights
Rockdale
Milford
Woodbrook
ST MARY'S SEMINARY
Cylburn Park
pCb
SZ
10
5
Fig. 5-2

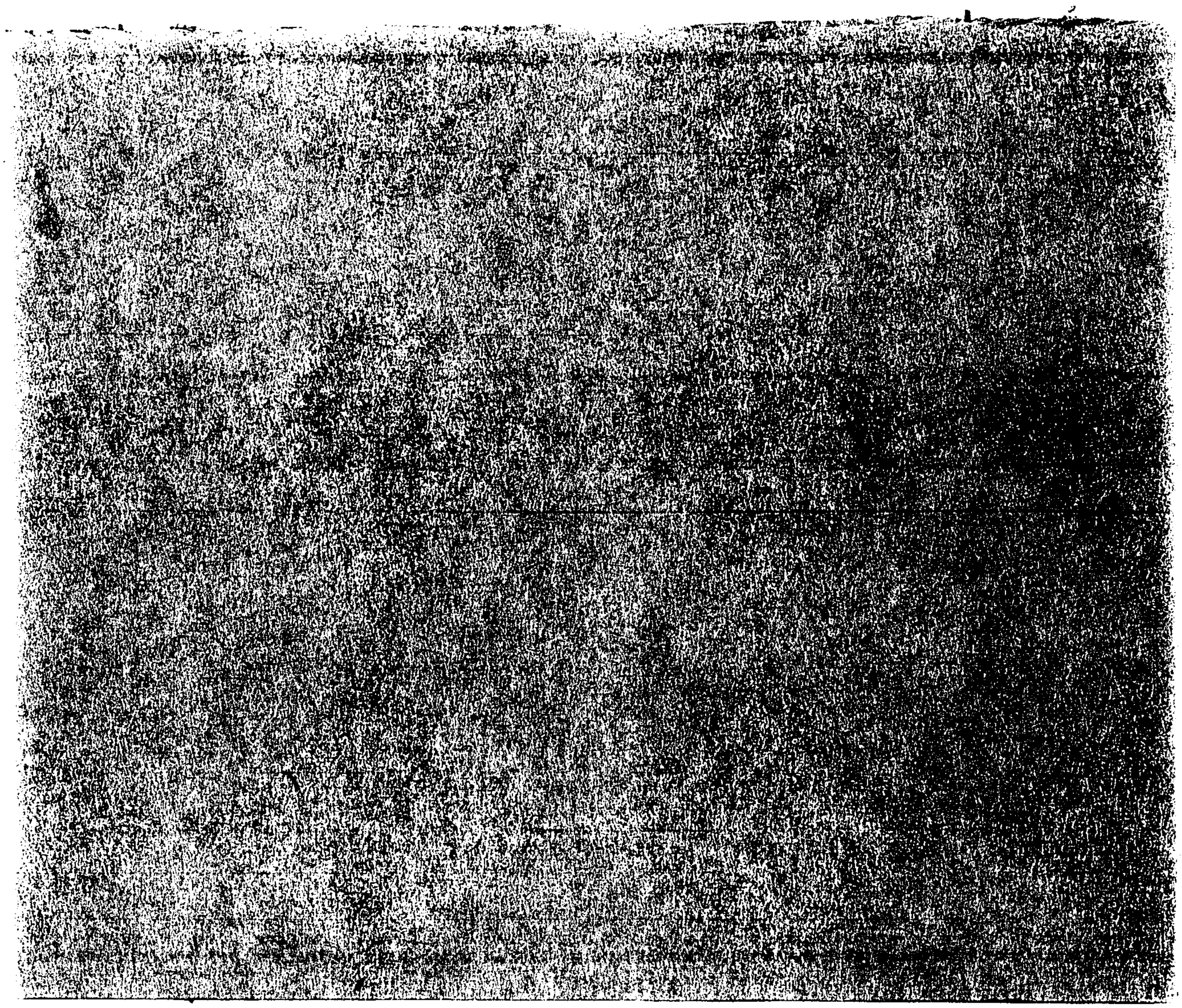

Figure 5-3: Second-order Gravity Trend Surface Map of the Chattolanee Dome

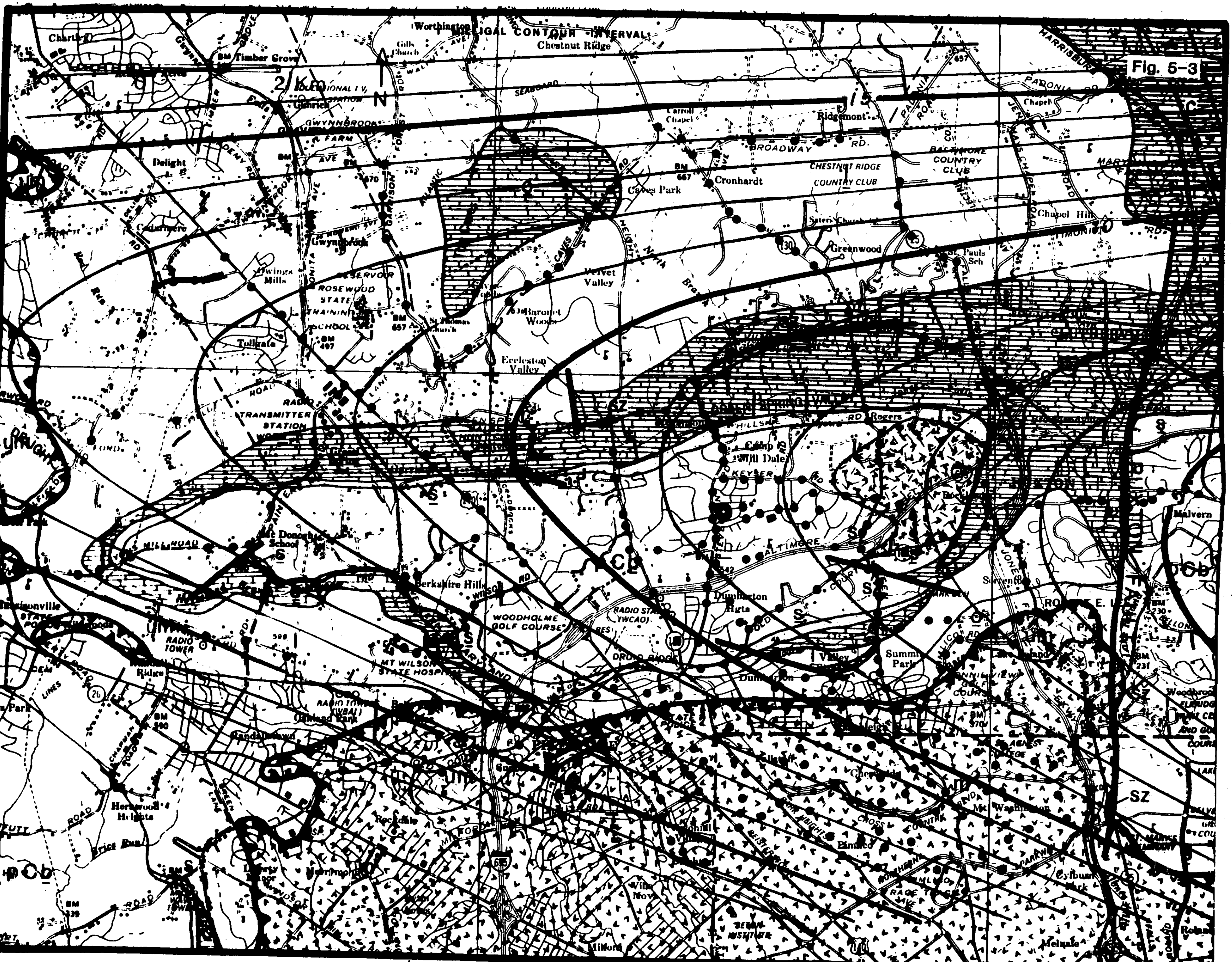
Worthington
Chestnut Ridge
Timber Grove
2 Km
N
Delight
Gwynnbrook
Owings Mills
ROSEWOOD STATE TRAINING SCHOOL
Tollgate
RADIO TRANSMITTER STATION
Caves Park
Cronhardt
Ridgemont
Carroll Chapel
BROADWAY
CHESTNUT RIDGE COUNTRY CLUB
BALTIMORE COUNTRY CLUB
Chapel Hill
Greenwood
Velvet Valley
Baronet Woods
Eccleston Valley
Camp Hill Dale
KEYSER
Berkshire Hills
WOODHOLME GOLF COURSE
Dumbarton Hgts
Summit Park
MT WILSON STATE HOSPITAL
RADIO TOWER
Ridge
Herwood Heights
Malvern
Woodbrook
Mt. Washington
Milford
SZ
CB
pCb

Fig. 5-3

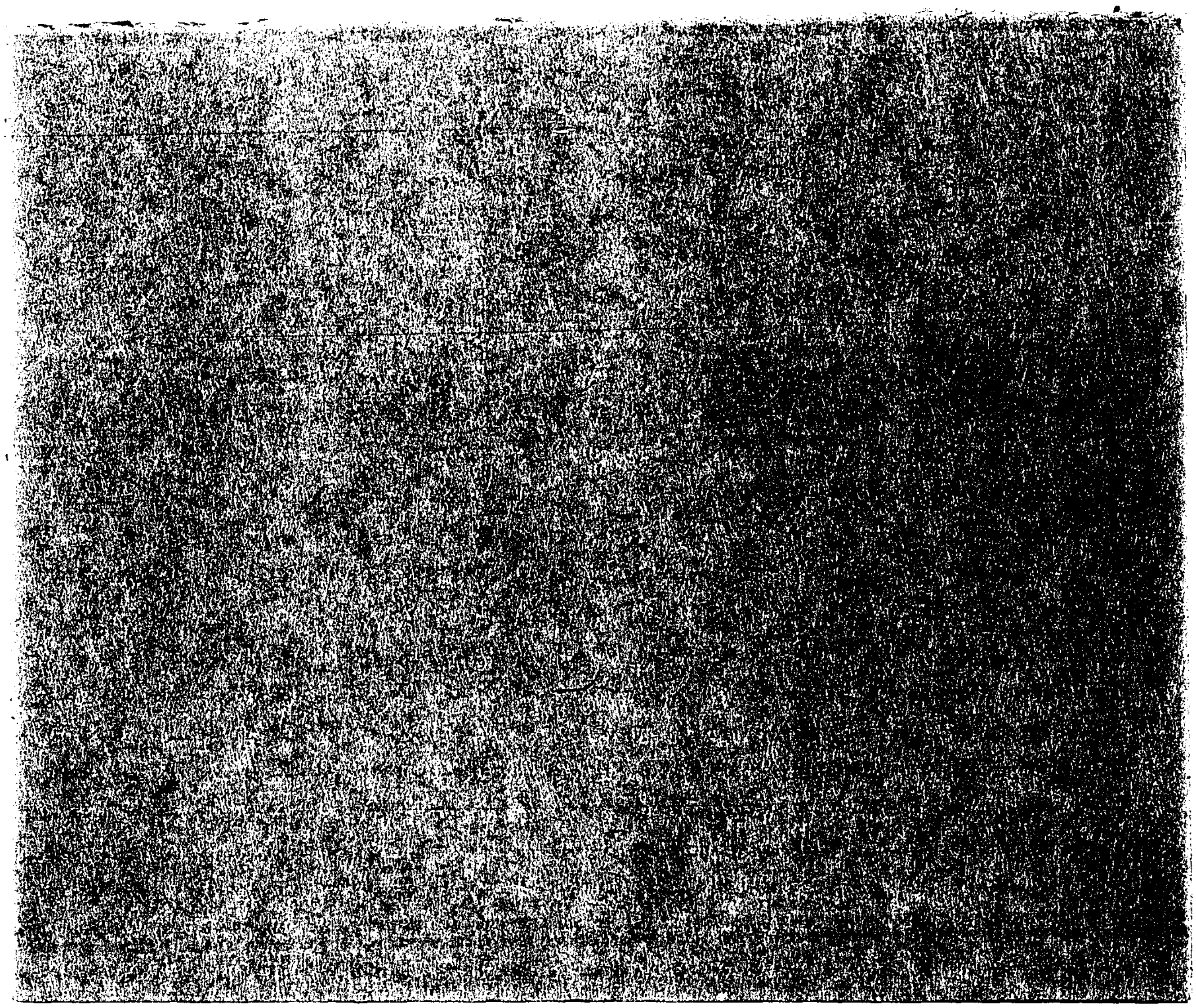

Figure 5-4: Index Map of Gravity Traverses

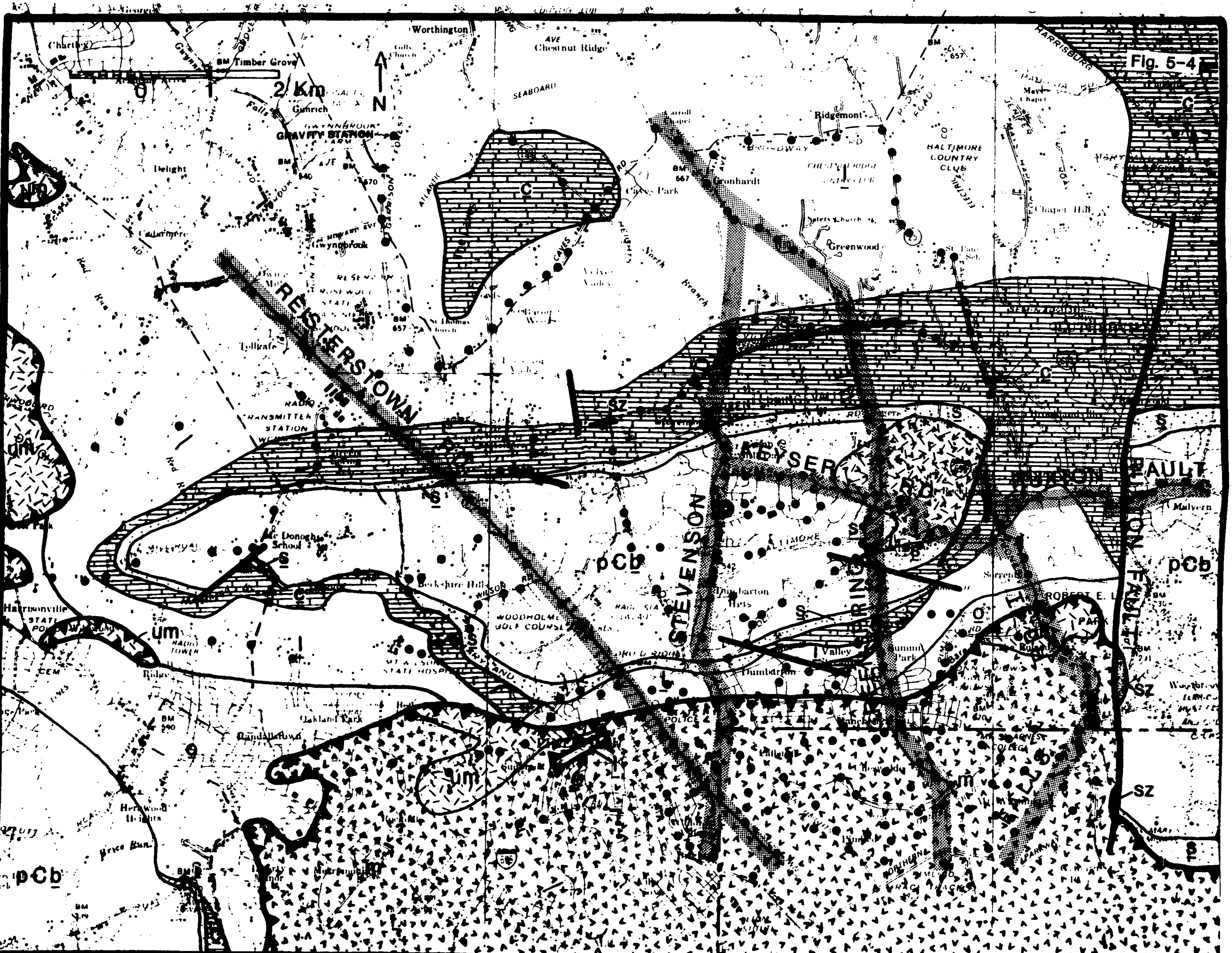
Fig. 5-4
2 Km
0
N
REISTERSTOWN
STEVENSON
KEYSER
RD
SPRING
FAULT
pCb
um
C
S
SZ
Worthington
Chestnut Ridge
Timber Grove
Gwynnbrook
Delight
Ridgemont
Cronhardt
Greenwood
Caves Park
Baltimore Country Club
Tollgate
Mc Donogh School
Berkshire Hills
Woodholme Golf Course
Dumbarton
Valley
Randallstown
Oakland Park
Harrisonville
Malvern
Robert E. Lee Park
Mt. St. Agnes College
Harrisburg
Seaboard
Radio Transmitter Station

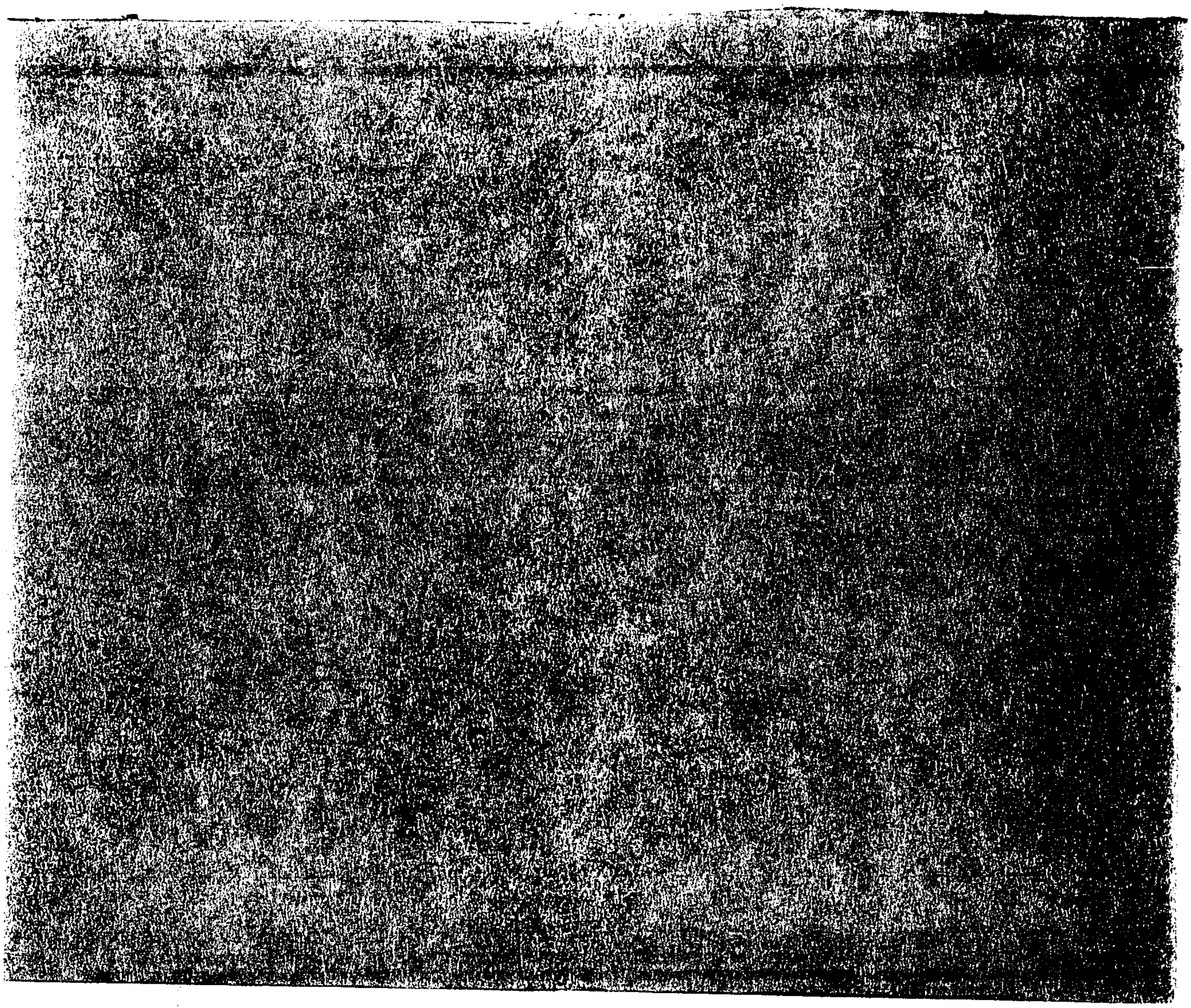

Figure 5-5: Geologic Map of the Phoenix Dome Along Falls Road

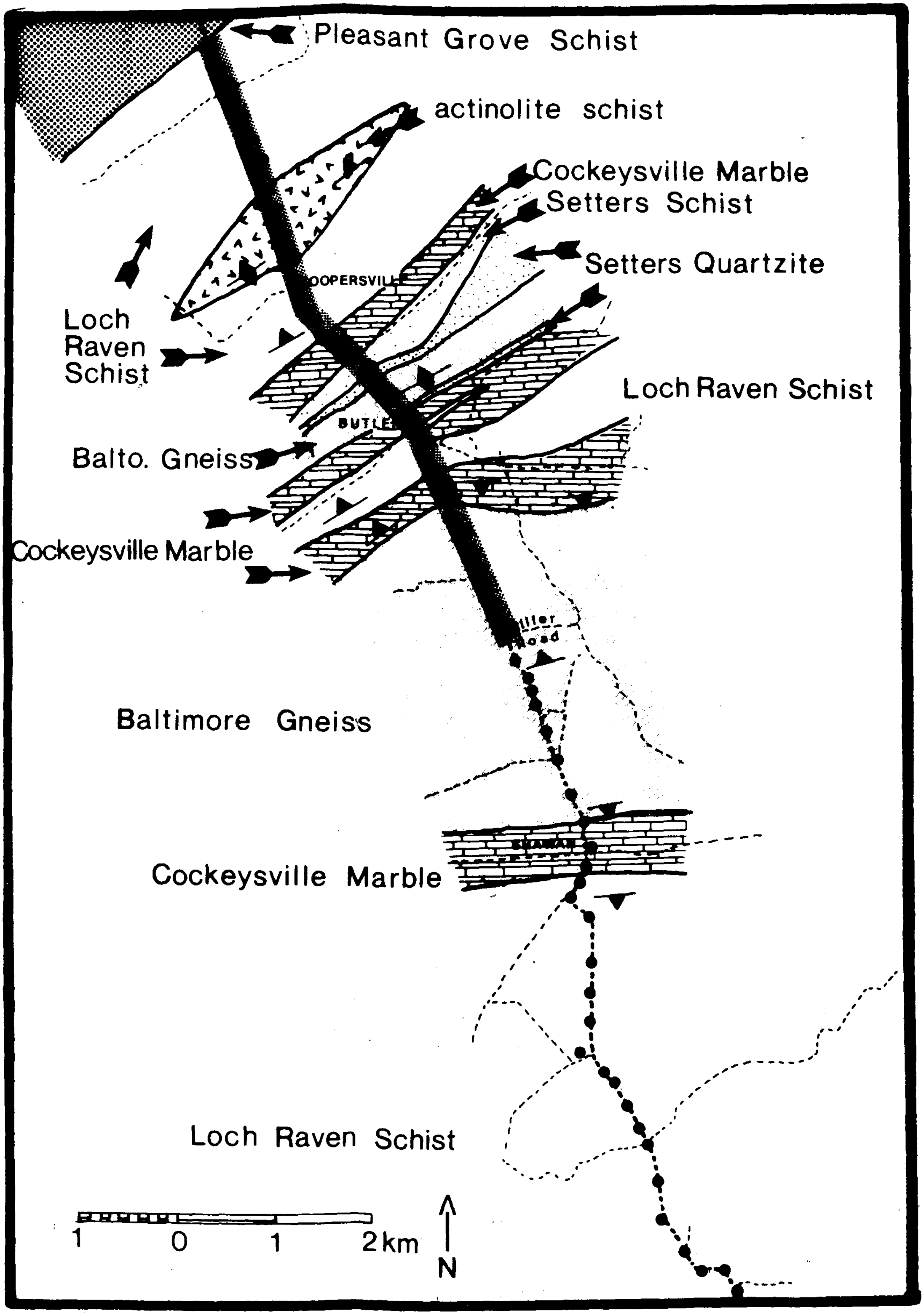
Pleasant Grove Schist
actinolite schist
Cockeysville Marble
Setters Schist
Setters Quartzite
Loch Raven Schist
Loch Raven Schist
Balto. Gneiss
Cockeysville Marble
Baltimore Gneiss
Cockeysville Marble
Loch Raven Schist
1 0 1 2km
N

VITA

David Alan Chapin
Born: October 13, 1957, Baltimore, Maryland
Parents: Jerry and Pauline Chapin
Academic Training:

1963-1975	Baltimore, Maryland Public Schools
1975-1979	George Washington University, B.S. Geology 1979
1979-1981	Lehigh University

Member:
Society of Exploration Geophysicists
American Geophysical Union
Sigma Xi
American Association for the Advancement of Science
National Geographic Society

Awards:
George Washington Award for Meritorious Service from George Washington Univ.

Married:
Sept. 13, 1981 to Rita Marlene Goldberg

Current Position:
Geologist
Gulf Science and Technology Co.
Houston Technical Services Center
P.O. Box 36506
Houston, Texas 77036